DEVELOPMENT OF A DOMESTIC ANIMAL MODEL OF ENDOMETRIOSIS

A Thesis Submitted to

the College of Graduate Studies and Research

in Partial Fulfillment of the Requirements

for the Degree of Masters of Science

in the Department of Veterinary Biomedical Sciences

University of Saskatchewan

Saskatoon, Saskatchewan, Canada

By

Emy Elizabeth Varughese

PERMISSION TO USE

TITLE OF THESIS: Development of a domestic animal model of endometriosis

NAME OF AUTHOR: Emy Elizabeth Varughese

Department of Veterinary Biomedical Sciences

DEGREE: Master of Science

In presenting this thesis in partial fulfillment of the requirements for a Master degree from the University of Saskatchewan, I agree that the Libraries of this University may make it freely available for inspection. I further agree that permission for copying of this thesis in any manner, in whole or in part, for scholarly purposes may be granted by the professor or professors who supervised my thesis work or, in their absence, by the Head of the Department or the Dean of the College in which my thesis work was done. It is understood that copying or publication or use of this thesis or parts thereof for financial gain shall not be allowed without my written permission. It is also understood that due recognition shall be given to me and to the University of Saskatchewan in any scholarly use which may be made of any material in my thesis.

Requests for permission to copy or to make other use of material in this thesis in whole or part should be addressed to:

Head of the Department of Veterinary Biomedical Sciences

Western College of Veterinary Medicine

52 Campus Drive

University of Saskatchewan

Saskatoon, Saskatchewan

S7N 5B4

ABSTRACT

Endometriosis is a reproductive disease affecting women in their prime reproductive years characterized by the presence of endometrial glands and stroma in ectopic locations. Animal models have been proven to be indispensable not only for the study of the disease but also to develop better non-invasive diagnostic imaging modalities. A major limitation with the diagnosis of endometriosis is the lack of a specific and sensitive non-invasive diagnostic test. Our objective was to develop a domestic animal model of endometriosis suitable for serial diagnostic imaging procedures and assessment of therapies. Two major studies were conducted to achieve this objective.

First study involved in vitro whole tissue-explant culture and surgical induction of endometriosis in dog, pig and sheep to choose the most suitable model. For in vitro co-culture, dog, pig and sheep endometrium was placed on visceral peritoneum for 24 to 72 h to assess the degree of attachment and adhesion characteristics of endometrium (epithelium, glandular and stromal cells). Surgical induction of endometriosis was tested in dog, sheep (n=5 each) and pig (n=4) using autologous endometrial (n=4 grafts per animal) and fat grafts sutured to visceral (urinary bladder surface in dog and pig, uterus in sheep) and parietal (abdominal wall) peritoneum. Sham surgeries were performed in control group animals (dog and sheep n=5, pig n=3) using fat grafts alone. Animals were euthanized between 80-110 days post-surgery. Size, gross characteristics and histopathologic features of endometriotic lesions were recorded. During in vitro explant culture, surface epithelial, stromal and glandular cells of endometrium were capable of attaching to visceral peritoneum within 24 hours with and without an intact layer of mesothelial lining in dog, pig and sheep. The proportion of successful endometrial attachments were greater at 24h compared to 72h (15/18 vs. 7/18, $p=0.008$; data combined among species) with intermediate attachment at 48h (12/15). Following surgical induction, there was no difference ($p>0.05$) in proportion of successful tissue grafts placed on serosal surface of visceral vs. parietal peritoneum in dog (10/10 vs. 10/10), pig (7/8 vs. 8/8) or sheep (7/10 vs. 8/10). A variety of outcomes (endometriotic cysts with sero-sangunous fluid, solid lesions, vesicles, absence of lesions) were found. The proportion of cystic lesions was greater ($p<0.01$) in dog (19/20 grafts) than in pig (8/16) and sheep (5/20). Further, the

area of endometriotic lesions at euthanasia was larger (0.89 ± 0.11 cm^2) compared to that at the time of surgery (0.50 ± 0.09 cm^2) in dog, whereas, the size of lesions decreased by half or more ($p<0.05$) in pig and sheep. Combined among grafting sites (visceral and parietal peritoneum) and species, a greater proportion ($p=0.015$) of surgical sites had adhesions in treatment (12/14) versus control group animals (5/13). The wall of majority of endometrial cysts in dogs were characterized by simple cuboidal/columnar epithelium, endometrial glands (normal, dilated and cystic), subepithelial capillary network and presence of stromal and smooth muscle cells. Hemorrhage and/or hemosiderin-laden macrophages were observed in the cystic lesions in dog. Development of a greater proportion of growing lesions in the form of endometriotic cysts in dogs compared to sheep and pig led us to conclude dog as a better suitable domestic animal model for endometriosis than sheep and pig.

Second study involved assessing the usefulness and limitations of ultrasonography, magnetic resonance imaging (MRI) and positron emission tomography-computed tomography (PET-CT) in detecting cystic endometriotic lesions in dog and sheep. Surgical induction of endometriois was performed in dogs (n=5) and sheep (n=5) using autologous endometrial grafts (n=4 grafts per animal) and fat grafts sutured to visceral peritoneum (urinary bladder in dogs, uterus in sheep) and parietal peritoneum (ventral abdominal wall). Weekly ultrasonography was performed from Week 1-9 post-surgery and day of euthanasia (Week 14-15). T1 and T2 weighted weighted MRI images (n=2 each for dog and sheep) and PET-CT (n=3 dog, n=1 sheep) using ^{18}F-fluorodeoxyglucose (^{18}F-FDG) as radiolabel was performed between Week 13-15 post-surgery in dog and sheep. Gray-scale B-mode ultrasonography was able to detect endometriotic cysts (0.25-1.75cm) on urinary bladder and abdominal wall in dogs; endometrial grafts Week 1 post-surgery appeared as a homogenous, hypoechoic masses, following which they grew larger with evidence of cyst formation by Week 5. Cysts were undetectable from Week 10-13, whereas they appeared as homogenous masses with a hypoechoic fluid-filled cavity with diffuse hyperechoic echoes and low vascularisation (Color-Doppler imaging) by Week 14-15. In sheep, endometrial grafts were detected as hypoechoic masses Week 1 post-surgery that became smaller until no detectable lesions were visible beyond Week 6-7. Cysts in dogs and sheep appeared hyperintense on T2 and hypointense on T1 weighted images. ^{18}F -

FDG PET-CT did not show hypermetabolic activity in endometriotic cysts in dogs and sheep. In conclusion, MRI appeared to provide the most definitive diagnostic images of endometriotic cysts in dogs and sheep, particularly for lesions in sheep which were not evident by ultrasonography. However, ultrasonography was sufficient to characterize most endometriotic cysts in dogs. Further research needs to be carried out to develop specific PET tracers for endometriosis.

ACKNOWLEDGEMENTS

For today and its blessings, I owe the world an attitude of gratitude.
~ Clarence E. Hodges

This thesis denotes the end of a long awaited journey, my journey through Masters. I have not traveled alone and any attempt to list the people and opportunities with which my life has been richly blessed would be like trying to count the stars in heaven. Yet among these, stand many who deserve special acknowledgement and contributed in many ways to the success of this study and made it an unforgettable experience for me.

All throughout, God's love has been independent of me without being indifferent towards me without which I would never have been what I am today. Thank you Lord for your unchanging love for me!!

Words fall short to express my sincere gratitude to my supervisor, Dr. Jaswant Singh and co-supervisor, Dr. Paul Babyn for their technical guidance and suggestions, constructive enthusiasm, and for inculcating in me the spirit of self reliance to work independently.

I am indeed thankful to Dr. Gregg Adams for his constant help and guidance at several occasions in carrying out my research which deserves immense appreciation. I would also like to thank Dr. Pritpal Malhi, Dr. Karen Machin, Dr. Daniel MacPhee, Dr. Barbara Ambros, Dr. Elisabeth Snead and Dr. Mary Kinloch for their support.

It is my pleasure to record deep sense of gratitude to Sylvia Fedoruk Canadian Centre for Nuclear Innovation and the Department of Veterinary Biomedical Sciences, Western College of Veterinary Medicine for their financial support.

I am forever grateful to Carlos Leonardi and Lawrence Araujo for their positive attitude and ever willing nature to help me in carrying out my experiments. I would like to thank all my colleagues, most notably, Rodrigo Carrassco, Fahrid Huanca, Awang Hazmi, Kylie Beck, Jessica Nicoletti and Steve Yang for being there in times of need.

I am highly thankful to Scott Mildenberger and all the technicians at PET-CT (RUH), Debbie Paisley, Jin Huang, Rachel Bloomfield, Jim Gibbons, Eiko Kawamuram, Ian Shirley,Susan Cook and Kim Tran for their valuable help during my research.

To my beloved parents Azhickal Oommen Varughese and Suma Sarah Varughese, I owe you my deepest sense of gratitude for encouraging and being there for me through every walk of my life, sharing my joys and sorrows and pursuing me to achieve all that I as a person can. To my brothers, Emil and Emilyn, thank you for keeping my spirits high from where you were. To my fiancé, Linz Philip, for just being you. I will continue to cherish the love and affection of my relatives, near and dear, for their unparallel affection, moral support and inspiration which will remain indelible in my life. Lastly, to great friends, Rose Peter, Shubhada Chothe, Varun Prabhakar and Jithin M.V.

All might not have been mentioned but none is forgotten.

TABLE OF CONTENTS

LIST OF TABLES

LIST OF FIGURES

LIST OF ABBREVIATIONS

BSA: Bovine serum albumin

BW: Body weight

CAMs: Cell adhesion molecules

cm: Centimetre

CT: Computed tomography

E2: Estradiol

E1: Estrone

DAPI: 4,6-diamidino-2-phenylindole

DMEM: Dulbecco's modified Eagle's medium containing 4.5g/L D-Glucose and L-Glutamine

DPBS: Dulbecco's phosphate buffer saline containing calcium and magnesium chloride

ECM: Extracellular matrix

EFI: Endometriosis Fertility Index

FCS: Fetal calf serum

^{18}F: Fluorine

^{18}F-FDG: ^{18}F-fluorodeoxyglucose

^{18}F-FDG PET-CT: ^{18}F-fluorodeoxyglucose Positron emission tomography-computed tomography

FSE: Fast spin-echo

^{68}Ga: Gallium-68

GAP-EDL: glutamate peptide estradiol

h: Hour

H&E: Hematoxylin and Eosin

HA: Hyaluronic acid

HA-Fe3O4 NPs: HA-modified magnetic iron oxide nanoparticles

HSD: Hydroxysteriod dehydrogenase

IL-1: Interleukin-1

kg: Killiogram

kv: Killovolt

LF: Least function

MCP-1: Monocyte chemotactic protein-1

mg: Milligram

MHz: Mega Hertz

mi: Microvilli

mm: Millimetre

µm: Micrometre

µSv/h: Microsievert per hour

MMPs: Matrix metalloproteinases

MRI: Magnetic Resonance Imaging

ms: Milliseconds

n: Number

NK: Natural killer

PAS: Periodic acid-Sciff

PET: Positron emission tomography

PET-CT: Positron emission tomography-computed tomography

PKA: Protein kinase A

PGE_2: Prostaglandin E_2

PMC: Peritoneal mesothelial cells

psi: pounds per square inch

rAFS: revised American Fertility Society

RANTES: Regulated on Activation Normal T-cell Expressed and Secreted

RIA: Radioimmunoassay

SAS: Statistical Analysis System

SE: Spin-echo

SEM: Standard Error of Mean

^{99m}Tc: Technetium-99m

TNF-α: Tumour necrosis factor-α

TSE: Turbo spin-echo

TVUS: Transvaginal ultrasonography

uPA: urokinase-type Plasminogen activator

VEGF: Vascular endothelial growth factor

v/v: volume by volume

W: Weighted

CHAPTER 1: INTRODUCTION

Endometriosis is defined as the presence of endometrial glands and stroma in ectopic locations, primarily the pelvic peritoneum, ovaries, and rectovaginal septum (Burney and Giudice 2012). An estimated 176 million women worldwide have endometriosis primarily during their prime reproductive years (Adamson et al 2010) with an overall prevalence of around 10%, higher in women aged 25-30 years (Meuleman et al 2009, Eskenazi and Warner 1997). The incidence of endometriosis in women undergoing laparoscopic evaluation for infertility is higher, as much as 50% (Senapati and Barnhart 2011), with serious implications for future reproduction. Endometriosis also has high economic importance as the total annual societal burden of endometriosis amounts to many millions of Euros (Simoens et al 2012).

Laparoscopy and histopathology are considered the gold standard for diagnosis and detection of endometriotic lesions in women (Dunselman and Beets-Tan 2012). As laparoscopy is invasive, expensive, and not the first diagnostic choice, endometriosis is often diagnosed many years (8-11 years) after the first complaint (Dunselman and Beets- Tan 2012). Various non-invasive imaging modalities including transvaginal ultrasonography (Mais et al 1993), magnetic resonance imaging (MRI) (Dallaudière et al 2013) and positron emission tomography- computed tomography (PET-CT) (Fastrez et al 2011) have been used in women with endometriosis with varying results. There remains need for better non-invasive diagnostic imaging tests that are more specific and sensitive especially in the detection of early endometriosis when lesions may be small and less invasive.

An ideal animal model would be a spontaneous primate model, however ethical and practical constraints prevent the study of pathogenesis and progression of endometriosis in women and non-human primates. Other models using mouse (Chen et al 2010), immunodeficient mouse (Defrère et al 2006), rat (Umezawa et al 2008), and rabbits (Rosa-e-Silva et al 2010) have been tried. Rodents and rabbits are cost effective

but the lesions that develop are small and difficult to identify (Tirado-Gonzalez et al 2010) making them less suited as models for imaging and other studies.

Our objective was to develop a domestic animal model suitable for performing sequential and repeated examinations that can be used for diagnostic imaging procedures and treatments. Two studies were conducted, the first involved in vitro whole tissue-explant culture and surgical induction of endometriosis in dog, pig and sheep to choose the most suitable model (Chapter 3). Second study involved assessing the usefulness and limitations of ultrasonography, MRI and PET-CT in detecting cystic endmoetriotic lesions in dog and sheep (Chapter 4). A general discussion of Chapters 3 and 4 is included in Chapter 5. Future directions for further studies are part of Chapter 6 and general conclusions from both studies are included in Chapter 7.

CHAPTER 2: LITERATURE REVIEW

Endometriosis is the presence of endometrial glands and stroma in locations other than the uterus, primarily the pelvic peritoneum, ovaries and rectovaginal septum (Burney and Giudice 2012).

2.1 Theories for Pathogenesis of Endometriosis in Women

Several theories have been proposed to explain the pathogenesis of endometriosis. In the theory of coelomic metaplasia, the serosa of peritoneum and epithelium of ovary undergo metaplasia to form endometrium (Nap 2012). This theory could explain the evidence of endometriosis outside the pelvis.
The theory of induction states that endogenous factors such as hormonal, biochemical or immunological factors could induce endometrial differentiation in undifferentiated cells (Merrill 1966, Nap 2012).
The theory of "Mullerianosis" states that migration of Mullerian ducts during embryogenesis retains its capacity to transform into endometriotic lesions (Burney and Giudice 2012) which could explain the presence of lesions in the rectovaginal pouch and broad ligaments (Nap 2012).

The theory of transplantation states that the endometrium is transplanted from the uterus to extrauterine locations through the lymphatic, and/or hematogenous route (Javert 1949). A more recent hypothesis relates to the role of endometrial stem/progenitor cells in the development of endometriosis (Sasson and Taylor 2008). Environmental factors such as endocrine disrupting chemicals (Crain et al 2008) and genetic predisposition (Simpson et al 1980) may also play a role in endometriosis.

However, the most popular and widely accepted theory is Sampson's retrograde menstruation theory (Sampson 1927). He suggested that during menstruation, a retrograde reflux of endometrial fragments from the uterus travels through the fallopian tube and falls into the peritoneal cavity, which implants and grows in ectopic sites such as peritoneum and ovary (Sampson 1921; Sampson 1927). Although 90% of

women with patent fallopian tubes have blood in the peritoneal cavity (Halme et al 1984), only 10% develop endometriosis (Eskenazi and Warner 1997) indicating that not all women with endometrial fragments in the peritoneal cavity develop the disease. This suggests that there are several other factors that facilitate the formation of endometriotic lesions from a normal phenomenon.

2.2 Types and Clinical Manifestations of Endometriosis in Women

The three main types of endometriosis are *peritoneal, ovarian and rectovaginal* (Donnez et al 2012). Peritoneal endometriosis can be explained by the retrograde menstruation theory wherein endometrial cells pass through the fallopian tube with subsequent implantation and peritoneal proliferation (Sampson 1927). The development of a peritoneal endometriotic lesion is facilitated by retrograde menstruation, escape from the immune system, adhesion and invasion into the peritoneum, survival and angiogenesis which is described in greater detail in section IV.

Peritoneal lesions visually may appear as red, black or white. An initial endometriotic lesion is called a "red" lesion as it has extensive vascular network and considerable amount of similarity with eutopic endometrium (Nissole and Doonez 1997). This provides evidence that red lesions are refluxed endometrial cells further supporting the retrograde menstruation theory (Nissole and Doonez 1997). After partial shedding, red lesions grow continuously, which induces a fibromuscular reaction leading to scarification and encapsulation (Donnez et al 2012). This embedded lesion becomes a "black" lesion due to intraluminal debris (Donnez et al 2012) with reduction in vascularization (Nissole and Doonez 1997). With time, the scarification process completely devascularizes the lesion, and white plaques of old collagen are retained known as a "white" lesion (Donnez et al 2012). Several other theories such as the theory of metaplasia (Ridley and Edwards 1958), mullerianosis (Von Recklinghausen 1896), transplantation (Sampson 1925) and role of stem cells (Sasson and Taylor 2008) have been considered to explain the pathogenesis of peritoneal endometriosis.

The pathogenesis of ovarian endometriosis is controversial. The invagination of the surface epithelium of the ovary into the cortex has been described (Motta et al 1992). These inclusions could be transformed into intraovarian endometriosis by the process of metaplasia (Donnez et al 1996; Zheng et al 2005). As the surface epithelium invaginates deeper into the ovary, follicles are seen surrounding the endometriotic cyst (Donnez et al 2012). As blood collects within the cyst over a period of time, it begins to turn brown and hence is referred to as "chocolate cyst". The presence of an endometrioma has been associated with a gradual reduction in dominant follicles and this deleterious effect was more evident in women with larger cysts or more than one cyst (Somigliana et al 2006). Other theories include invagination of cortex after accumulation of menstrual debris from bleeding of endometrial implants located on the ovarian surface (90%; Hughesdon 1957) or via secondary involvement of ovarian cysts to from endometriomas (Nezhat et al 1992).

The third main type has been defined as rectovaginal endometriosis or deep endometriosis and sometimes also referred to as deep-infiltrating endometriosis (Donnez and Squifflet 2004, Chapron et al 2006). The pathogenesis of these lesions has been hypothesized to have a retroperitoneal origin or mullerianosis in some cases (Donnez et al 2012). However, it is evident that 90% of deep lesions originate from the cervix or are at least strongly related to it (Donnez et al 2012). These lesions originate from tissues of the rectovaginal septum or the posterior part of the cervix, and consist of smooth muscle (90%) with active glandular epithelium and scanty stroma (Donnez et al 2012; Nissole and Donnez 1997).

Extra-abdominal endometriosis has been described in other locations including the thoracic, extremities, skin and central nervous systems (Honoré 1999). However, it is rarely seen in clinical practice (Bobbio et al 2012).

The most common symptoms identified in women with endometriosis are dysmenorrhea, dyspareunia, severe pelvic pain, gastrointestinal symptoms such as painful defecation, diarrhea, constipation or both, nausea and vomiting, and bladder symptoms such as painful dysuria, urgency-frequency and painful bladder sensation (Arnaud et al 2013).

2.3 Clinical Staging of Endometriosis

In the past, there have been several attempts to classify endometriosis (Sampson 1921, Acosta et al 1973, Kistner et al 1977, Buttram 1978), but a major limitation in all of them is the inability to predict clinical outcome.

Endometriosis Fertility Index (EFI) is a clinical classification tool that predicts pregnancy rates for patients following surgical staging of endometriosis. It is the first classification tool for endometriosis that has been validated among different countries (Adamson 2013). It is based on assigning scores to factors in two broad categories: Historical factors and Surgical factors. Historical factors included age (<35, 36-49 and>40 yrs), years infertile (< 3yrs or > 3yrs) and prior pregnancy (yes or no) (Adamson and Pasta 2010). The results of abdominal surgery were recorded in detail for the comparison of three operative coding systems: 1) revised American Fertility Society (rAFS) total, lesion, adhesion, and cul-de-sac scores, 2) percentage of filmy and dense adhesions on the ovaries and tubes bilaterally, and 3) intraoperative pretreatment and post-treatment functional score named the least function (LF) score (Adamson and Pasta 2010). The LF score is determined by the surgeon for each tube, fimbria, and ovary bilaterally where 0= absent or nonfunctional; 1, 2, and 3= severe, moderate, and mild dysfunction, respectively; and 4 = normal with respect to the capacity of the organ/structure to effect its purpose in reproduction. It is calculated as the sum of the lowest function score on each side from among the fallopian tube, fimbria and ovary (Adamson and Pasta 2010).

The EFI score ranges from 0 to 10 with 0 representing poorest prognosis and 10 the best prognosis (Adamson and Pasta 2010). Half the points come from historical factors and the other half from surgical factors. EFI is a simple, robust, and validated clinical tool that predicts pregnancy rate for patients after surgical staging of endometriosis (Adamson and Pasta 2010). It can also be used to decide the type, length, duration and cost of treatment before considering assisted reproductive technologies following endometriosis surgery (Adamson and Pasta 2010).

2.4 Pathogenesis

2.4.1 Escape from the Immune System

Since retrograde menstruation is a normal phenomenon in women, minimal peritoneal lesions are probably seen in all women with patent fallopian tubes (Donnez and van Langendonckt 2004). However in most women, the immune system is capable of clearing the endometrial fragments from the peritoneal cavity. In a small percentage of women (10%), endometriosis sets in due to inefficient functioning of components of the immune system. The endometrial cells secrete intercellular adhesion molecule-1 which binds to lymphocyte function-associated antigen-1 that prevents endometrial cells from being recognized by lymphocytes (Vigano et al 1998) and subsequently escape natural killer (NK) cell-mediated clearance (Somigliana et al 1996). It has also been found that eutopic endometrium of women with endometriosis is more resistant to NK cell-mediated cytotoxicity when compared to that of women without endometriosis (Oosterlynck et al 1991). A significant increase in activated macrophages in peritoneal fluid (Badawy et al 1984) and monocytes expressing CD14+ and high levels of CD44 (Gagné et al 2003) in blood has been demonstrated in women with endometriosis. This provides evidence for the inflammatory nature of the disease, and with compromised function, these cells do not clear endometrial cells from the system thereby facilitating the development of the disease.

2.4.2 Escape from Apoptosis

After entering into the peritoneal cavity, the endometrial cells must survive to develop lesions. There are several proteins that regulate apoptosis. Protein p53 accelerates apoptosis whereas; bcl-2 inhibits apoptosis (Stewart 1994). Under normal circumstances, the cells are either cleared by the immune system or enter apoptosis. However, in women with endometriosis, endometriotic lesions showed an increased expression of bcl-2 compared with eutopic endometrium which could account for the survival of endometriotic tissue at ectopic sites (Béliard et al 2004).

2.4.3 Adhesion to the Peritoneum

Cell adhesion molecules (CAMs) are transmembrane receptors that facilitate intercellular binding and interactions with the extracellular matrix (Donnez et al 2012). They facilitate cell-cell and cell-matrix adhesion (Donnez et al 2012). CAMs are members of a limited number of families that include integrins, immunoglobulin superfamily, cadherins, and selectins (Humphries 2000).

CD44, a transmembrane glycoprotein, is the receptor for hyaluronic acid (HA) expressed by endometrial cells (Yaegashi et al 1995). HA is present on the surface of peritoneal mesothelial cells (PMCs) (Jones et al 1995) and is involved in the initial attachment of endometrial cells to PMCs (Witz 2003). Although integrins ($\alpha 2\beta 1$ and $\alpha 3\beta 1$) has been demonstrated to be present on PMCs, their involvement in cell adhesion is questionable (Witz et al 2002a).

Cadherins are calcium-dependant transmembrane proteins that are involved in cell-cell adhesion and cadherins from two adjacent cells interact in a homophilic manner (Klemmt and Starzinski-Powitz 2012). Of the classic cadherins, E-cadherin is a marker of differentiated epithelial tissue like endometrium, ovary, etc and N-cadherin is a mesenchymal cadherin present in synapses of neurons and intercalating

disks of the heart (Klemmt and Starzinski-Powitz 2012). Caderins are associated with proteins such p120 catenin and β-catenin. Cytokines such as epidermal growth factor and hepatocyte growth factor can promote the transition of epithelial cells to mesenchymal cells which leads to downregulation of E-cadherin and upregulation of N-cadherin (Klemmt and Starzinski-Powitz 2012). Immunohistochemitry of endometriotic lesions demonstrated that E-cadherin-negative epithelial cell type was increased in sections of endometriosis tissue as compared with sections of eutopic endometrium (Gaetje et al 1997) and some of the endometriotic glands expressed N-cadherin (Klemmt and Starzinski-Powitz 2012). Therefore, E-cadherin-negative/N-cadherin-positive cells could exhibit invasive potential, promoting the relatively high recurrence rate of endometriosis (Klemmt and Starzinski-Powitz 2012). This could also account for recurrence of endometriosis in surgically treated areas since it is known to extend beyond margins visible under white light at laparoscopy (Taylor and Williams 2010) thereby suggesting invasive potential.

Integrins bind to major components of extracellular matrix (ECM) such as collagen, fibrinonectin, laminin, tenascin, thrombospondin, vitronectin and fibrinogen (Klemmt and Starzinski-Powitz 2012) and mediate cell-ECM adhesion (Baraczyk et al 2010). The ECM components of peritoneum such as collagens (type I and IV), fibrinonectin and laminin (Witz et al 2001) are similar to endometrium (Stovall et al 1992, Béliard et al 1997). Fibrinoectin receptors such as integrin α5β1 were the only receptors found to be differently localized in endometriotic and endometrial samples and could play a role in the persistence of endometriosis (Beliard et al 1997, Klemmt and Starzinski-Powitz 2012).

2.4.4 Invasion of Peritoneum by Endometrial Cells

The invasion of endometrial cells into the peritoneum requires the breakdown of ECM which is achieved by two types of proteolytic enzymes: matrix metalloproteinases (MMPs) and plasminogen/plasmin activation system (Rodgers et al 1994).

MMPs are a family of extracellular zinc-dependant proteinases that are capable of degrading ECM components (Matrisian 2000). Estrogen is associated with growth related expression of MMPs through specific steroid receptor interaction with the activator protein-1 site whereas progesterone has a suppressive effect on MMPs along with the local action of transforming growth factor-β (Kushner et al 2000, Bruner-tran et al 2002). Therefore, the proliferative phase is associated with an increased expression of MMP-7 in epithelial cells while stromal cells express specific mRNAs for MMP-1, MMP-2 and MMP-11, but the secretory phase is associated with a decreased expression of most MMP genes (Osteen et al 2003). Tissue inhibitors of metalloproteinases are coexpressed with MMPs to provide balance and control in tissue remodeling (Osteen et al 2003). However, there is an altered expression of MMPs in women with endometriosis (Osteen et al 2003). It has been demonstrated that the failure of progesterone in the secretory phase to suppress MMP-3 or MMP-7 secretion in vitro was linked to an increased ability of endometriotic tissues collected from women with endometriosis to subsequently establish experimental endometriosis (Bruner-tran et al 2002). Thus an increased expression of MMPs may lead to breakdown of ECM and endometrial invasion of the peritoneum.

Plasminogen, a protein secreted by the liver, is activated to plasmin by two types of activators, tissue-type plasminogen activator and urokinase-type plasminogen activator (uPA) (Sillem et al 1998). In endometriosis, plasminogen and uPA have been detected in higher concentrations (Sillem et al 1998).

2.4.5 Survival of Ectopic Endometrial Cells

Growth and survival of endometriotic cells is regulated by ovarian hormones, cytokines and growth factors.

2.4.5.1 Ovarian Hormones

During the proliferative phase of the menstrual cycle, endometrium proliferates in response to estrogen followed by differentiation in response to progesterone (P4) during the secretory phase. However in endometriosis, several regulatory enzymes are expressed differently.

Firstly, there is increased expression of aromatase, which converts androgens to estrogen, in eutopic as well as ectopic endometrium of patients suffering from endometriosis (Noble et al 1996). This is absent in normal human endometrium (Bulun et al 2002). Also, due to the inflammatory nature of the disease, several cytokines and prostaglandins are overexpressed. Both aromatase expression and activity are stimulated by prostaglandin E2 (PGE2) (Bulun et al 2002). This results in local production of estrogen, which induces PGE2 formation through cyclo-oxygenase type 2 enzyme and establishes a positive feedback cycle (Bulun et al 2002).

Secondly, the enzyme 17β-hydroxysteriod dehydrogenase (HSD) is involved in regulation of estrone (E1) and estradiol (E2) concentrations. The highly active E2 is inactivated to weak estrone (E1) by 17β HSD-2 whereas 17 β HSD-1 promotes activation of E1 to E2. In the proliferative phase, endometrial E2 conentration was higher than in serum, whereas in the secretory phase the E2 concentration was lower than in serum (Huhtinen et al 2012). However in endometriosis lesions, E2 levels predominated over those of E1 throughout the menstrual cycle (Huhtinen et al 2012). These results suggest that endometriosis is an estrogen-dependant disease.

Postovulatory rise in P4 leads to transformation of endometrial stromal cells into specialized decidual cells, influx of immune cells and inhibition of endometrial proliferation (Gellersen et al 2007). However in endometriosis, inflammatory signals associated with the disease could induce progesterone resistance by altering the expression of P4 receptor isoforms, chaperone proteins like FKBP52, or co-regulators such as HIC-5/ARA55 (Khanjani et al 2012) which contributed to the persistent proliferative nature of the endometrium (Burney et al 2007). Furthermore, it has also been observed that endometrial stromal cells

become sensitive to P4 only after the activation of protein kinase A (PKA) pathway which is associated with decidualization of stromal cells (Gellersen and Brosens 2003). A recent study has revealed that there is an inherent abnormality in PKA pathway (Aghajanova et al 2010) which may be an important contributing factor causing P4 resistance. Therefore, endometriosis is considered an estrogen dependant-P4 resistance disease.

2.4.5.2 Cytokines and Growth Factors

RANTES (Regulated on Activation, Normal T-cell Expressed and Secreted) is a chemokine that is a potent chemoattractant of monocytes, macrophages, T-lymphocytes and eosinophils (Schall et al 1990). Expression of the RANTES gene is up-regulated in endometriotic stromal cells in response to interleukin-1 (IL-1)-β, a macrophage-derived cytokine which is also upregulated in endometriosis (Mori et al 1992; Lebovic et al 2001). The cognate chemokine receptor has high affinity for RANTES and is seen expressed on the surface of neutrophil/mononuclear leukocytes (Rossi et al 2000). The expression of cognate chemokine receptor-1 mRNA was found to be higher in peripheral blood leucocytes of women with endometriosis compared to healthy women (Agic et al 2007).

Interleukins play an important role in inflammation and immune responses. IL-1 has two receptor agonists (IL-1α and IL-1β) and a receptor antagonist (IL-1ra) which blocks the binding of both IL-1α and IL-1β to IL-1 receptor type 1 (Lebovic et al 2001). It has been demonstrated that the expression of IL-1β mRNA in peritoneal macrophages was greater in women with mild endometriosis but the expression of IL-1ra mRNA was greater in macrophages of women with moderate to severe endometriosis (Mori et al 1992). IL-1β is also considered to enhance angiogenesis by induction of vascular endothelial growth factor (VEGF) and IL -6 in endometriotic stromal cells but not in endometrial stromal cells (Lebovic et al 2000). Therefore, these factors promote the growth and survival of endometriotic lesions. IL-6 is also an important regulator of inflammation. Secretion of IL-6 by macrophages is mediated by IL-1 (Sironi et al

1989) and IL-6 also activates macrophages (Akira et al 1993). Both epithelial and stromal cells of the endometrium produce IL-6 in the presence of E2 and P4, epithelial cells producing in greater amounts (Laird et al 1993). It has been shown that E2 and P4 have a stimulatory effect on the production of IL-6 by epithelial and stromal cells during the proliferative and early secretory phases, but exhibit an inhibitory effect on IL6 production during the late secretory phase, suggesting its possible role in endometrial proliferation (Laird et al 1993). There have been reports of increased levels of IL-6 in the peritoneal fluid of women with endometriosis (Martinez et al 2007; Fassbender et al 2011). Indeed, IL-6 may promote increased soluble ICAM-1 production by endometriotic lesions, leading to a reduction in NK cytotoxicity, promoting endometriosis (Fassbender et al 2011).

Tumour necrosis factor-α (TNF-α), an important regulator of inflammation and angiogenesis, is produced by neutrophils, activated macrophages and lymphocytes. Several factors regulate the production of TNF-α by human endometrial epithelial cells (Laird et al 1996). IL-1, P4 alone or in conjunction with E2 and placental protein 14 cause a significant increase in TNF-α by human endometrial epithelial cells prepared from the proliferative phase which suggests that TNF-α might have a paracrine control of endometrial function (Laird et al 1996). TNF-α can also increase the production of PGE2 by endometrial cells which could play a potential role in adhesion of cells to mesothelium (Zhang et al 1993, Chen et al 1995) along with IL-1 (Chen et al 1995). TNF-α promotes the proliferation and angiogenetic potential of endometriotic stromal cells through the expression of IL-8 (Iwabe et al 2000; Barcz et al 2002). It has also been shown that IL-6, IL-8 and TNF-α are significantly elevated in peritoneal fluid and up-regulated in granulosa cells of women with endometriosis compared to healthy women (Keenan et al 1994, Rana et al 1996, Carlberg et al 2000).

Monocyte chemotactic protein-1 (MCP-1) promotes chemotaxsis and activation of monocytes and macrophages. Levels of MCP-1 in peritoneal fluid were higher during the proliferative phase than secretory phase of control women and increased in moderate to severe endometriosis (Arici et al 1997).

The regulated expression of MCP-1 may recruit macrophages into peritoneal fluid and contribute to the pathogenesis of endometriosis (Arici et al 1997).

Growth factors such as transforming growth factor-α and β, epidermal growth factor and fibroblast growth factor released by peritoneal macrophages or endometrial stromal cells in endometrial stromal tissue may promote implantation and proliferation of ectopic endometrium in the peritoneal cavity (Hammond et al 1993). It has been demonstrated that the production of hepatocyte growth factor (influenced by IL-6 and TNF-α) by stromal cells derived from the eutopic endometrium of women with endometriosis was significantly higher than that of cells from women without endometriosis (Khan et al 2005). The role of VEGF as a growth factor is described in section 2.4.6.

2.4.6 Endometrial Angiogenesis

Endometriosis is one among the many angiogenic diseases and excessive endometrial angiogenesis has been observed in women with endometriosis compared to normal subjects (Healy et al 1998). VEGF is a heparin-binding glycoprotein with potent angiogenic, endothelial cell-specific mitogenic and vascular permeability activities (Donnez et al 1998). It is considered the most important vasoactive factor (Groothuis 2012) and is found to be elevated in the peritoneal fluid of women with endometriosis (McLaren et al 1996). The angiopoietin-1/Tie-2 system is responsible for last stage blood vessel development, stabilization and maturation of newly formed blood vessels in endometrium whereby angiogenesis is facilitated in the presence of VEGF (Groothuis 2012).

High levels of VEGF were observed in uterine glandular epithelium and stroma of red peritoneal lesions as compared to black lesions that were characterized by poor angiogenesis (Donnez et al 1998). Based on the study by Donnez et al 1998, it was suggested that during retrograde menstruation, endometrial implants with high VEGF-expressing glandular cells enter the peritoneal cavity. Following attachment,

VEGF could provoke an increase in subperitoneal vascular network and facilitate implantation and viability (Donnez et al 1998).

2.5 Models of Endometriosis

2.5.1 In vitro Culture Models

Several attempts have been made in the past to study the interaction between endometrial components such as stromal and glandular cells and peritoneum. These studies were carried out using whole explants of peritoneum and endometrium i.e by separating endometrium from uterus collected from women undergoing surgical procedures (Witz et al 1999) or using shed menstrual effluent (Witz et al 2002b).

Whole explant models using peritoneum and endometrium revealed attachment of endometrium (collected during proliferative and secretory phases), mainly via stromal cells, to mesothelium of peritoneum (Witz et al 1999). Menstrual effluent collected from women when cultured with peritoneal explants attached within 1 hour and an intact layer of cytokeratin positive mesothelial cells was identified below sites of attachment (Witz et al 2002b). It was also noted that there lacked an identifiable mesothelium beneath the endometrial implants, instead found adjacent which suggested early invasion (<24 hours) (Witz et al 1999). Further studies were conducted to study early attachment and invasion characteristics and it was found that endometrial (both stromal and glandular cells) adhesion to peritoneum occurs within 1 hour and transmesothelial invasion occurs within 18 hours (Witz et al 2001).

2.5.2 In vivo Animal Models

To understand the pathogenesis of such a complex disease has been a challenge combined with the fact that it is unethical, impractical and difficult to study the progression of the disease in women. Therefore,

animal models are indispensable to increase our understanding of this disease that is affecting many women of today's age. Several species have been tried and documented.

2.5.2.1 Rodent Models

In a mouse model (Chen et al 2010), induction was performed by intraperitoneal injection of endometrial-rich fragments collected from the uterine tissue of donor mice into recipient mice. Following this, the recipient mice developed bright red lesions, adhesions and white lesions on the surface of organs or peritoneum in 6, 9 and 15 days respectively. A change in pattern of cytokines was noted and thought to bear relationship with the progression of the disease. One study (Uchiide et al 2002) demonstrated that stromal tissues of the peritoneum adjacent to implanted uterine tissue showed infiltration by mast cells, eosinophils, plasma cells, lymphocytes, and macrophages which may reflect a hypersensitivity reaction. Another study on rats (Umezawa et al 2008) showed that expression levels of IL-6, IL-10, MCP-1, RANTES, and cognate chemokine receptor-1 were significantly increased in the endometriotic lesions of rats with endometriosis (induced by surgical implantation of endometrium) compared to controls rats. This supports the findings of the previous study (Uchiide et al 2002) by providing evidence that the increased levels of cytokines may be due to activation of immune cells.

From the above studies and section 2.4.5.2, it is also evident that the expression of inflammatory mediators is similar in both humans and rats induced with the disease. It has been demonstrated that the expression of inflammatory mediators such as cytokines and chemokines in rat and gene expression in mice developing endometriosis after induction is similar to that in humans (Umezawa et al 2008; Pelch et al 2010). This provides substantial evidence that animal models provide insight into the pathogenesis of the disease in humans.

Heterologous models are based on the induction of disease using human endometrial tissue in immunodeficient mice without graft rejection. The progression of endometriosis by surgical

transplantation of endometrium from patients with and without endometriosis has revealed that there is no significant difference in histology, VEGF, MMP-9 expressions, and the positive rate of steroid receptors between the two groups (rats grafted with endometrium from patients with endometriosis and without endometriosis) (Wang et al 2005). This provides evidence that endometrial tissue has the capacity to proliferate, invade and establish endometriosis in nude mice. This experiment also suggests that endometriosis may be governed by genetic, immune or other factors (Wang et al 2005) owing to the establishment of disease in both groups. The mean size of endometriosis like-lesions in a nude mice model was 0.49 ± 0.02 cm and ranged from 0.30-0.70 cm (Banu et al 2009).

One of the major problems in mouse models is that endometrial lesions appear small and are difficult to identify, which initiated the development of "fluorescent murine models" (Tirado-Gonzalez et al 2010). Fluorescent models have been developed in autologous (Hirata et al 2005) and heterologous (Defrère et al 2006) murine models. Fluorescent labeling was achieved by incubating minced human menstrual endometrium with a fluorescent dye (carboxyfluorescein diacetate succinimidyl ester) (Defrère et al 2006). Following this, retrograde menstruation was mimicked by intraperitoneal injection of labeled menstrual endometrium in nude mice (Defrère et al 2006). This technique allowed the recovery of lesions that were grossly not visible, one gland surrounded by one layer of stromal cells (<0.5mm), that constituted 15% of all recovered lesions (Defrère et al 2006). Failure to detect microscopic lesions that could proliferate and produce endometriotic lesions is a serious limitation as it could lead to under staging of the disease. However, fluorescence may be overestimated since it also stains necrotic tissue and some murine organs such as pancreas may autofluoresce (Defrère et al 2006). Therefore, fluorescent labeling complemented with immunohistochemical analysis provided precise localization and detection of microscopic lesions (Defrère et al 2006).

One of the major limitations of nude mice models is the limited life span of transplanted human endometrial tissue which limits long term experiments (Grummer et al 2001). Also, since endometriosis is

governed by immunological and inflammatory factors, immunodeficient models eliminate the study of any immunoregulatory component which is another major drawback.

2.5.2.2 Rabbit Model

Surgical implantation of autologous endometrial tissue to the peritoneum of rabbits also led to the development of endometriotic lesions (Rosa-e-Silva et al 2010). Ectopic lesions (stromal and glandular cells) at 4 and 8 weeks after induction (endometrium sutured onto peritoneum) appeared to have a higher cell proliferation index than eutpoic endometrium (Rosa-e-Silva et al 2010). Glandular tissue of ectopic lesions at 8 weeks had lower apoptotic index compared to eutopic endomerium (Rosa-e-Silva et al 2010).

2.5.2.3 Primate Models

Other than women, the only other species to have a menstrual cycle are non-human primates and this makes them ideal as models for endometriosis. Most non-human primates are endangered and protected, hence baboons offer a great advantage and have been used extensively to study lesion development and progression of the disease (D'Hooghe et al 1995). Spontaneous endometriosis is seen in baboons (D'Hooghe et al 1996) and experimental retrograde menstruation has been attempted successfully using methods like cervical occlusion (D'Hooghe et al 1995) and retroperitoneal/intrapelvic injection of menstrual endometrium (D'Hooghe et al 1994).

Similar to humans, following intrapelvic injection of menstrual tissue and fluid, endometriotic lesions in baboons were found in the peritoneum, especially in the rectovaginal pouch, bladder and the perimetrium (Harirchian et al 2012). The colours of lesions were noted and it was observed that early lesions were usually red lesions which later transformed into different colours (Harirchian et al 2012). Most lesions observed in this study were black (which remained black or turned blue or white) and blue (which usually

remained blue) (Harirchian et al 2012). White lesions were seen at later stages and disappeared or became scar tissue (Harirchian et al 2012).

Despite the numerous advantages associated with using non-human primates as models, they are expensive to maintain and is ethically sensitive to carry out such experiments in these animals (Tirado-Gonzalez et al 2010).

2.6 Imaging Modalities for Diagnosis of Endometriosis

2.6.1 Imaging in Women

Laparoscopy and/or histopathology remains the gold standard diagnostic test for detection of endometriotic lesions (Dunselman and Beets-Tan 2012). Since laparoscopy is invasive and expensive, it is not the first diagnostic choice; hence, endometriosis is often diagnosed several years (8-11 years) after the occurrence of the first complaint (Dunselman and Beets-Tan 2012). Laparoscopy has limitations including procedure related complications and experience of the laparoscopist (Rogers et al 2013), limited knowledge on efficacy (Rogers et al 2013), long term outcome and cost-effectiveness of the procedure (Hori and SAGES Guidelines Committee 2008). Therefore, there seems to be an ever-increasing need for a non-invasive test for the detection of early endometriosis where the lesions are particularly small and sometimes micro-invasive.

Several imaging modalities have been explored to date and are detailed below.

Transvaginal ultrasonography (TVUS) is probably the most available imaging tool and has been proven to have an efficacy of 88% in differentiating endometriomas from other ovarian masses (Mais et al 1993). It has also been documented to have better sensitivity, specificity and accuracy in cases of deep infiltrating

endometriosis compared to Magnetic Resonance Imaging (MRI) and digital examination (Abrao et al 2007).

MRI has been used extensively to detect pelvic (intraperitoneal and subperitoneal) and extrapelvic endometriosis (Dallaudière et al 2013). Endometriomas have a characteristic appearance of being persistently hyperintense in T1 weighted-fat suppressed sequences and hypointense with T2-weighted images (Dallaudière et al 2013). However, ovarian cysts appear hypointense with T1-weighted images and hyperinetnse on T2-weighted images (Dallaudière et al 2013). Peritoneal lesions are seen as simple thickening or isolated nodule on the peritoneum which is sometimes difficult to distinguish on MRI (Dallaudière et al 2013). MRI was particularly useful in women with significant pain in the rectovaginal pouch or those with large ovarian cysts which limited the use of TVUS (Abrao et al 2007). Intraperitoneal and subperitoneal bowel endometriosis lesions were hypointense in T2-weighted images (Dallaudière et al 2013). Posterior wall and dome of bladder are common areas of bladder endometriosis and unlike cystoscopy, MRI appeared better at ascertaining the relationship of bladder endometriosis to the uterus and other pelvic structures (Umaria and Olliff 2000). Extrapelvic endometriosis lesions is most common in muscle and subcutaneous tissues (Dallaudière et al 2013). Thoracic endometriosis lesions may also occur with signal intensities similar more common to intrapelvic lesions (Dallaudière et al 2013).

Positron emission tomography (PET) is a non-invasive imaging modality that is gaining increasing popularity due to its high resolution imaging and ability to demonstrate function of organs being imaged. PET is complemented with computed tomography (CT) or more recently MRI to provide accurate anatomical localization. Hence, most scanners now have a PET and CT component which provides separate as well as combined PET and CT images. The PET camera measures the distribution of positron-emitting tracers within an object and the most widely used positron-emitting isotope is fluorine (^{18}F), conjugated with glucose to make ^{18}F-fluorodeoxyglucose (^{18}F -FDG) (Baghaei et al 2013).

^{18}F -FDG follows the glucose pathway but unlike glucose remains trapped in the cell as it does not undergo further metabolism due to its negative charge, which is used for imaging purposes (Baghaei et al 2013). Since tumour cells have higher glycolytic rate (DeBerardinis et al 2008) which follows uptake of ^{18}F -FDG (Lee et al 2013) compared to normal tissue, most studies on PET are primarily, but not necessarily related to oncology in both human (Walker et al 2012) and animal patients (Hansen et al 2011). However, uptake of ^{18}F -FDG is not only related to malignant tissue, but may be seen normally in skeletal muscle after exercise, myocardium, brain, parts of the gastrointestinal tract especially stomach and cecum, and in the urinary tract (Lee et al 2013).

^{18}F-FDG is said to accumulate greatly in inflammatory conditions such as rheumatoid arthritis due to inflammatory cytokines (Matsui et al 2009). Following this concept, there have been reports that suggest that ^{18}F-FDG PET is particularly useful in cases of inflammatory endometriosis (Jeffry et al 2004).
The utility of PET-CT in the diagnosis of endometriosis was studied by Fastrez et al in 2011, who concluded that no hypermetabolic anomaly related to endometriosis could be detected using ^{18}F -FDG PET-CT. Since ^{18}F -FDG is not highly specific for endometriosis, it was concluded that there is a need to develop more specific tracers for the disease (Fastrez et al 2011).

2.6.2 Imaging Endometriotic Lesions in Animal Models

Gamma scintigraphy and PET studies has been performed in rabbit to assess the uptake of radiolabelled {Technetium-99m (^{99m}Tc) or Gallium-68 (^{68}Ga)} glutamate peptide estradiol (GAP-EDL) via estrogen-receptor mediated process (Takahashi et al 2007) provided promising results. There was increased uptake of ^{99m}Tc-GAP-EDL via gamma scintigraphy and ^{68}Ga-GAP-EDL via PET in uterine graft implants proving to be useful functional estrogen receptor imaging agents (Takahashi et al 2007).

High-resolution high-frequency ultrasound imaging with a centre frequency of 40MHz and maximal depth of 6mm in a mice model of endometriosis has been carried out recently (Laschke et al 2010). On ultrasonography, endometriotic lesions were characterized by anechoic cysts presented as a homogenous tissue mass. Volume measurements of endometrial cysts and stroma indicated that the initial establishment of lesions is associated with enhanced cellular proliferation, followed by a phase of increased secretory activity of endometrial glands (Laschke et al 2010). It also helped differentiate between endometrial cysts and stroma. Therefore, this non-invasive techonology allowed repetitive quantitative analysis of growth, cyst development, and adhesion formation of endometriotic lesions (Laschke et al 2010).

In vivo MRI of surgically induced endometriotic lesions in rats using hyaluronic acid (HA)-modified magnetic iron oxide nanoparticles (HA-Fe3O4 NPs) as a T2 -negative contrast agent proved to be a useful application (Zhang et al 2014). Quantification of iron concentration at different time points after administration of HA-Fe3O4 NPs disclosed that the accumulation of iron in endometriotic lesions achieved highest concentration at 2 h post injection with clearly outlined lesions and provided better lesion to background contrast compared to T1 weighted images (Zhang et al 2014).

A fluorescent nude mouse model of endometriosis was established by transfecting endometrial epithelial and stromal cells with adenovirus encoding red fluorescent protein (Wang et al 2014). Transfected cells were injected subcutaneously or intraperitoneally and an invivo imaging system was used to observe lesions. Higher fluorescent positive rates were observed from Day 5 in cells injected subcutaneously but similar fluorescence persistence as the intraperitoneal injection model (Wang et al 2014).

CHAPTER 3: OBJECTIVES

Thesis Objective:

Domestic animal models can be developed for endometriosis which can be used for therapeutical imaging purposes.

Objective 1A:

To evaluate, in vitro, the ability of endometrial tissue to adhere/attach to serosal surface in dogs, pig and sheep (Chapter 3).

Objective 1B:

To surgically induce endometriosis and characterize endometriotic lesions in dogs, pig and sheep (Chapter 3).

Objective 1C:

To compare the characteristics of lesions with previously described lesions in women to determine which of the species is the most suitable animal model (Chapter 3).

Objective 2A:

To demonstrate the feasibility of the induced model to evaluate potential imaging techniques including ultrasonography, magnetic resonance imaging and positron emission tomography-computed tomography in dog and sheep (Chapter 4).

CHAPTER 4: DEVELOPMENT OF A DOMESTIC ANIMAL MODEL FOR ENDOMETRIOSIS: INVITRO CULTURE AND SURGICAL INDUCTION IN DOG, PIG AND SHEEP

Emy E. Varughese, Gregg P. Adams, Carlos Leonardi, Pritpal Malhi, Paul Babyn, Mary Kinloch, Jaswant Singh

4.1 Abstract

Endometriosis affects one in ten women of reproductive age but is often diagnosed only at advanced stages. Our objective was to develop a domestic animal model suitable for performing sequential and repeated examinations which may be used for imaging and therapy assessment. In vitro tissue-explant culture and surgical transplantation were carried out in dogs, pig and sheep to determine the most suitable model. For in vitro culture, dogs, pig and sheep endometrium was placed on visceral peritoneum for 24 to 72 h to assess the degree of attachment and adhesion characteristics of endometrium (epithelium, glandular and stromal cells). Surgical induction of endometriosis was tested (treatment group; dogs and sheep n=5, pig n=4) using autologous endometrial (n=4 grafts per animal) and fat grafts sutured to visceral (urinary bladder surface in dogs and pig, uterus in sheep) and parietal (abdominal wall) peritoneum. Sham surgeries were performed in control group animals (dogs and sheep n=5, pig n=3) by placing fat grafts and omitting endometrial grafts. Animals were euthanized between 80-110 days post-surgery. Size, gross characteristics and histopathologic features of endometriotic lesions were recorded. During in vitro culture, surface epithelial, stromal and glandular cells of endometrium were capable of attaching to visceral peritoneum within 24 hours with and without an intact layer of mesothelial lining in dogs, pig and sheep. The proportion of successful endometrial attachments were greater at 24h than at 72h (15/18 vs. 7/18, $p=0.008$; data combined among species) with intermediate attachment at 48h (12/15). There was no difference ($p>0.05$) in proportions of successful tissue grafts after surgery on serosal surface of visceral vs. parietal peritoneum in dogs (10/10 vs. 10/10), pig (7/8 vs. 8/8) or sheep (7/10 vs. 8/10). A variety of outcomes (endometriotic cysts with sero-sangunous fluid, solid lesions, vesicles, absence of lesions) were noticed. The proportion of cystic lesions was greater ($p<0.01$) in dogs (19/20 grafts) than in pig (8/16) and sheep (5/20). The area of endometriotic lesions at euthanasia was larger (0.89 ± 0.11 cm^2) than at the time of surgery (0.50 ± 0.09 cm^2) in dogs, whereas, the size of lesions decreased ($p<0.05$) by half or more in pig and sheep. Combined among grafting sites (visceral and parietal peritoneum) and species, a greater proportion ($p=0.015$) of surgical sites had adhesions in

treatment (12/14) versus control group animals (5/13). The wall of majority of endometrial cysts in dogs were characterized by simple cuboidal/columnar epithelium, endometrial glands (normal, dilated and cystic), subepithelial capillary network, stromal and smooth muscle cells with hemorrhage and/or hemosiderin-laden macrophages. Development of a greater proportion of growing lesions in the form of endometriotic cysts in dogs compared to sheep and pig led us to conclude that dogs are a better suited domestic animal model for endometriosis.

Keywords: Animal models, Dogs, Endometriosis, Endometriotic cyst, Endometrium, Pig, Sheep, Uterine Pathology, Uterus

4.2 Introduction

Endometriosis is defined as the presence of endometrial glands and stroma in ectopic locations, primarily the pelvic peritoneum, ovaries, and rectovaginal septum (Burney and Giudice 2012). It is believed to establish when retrograde reflux of endometrial fragments from the uterus enter the oviduct (fallopian tube), fall into the peritoneal cavity, implants and grows in ectopic sites (Sampson 1921; Sampson 1927). Although 90% of women with patent oviducts have blood in the peritoneal cavity (Halme et al 1984), endometriosis has a prevalence rate of 10% (Eskenazi and Warner 1997) indicating that not all women with endometrial fragments in the peritoneal cavity will develop the disease. One of the possible reasons for development of endometriotic lesions in some but not all women is perhaps inefficient functioning of the immune and/or phagocytic system (Somigliana et al 1996; Vigano et al 1998)

Interactions between endometrial components and serosal surfaces have been studied in vitro using whole explants of the peritoneum and endometrium; using uterine tissue collected from women undergoing surgical procedures (Witz et al 1999) or using shed menstrual effluent (Witz et al 2002b). Whole explant models indicate attachment of endometrium to mesothelium of peritoneum (Witz et al 1999). Such in vitro models provide useful information regarding initial attachment characteristics between the

endometrium and serosal surfaces but fail to provide information regarding long-term tissue interactions. Ethical and practical constraints prevent the study of pathogenesis and progression of endometriosis in women. Therefore, several animal models have been used to understand the disease. Non-human primates are the only animal species to undergo menstruation at the time of endometrial shedding and to develop spontaneous endometriosis (D'Hooghe et al 1996). Despite the advantages associated with using non-human primates as models, they are expensive to maintain and it is ethically sensitive to carry out invasive experiments in these animals (Tirado-Gonzalez et al 2010). Induction of endometriosis has been tried by injection of endometrial fragments into the peritoneal cavity or by surgical transplantation of endometrium onto organs in the peritoneal cavity in mouse (Chen et al 2010), rat (Umezawa et al 2008), immunodeficient mouse (Defrere et al 2006) and rabbits (Rosa-e-Silva et al 2010). Rodent models are cost effective but they develop lesions that are small and difficult to identify (Tirado-Gonzalez et al 2010) making them less suitable as animal models for sequential studies. Further, the use of immunodeficient mice confounds the investigation of immunoregulatory component involved in the pathogenesis of the disease (Fazleabas 2012). Rabbits are induced ovulators and lack a luteal phase (D'Hooghe 1997). Therefore, there is a need for a suitable animal model which can develop macroscopically visible lesions characteristic of endometriosis in women. An animal model with body size comparable to women will be valuable to perform repeated and sequential imaging can be performed for diagnostic and treatment trials.

Domestic animal species (eg. dogs, pig and sheep) as models for endometriosis have not been reported. However, prior to conducting trials in animals, a preliminary in-vitro culture trial may provide information regarding relative adhesion and attachment characteristics of endometrial components to serosal surfaces in animals. Therefore, the objectives of the present study were: (1) To evaluate, in vitro, the ability of endometrial tissue to adhere/attach to serosal surface in dogs, pig and sheep, (2) to surgically induce endometriosis and characterize endometriotic lesions in these three species, and (3) to compare the characteristics of lesions with previously described lesions in women to determine which of the species is the most suitable animal model.

4.3 Materials and Methods

Two experiments were conducted to address the objectives of this study. First experiment comprised of in vitro whole-tissue explant cultures of endometrium and visceral peritoneum of dogs, pig and sheep. In the second experiment, surgical induction of endometriosis was performed in dogs, pig and sheep. Both experiments were approved by University Committee on Animal Care and Supply, Animal Research Ethics Board, University of Saskatchewan.

Dulbecco's phosphate buffer saline containing calcium and magnesium chloride (DPBS; Catalog no. 14040-133), Dulbecco's modified Eagle's medium containing 4.5g/L D-Glucose, L-Glutamine (DMEM; Catalog no. 11965-092), 1% antibiotic/antimycotic solution (Catalog no. 15140-122) were purchased from Thermo Fisher Scientific, NY, USA. Fetal calf serum (FCS), poly-L-lysine (Catalog no. SLBJ5688V), and bovine serum albumin (BSA; Catalog no. SLBM2718V) were purchased from Sigma-Aldrich, MO, USA. Pan-cytokeratin (H-240) polyclonal rabbit antibody (sc-15367; concentration 200µg/mL) was purchased from Santa Cruz Biotechnology, Santa Cruz, CA, USA, Alexa Fluor ® 488 goat anti-rabbit IgG (Alexa 488; concentration 2mg/mL) from Molecular Probes, CA, USA and 4,6-diamidino-2-phenylindole (DAPI) containing Vectashield mounting media was purchased from Vector Laboratories, CA, USA.

4.3.1 In vitro whole-tissue explant culture of endometrium and visceral peritoneum

4.3.1.1 Experimental design

Tissues were collected from dogs (mixed-breed Husky; n=3; aged between 2-4 years) following routine ovariohysterectomy and from sheep (Suffolk; n=3; aged between 1.5-3 years) and pig (Mixed breed; n=3; aged between 8 months-1 year) immediately following slaughter at local abattoirs. The stage of estrous cycle was estimated by gross examination of ovaries in sheep and pig for the presence of corpora lutea and by exfoliative vaginal cytology in dogs (Concannon 2011). All sheep (n=3) were in diestrus (large corpus luteum), two pigs were in diestrus (multiple corpora lutea) and one in proestrus-estrus stage

(multiple large follicles), one dog was in anestrus (parabasal cells) and other two dogs in diestrus (intermediate and parabasal cells). For consistency, visceral peritoneum was collected from the superficial leaf of greater omentum in sheep (Yung et al 2006) as it was abundant and easily accessible. For dogs and pig, broad ligament was chosen as a representative location of visceral periteonum since it is a wide extension of peritoneal fold in these two species.

Uterus and visceral peritoneum was collected aseptically and immediately placed in 1X DPBS and transported to the laboratory. Tissue handling and processing in the laboratory was carried out in a biosafety cabinet to minimize contamination. Visceral peritoneum was cut into 1 X 1cm pieces, endometrium was separated from myometrium as much as possible by careful dissection and cut into 0.5 X 0.5 cm pieces. Fat was separated from visceral peritoneum and also cut into 0.5 X 0.5 cm pieces. Pieces of endometrium, fat and visceral peritoneum were washed once in DPBS and twice in culture media (DMEM plus 10% FCS with 1% antibiotic/antimycotic). Explants of visceral peritoneum were placed in six-well plates (Bioniche Animal Health, USA) with culture media. One endometrial piece was gently placed on top of visceral peritoneum in each of the treatment wells. Fat pieces were placed in control wells in a similar manner. Tissues were incubated at 37°C with 5% carbon dioxide and high humidity for 24h, 48h or 72h. Culture media was changed every 24h and two replicates were incubated for each time point for each animal.

4.3.1.2 Histology and Immunohistochemistry

At the end of incubation, visceral peritoneum was held from the edge and lifted vertically so that loose endometrium or fat that were not attached would fall off. Replicates from which endometrium or fat fell off were not processed further and were considered as non-attached. Tissues were fixed in freshly prepared 4% paraformaldehyde for 24h. For comparison between fresh and cultured tissue, samples of visceral peritoneum, endometrium and uterus were fixed separately prior to culture (i.e. 0h).

Tissues were embedded in paraffin, sectioned at thickness of 5µm and placed on poly-L-lysine coated glass slides. While sectioning, when attachment area was detected between endometrium/fat and visceral peritoneum, serial sections were cut at thickness of 5µm and used for staining purposes. Hematoxylin and eosin (H & E) staining was used for routine analysis of sections (modified from Culling 1974). Masson's trichrome staining (to differentiate between cellular components and connective tissue), Periodic acid-Schiff stain (PAS) staining (to detect basement membrane) and immunohistochemistry for CD3 (T-cell) and CD20 (B-cell) was performed on a few selected sections by a commercial service (Prairie Diagnostic Centre, Western College of Veterinary Medicine, Saskatoon, Saskatchewan, Canada). Evaluation of the tissue sections was performed using light microscopy (Olympus BX41TF, Tokyo, Japan).

To identify the presence or absence of mesothelial cells on visceral peritoneum and to differentiate between endometrial glandular epithelial cells and stromal cells, immunohistochemsitry was performed using a rabbit polyclonal pan-cytokeratin antibody (sc-15367, primary antibody). Each slide had a positive (incubated with 1:100 dilution of primary antibody in 1% BSA) and a negative control (incubated with 1% BSA) tissue section. Unmasking of antigen was performed by placing slides in citrate buffer (10mM, pH-6.0) in a water bath at 80°C for 1h. Sections were blocked by adding 1% BSA for 1h at room temperature. Primary antibody was placed over sections for 12h at 4°C followed by incubation with Alexa 488 secondary antibody (1:100 dilution) for 2h at room temperature. Sudan black (0.1% in 70% ethanol) for 1h was used to suppress autofluorescence background staining. Nuclear counterstaining was performed with DAPI containing mounting media. Evaluation of the sections was performed using confocal laser scanning microscopy (Leica, TCS SP5, Germany) with Argon ion laser with excitation at 488 nm and emission at 500-525 nm.

4.3.1.3 Evaluation of degree of attachment and health of tissues

The sections were evaluated at different magnifications for assigning scores. Identities of all sections were hidden and one investigator (EEV) scored all sections. A scoring system was developed to assess the

degree of attachment between endometrial tissue/fat and visceral peritoneum (Table 4.1) and health of visceral peritoneum (smooth muscle) and endometrium (endometrial glands and uterine epithelium; Table 4.2). The intactness of mesothelial cells was also scored based on the extent to which it was observed. Adipocytes and stromal cells of uterus did not undergo significant changes over the culture period, hence they were not included in the scoring evaluation.

Table 4.1 Scores (0-3) used to assess degree of attachment between endometrium/fat and visceral peritoneum in dogs, pig and sheep.

Score	**Assessment regarding degree of attachment**
0	No attachment
1	Attached at several points with ≤30% contact area
2	30-60% contact with/without endometrial stromal/glandular cells/uterine epithelium making direct contact with visceral peritoneum.
3	60-100% contact with little distinction between endometrium/fat and visceral peritoneum with/without invasion.

Table 4.2 Scores (0-3) used to assess extent of presence/absence of mesothelial cells on visceral peritoneum, health of smooth muscle of visceral peritoneum and health of endometrium (uterine epithelium and endometrial glands).

Mesothelial cells of visceral peritoneum	**Smooth muscle fibres of visceral peritoneum (if present)**	**Endometrium**
Score 0 Mesothelial cells are present at the site of attachment and along most of the section	Score 0 No degenerative changes	Score 0 Intact uterine epithelium (if present). Endometrial glands are intact and uniform. <20% of glandular epithelial cells detach from the basement membrane.
Score 1 Mesothelial cells are present at the site of attachment and in a few places along the section	Score 1 Mild degenerative changes in muscle fibres	Score 1 Mild sloughing of uterine epithelium cells (if present). 20-50% of glandular epithelial cells detach from the basement membrane.
Score 2 Mesothelial cells are absent at the site of attachment but present in a few places along the section or upto site of attachment.	Score 2 Moderate degenerative changes seen in most muscle fibres	Score 2 Moderate sloughing of uterine epithelium cells (if present). 50-80% of glandular epithelial cells detach from the basement membrane.

Score 3 Mesothelial cells are absent along the entire section	Score 3 Severe degenerative changes with significant gaps between muscle fibres.	Score 3 Severe sloughing of uterine epithelium cells (if present). >80% of glandular epithelial cells detach from the basement membrane.

4.3.2 Surgical induction of endometriosis by autologous tissue grafting

4.3.2.1 Animals

Surgeries were performed in dogs (mixed-breed Husky; n=10; body weight= 15-20kg; age = 2-4 years), pig (Mixed breed; n=8; body weight=100-110kg; age = 7 months-1 year post puberty) and sheep (Suffolk; n=10; body weight=80-90kg; age = 1-2 years). Sheep and pig were randomized in treatment (Sheep n=5, pig n=4) and control (Sheep n=5, pig n=4) groups based on body weight. Dogs were assigned to groups (n=5 each in treatment and control group) by randomized block design based on exfoliative vaginal cytology and body weight. At the time of surgery, treatment group dogs were in proestrus (n=2) and anestrus (n=3) whereas those in control were in proestrus (n=1), diestrus (n=1) and anestrus (n=3).

4.3.2.2 Surgery

Dogs, pigs and sheep were fasted for 12 hours, 24 hours and 48 hours respectively, prior to surgery. Animals were premedicated for surgery, anesthesia induced by intravenous injection (dose and drugs described in Table 4.3), intubated and maintained on general anesthesia with isoflurane (Isoflurane USP, Pharmaceuticals partners of Canada Inc., Richmond Hill, Ontario, Canada).

Table 4.3 Dose, type and method of administration of drugs used for premedication and induction of anesthesia and post-operative analgesia (BW- body weight).

Species	Premedication (Intramuscular)	Anesthesia Induction (Intravenous)	Post-operative Analgesia (Intramuscular)
Dogs	Hydromorhone[a] (0.1 mg/kg BW) and Acepromazine[b] (0.02-0.04 mg/kg BW; depending on temperament of the dogs)	Diazepam (0.25 mg/kg BW) and Ketamine (5 mg/kg BW) via cephalic vein	Hydromorhone (0.05 mg/kg BW)
Pig	Butorphanol[c] (0.2 mg/kg BW), Xylazine[d] (1 mg/kg BW) and Ketamine[e] (5 mg/kg BW)	Xylazine (1 mg/kg BW) and Ketamine (2 mg/kg BW) via ear vein ± Induction via masking with Isoflurane if required	Butorphanol (0.2 mg/kg BW
Sheep	Butorphanol (0.2 mg/kg BW) and Xylazine (0.2 mg/kg BW)	Diazepam[f] (0.25 mg/kg BW) and Ketamine (5 mg/kg BW) via jugular vein	Butorphanol (0.2 mg/kg BW

a- Hydromorphone Hydrochloride Injection USP, Sandoz, Canada
b- Atravet, Boehringer Ingelheim, Burlington, Ontario, Canada
c- Torbugesic, Ayerst Laboratories, Montreal, Canada
d- Rompun, Bayer Inc, Toronto, Canada
e- Vetalar, Bioniche Animal Health Canada Inc, Belleville, Ontario, Canada
f- Diazepam Injection USP, Sandoz, Canada

4.3.2.2.1 Treatment group surgeries

In the treatment group, both endometrial and fat grafts were used, therefore, treatment animals also served as their own internal control. Ventral abdomen was aseptically prepared for laparotomy. Median (7.5-10 cm long, 7.5 cm caudal to umbilicus in dogs and 7.5-10 cm cranial to udder in sheep) or right paramedian (7.5-10 cm dorsal to mammary glands at the level of 5-7th teat in pig) incision was made to approach organs of interest. Unilateral hysterectomy of the left uterine horn was performed in the treatment group. Following this, the excised uterus was cut open longitudinally, endometrium separated aseptically and carefully dissected into small pieces (approximately 1 X 1 cm in dogs and 2 X 1 cm in pig and sheep). Epithelial side and non-epithelial side of the endometrium were identified. Fat was dissected out from the falciform ligament (dogs) or ligaments of the urinary bladder (sheep and pig) and serosal and non-serosal sides of fat were also identified. Endometrial and fat grafts were sutured on the parietal peritoneum (ventral abdominal wall on either side of the incision) and visceral peritoneum (caudodorsal aspect of

urinary bladder in dogs and pig, caudodorsal aspect of uterus in sheep) using 4-0 absorbable (PDS*II, Ehicon Inc., Mexico) suture material (Fig 4.1 and Fig 4.4). Uterus was chosen as the site of grafting in sheep as urinary bladder was difficult to access from the incision opening. Fat grafts were placed cranial to endometrial grafts. To test the difference (if any) between epithelial/serosal versus non-epithelial/non-serosal grafts, grafting on the left side of body was done with non-epithelial side of endometrium/non-serosal side of fat touching the visceral/parietal peritoneum and those on the right side of body with epithelial/serosal side touching the visceral/parietal peritoneum. Plastic jewelry beads (4mm diameter) were sutured using 4-0 non-absorbable (Novafil, Covidien IIc, Mansfield, MA, USA) suture material and served as markers to identify grafts during imaging and euthanasia. Locations of the beads are shown in Fig 4.1 and Fig 4.4).

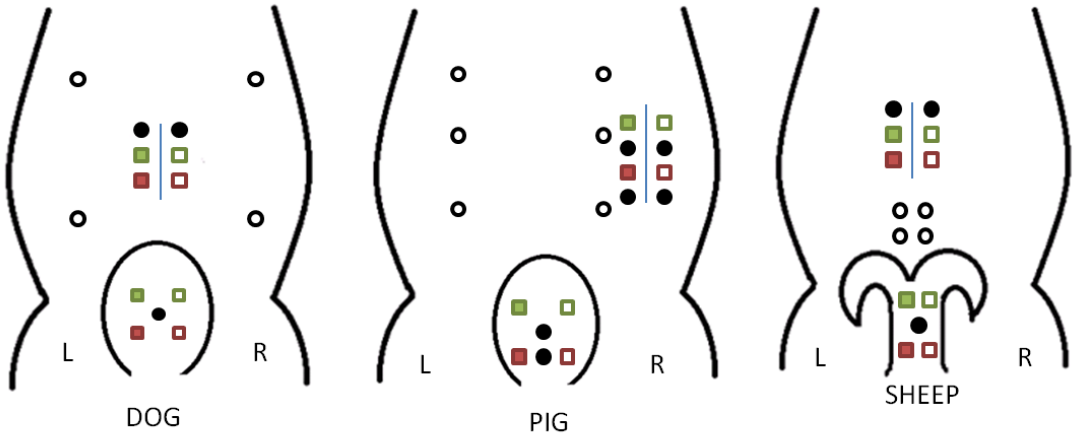

Figure 4.1. Dorsoventral view of abdomen showing the site of incision (line) on the ventral abdominal wall in relation to mammary glands (teats shown as open circles) in dogs, pig and sheep. In the treatment group, endometrial (red) and fat (green) grafts were sutured on the dorsal aspect of urinary bladder (dogs and pig) or uterus (sheep) and on abdominal wall on either side of incision. In control group, only fat grafts were sutured. Grafts were placed with either uterine epithelium (epithelial; clear boxes; right side of body) or non-epithelial (stroma and glands) side (solid boxes; left side of body) of endometrium touching the visceral/parietal peritoneum. Plastic beads (solid circles) served as markers for imaging.

Surgical procedure and site of graft placement for the control group were identical to the treatment group but only fat grafts were used. In brief, two fat grafts were sutured on visceral peritoneum (urinary bladder

in dogs and pig, uterus in sheep) with a plastic bead in between grafts. Two fat grafts were placed on the parietal peritoneum, one on either side of ventral incision with a bead cranial to the graft. Fat graft on the left and right side was placed with the non-serosal side and serosal side respectively, facing the visceral/parietal peritoneum. In addition to serving as sham surgery controls, these animals were used to compare the effect of endometrial grafts on plasma levels of estrogen and progesterone.

In both treatment and control groups, the sizes (length and width) of grafts were measured before closing the abdomen. Linea alba and subcutaneous tissue was closed in a simple continuous manner using absorbable suture material (PDS*II, Ehicon Inc., Mexico; No.0/2-0 in dogs, No.1/2 in pig and No.0/1 in sheep). Skin was closed using non-absorbable suture material (Covidien IIc, Mansfield, MA, USA; No. 2-0 Novafil in dogs and 0 Monosof in sheep and pig).

Post-operative analgesics (Table 4.3) were administered in animals that showed signs of pain. All animals recovered uneventfully except for one pig in the treatment group which developed an abdominal hernia. A second corrective surgery was performed to reduce herniated mass, however, the pig had to be euthanized due to complications. Skin sutures were removed after 14 days or after complete healing of the incision site. None of the animals developed any complications related to daily activities such as feeding, voiding etc during the study period.

4.3.2.3 Recovery of tissue grafts

All animals were euthanized between 80-110 days post-surgery and transplanted grafts were recovered except for the five control dogs that were re-used later for another experiment. Pentobarbital Sodium (Euthanyl Forte, Bimeda-MTC Animal Health Inc, Cambridge, Ontario, Canada) at a dose of 1mL/5kg body weight was injected intravenously (cephalic vein in dogs, ear vein in pig and jugular vein in sheep). Pigs were premedicated prior to euthanasia for safety reasons.

The abdominal wall was reflected, all lesions were macroscopically visible and identified by relative position from the plastic beads. The sizes (length and width) of grafts were measured using a measuring

scale. Lesions were cut out, fixed in 4% paraformaldehyde for 24-48h, tissues embedded in paraffin, sectioned at 5µm thickness and slides were stained with H & E (as described for in vitro culture study)

4.3.2.4 Blood sampling and estimation of plasma estrogen and progesterone

Blood samples were collected in heparinized 10 mL vaccutainer tubes (Becton and Dickinson Vaccutainer Systems, Franklin Lakes, NJ, USA) immediately prior to surgery, weekly for thirteen, five and twelve weeks in dogs, pigs and sheep respectively. Samples were centrifuged at 1500Xg for 20 min, plasma was collected and stored at -20°C for radioimmunoassay (RIA).

Plasma estrogen concentration was estimated using previously described RIA procedure (Joseph et al 1992). The intra-assay coefficients of variation for low and high-reference samples was 11% and 7.3% respectively. The inter-assay coefficients of variation for low and high-reference samples was 12.5% and 11.6% respectively Plasma progesterone concentrations were measured using a commercial RIA kit (ImmuChem^{TM} Progesterone^{125} kit, ICN Pharmaceuticals, Inc. Diagnostic Division, Costa Mesa, CA, USA).The intra-assay Effects of time after ovariectomy, season and oestradiol on luteinizing hormone and follicle-stimulating hormone secretion in ovariectomized ewes were 10.8% and 4.9% respectively, for low and high-reference samples. The inter-assay coefficients of variation were 11.1% and 6.5% respectively, for low and high-reference samples.

4.3.2.5 Scanning Electron microscopy

In order to examine the microscopic features of the lining epithelium of cystic lesions, a subset of samples from dogs (n=2 lesions) were processed for scanning electron microscopy. Briefly, tissue samples (fixed in 4% paraformaldehdye) were dehydrated in increasing concentrations of ethanol; ethanol was substituted with 50% and 75% amyl acetate (v/v in ethanol; 15 min each) followed by three changes in 100% amyl acetate; tissues were critical-point-dried in liquid carbon dioxide (1200psi pressure setting in Polaron E3000; Polaron, Watford, England) and finally coated with gold in a sputter coater (Edwards

S150B, Edwards Co., England). Samples were examined using Hitachi SU8000 Scanning electron microscope at an accelerating voltage of 1.5kV.

4.3.3 Statistical Analysis

Proportions were compared using Chi-square test or Fisher's Exact test. The size (area) of the graft at surgery and lesion at euthanasia (for both endometrial and fat grafts placed on bladder/uterus or abdomen) was analyzed using paired sample t-test using SPSS 22 software (SPSS Inc, USA). Sequential data from weekly plasma estrogen and progesterone estimations were analyzed using mixed procedure repeated measures analysis using Statistical Analysis System software package (SAS 9.4; SAS Institute Inc., Cary, NC, USA). The statistical model included treatment, week and treatment*week interaction as explanatory variables and animal ID as repeated factor. All data are reported as mean ± SEM unless specified otherwise. Probabilities (P) values ≤ 0.05 were considered significant, whereas $P > 0.05$ but ≤ 0.10 were considered trends approaching significance.

4.4 Results

4.4.1 In vitro whole-tissue explants culture of endometrium and visceral peritoneum

Fig 4.2 illustrates varying degrees of attachment between endometrium and visceral peritoneum (broad ligament in dogs and pig, omentum in sheep) based on the scoring system (Table 4.1) and health scores of tissues (classification based on Table 4.2). Changes in degree of attachment, presence of mesothelial cells on visceral peritoneum and health scores for endometrium and smooth muscle fibres of visceral peritoneum after in vitro culture for 24 to72 h are depicted for dogs, pig and sheep in Fig 4.3. Proportions of successful endometrial and fat attachments to the visceral peritoneum and tissue scores are presented in Table 4.4 and 4.5, respectively.

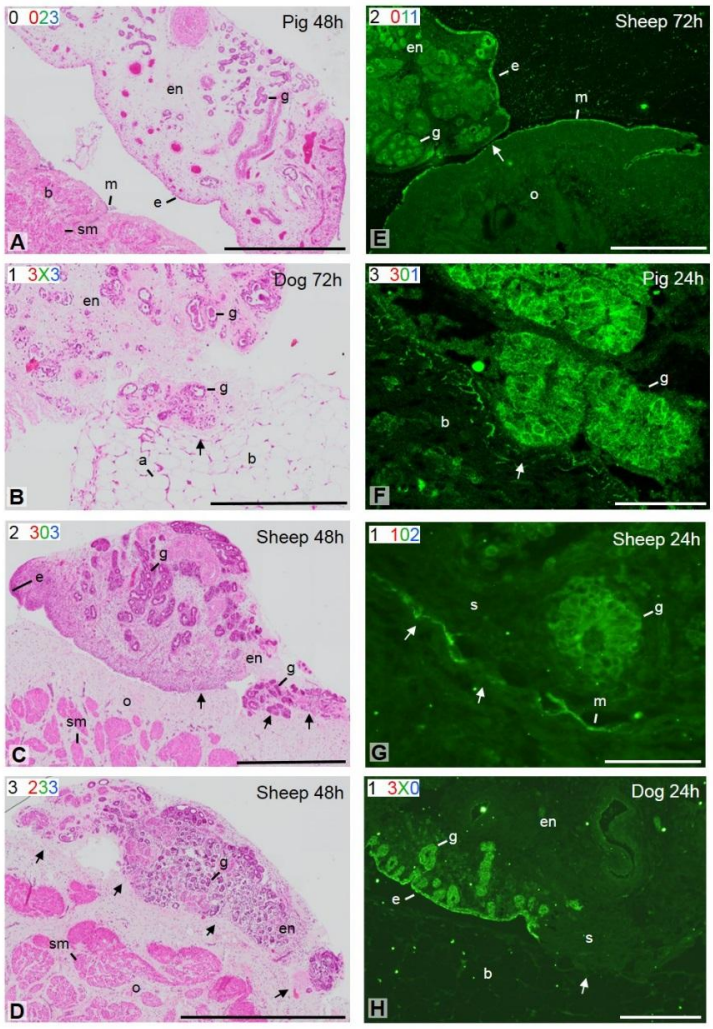

Figure 4.2 Degree of attachment between endometrial components (epithelium, glands and stromal cells) and visceral peritoneum after whole-tissue explant culture for 24 to 72 h. Species and incubation time are indicated at the upper right corner of each figure. Numbers (left to right) in the white boxes (upper left corner of each figure) indicate the scores for degree of attachment (black number; based on Table 4.1), presence of mesothelial cells (red), health of smooth muscles in peritoneum (green) and health of endometrium (blue; based on Table 4.2). All scores were from 0 to 3; X indicates that the given tissue for scoring was not present in the section. Scoring for Figs. E to H are based on adjacent sections stained with H & E. Left column (Fig. A-D) is arranged to show progressively increasing degree of attachment (H&E staining and bright-filed microscopy). Right column (Fig.E-H) distinguishes epithelial cells (green fluorescence; surface epithelium of uterus, endometrial glands, mesothelium) from connective tissue components of endometrium (stromal cells) and peritoneum (pancytokeratin immunohistochemistry and confocal microscopy). Endometrial epithelial (Fig. E), glandular (Fig. F) and stromal cells (Fig. G and H) are capable of attaching to peritoneum with (Fig E and G) or without (Fig. F and H) an intact layer of mesothelial cells. Contact points between endometrium and peritoneum are indicated by arrows.; a, adipocytes; b, broad ligament; e, surface epithelium of uterus; en, endometrium; g, endometrial glands; m, mesothelium; o, ometum; s, stromal cells; sm, smooth muscle fibers. Scale bars: A-D = 500µm, E=300 µm, F,G= 50 µm, H= 200 µm.

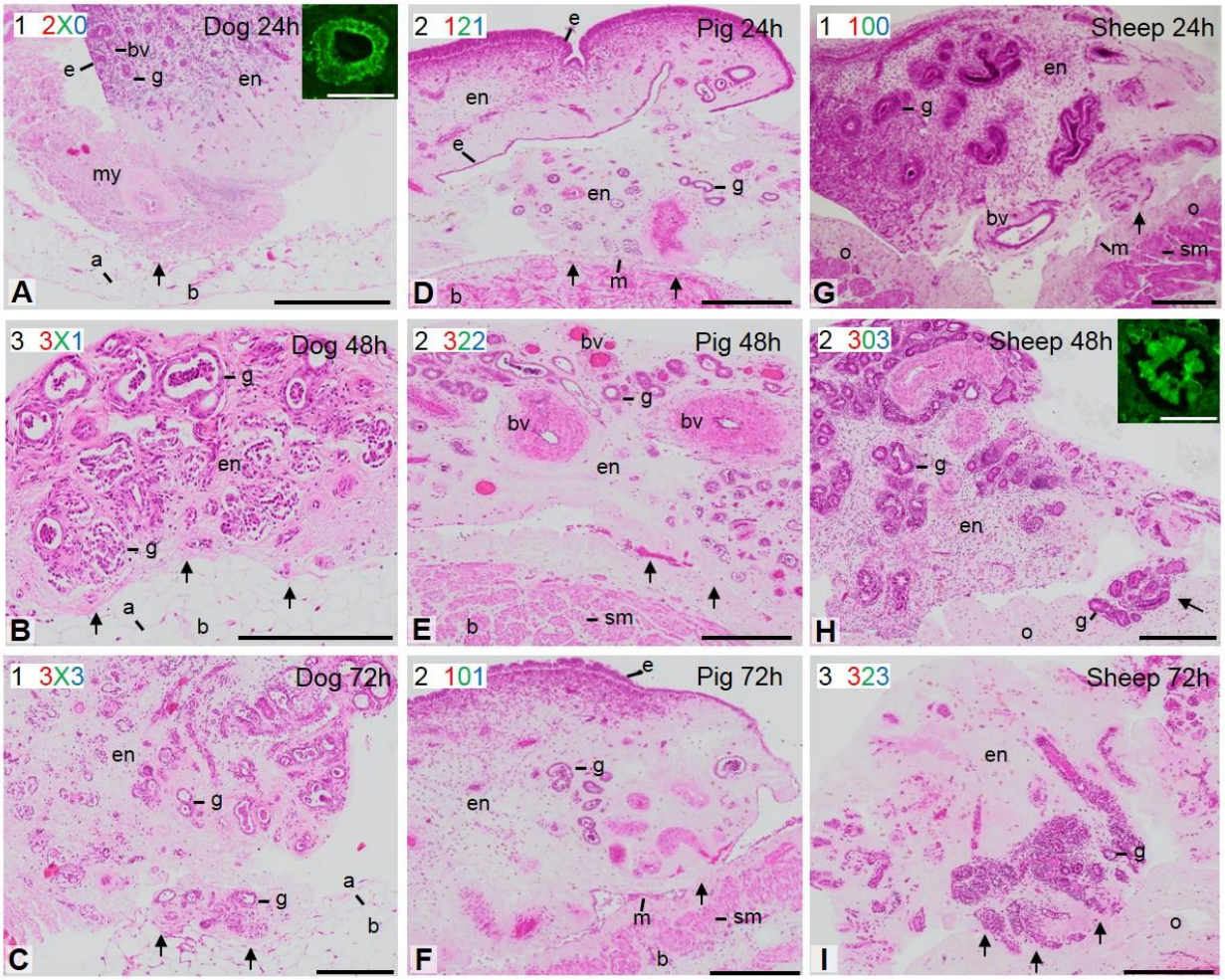

Figure 4.3 Attachment between endometrium and visceral peritoneum (omentum in sheep, broad ligament in dogs and pig) after whole-tissue explant culture for 24 to 72 h in dogs (Fig. A-C), pig (Fig. D-F) and sheep (Fig. G-I). Numbers (left to right) in the white boxes (upper left corner of each figure) indicate the scores for degree of attachment (black number; based on Table 4.1), presence of mesothelial cells (red), health of smooth muscles in peritoneum (green) and health of endometrium (blue; based on Table 4.2). All scores were from 0 to 3; X indicates that the given tissue for scoring was not present in the section (H&E staining and bright-filed microscopy). Endometrium and smooth muscle fibres of peritoneum remained healthy until 24 hours of culture (Fig A and G), but began to show degenerative changes by 48 (Fig E and H) and 72 (Fig C and I) hours. Insets show endometrial gland with intact epithelial cells attached to basement membrane (Inset A) and endometrial gland with epithelial cells detached from basement membrane (Inset H) using Pancytokeratin immunohistochemistry and confocal microscopy. Contact points between endometrium and peritoneum are indicated by arrows; a, adipocytes; b, broad ligament; bv, blood vessel; e, surface epithelium of uterus; en, endometrium; g, endometrial glands; m, mesothelium; my, myometrium of uterus; o, ometum; sm, smooth muscle fibers. Scale bar: A-I = 250µm, Inset A and H= 50 µm.

4.4.1.1 Nature and degree of attachment between endometrium/fat and visceral peritoneum

Attachments between tissues (endometrium/fat) and visceral peritoneum were successful in more than half of the tissue samples except at 72 h in dogs and pig (Table 4.4). The proportion of successful samples with endometrium to visceral peritoneum attachment in dogs, pig and sheep at three time points (24, 48 and 72h) did not differ ($p > 0.05$, Chi-square test) except between 24h and 72h in pig ($p=0.008$, Fisher's Exact test). When data were combined among species, the proportion of successful endometrial samples with attachments were greater at 24h compared to 72h (15/18 vs. 7/18, $p=0.008$) with intermediate attachment at 48h (12/15). Disregarding time points, 64% of the successful endometrial samples in dogs (7/11) had an attachment score of 1 (<30% contact) vs. 40% in pig (4/10) and 23% sheep (3/13). The proportion of endometrial samples with an attachment score of 2 or 3 had a tendency to be higher in sheep (10/13) compared with combined data from dogs and pig (9/21, $p=0.06$ Fisher's Exact test). Combined over time points and species, the proportion of successful attachments to the visceral peritoneum did not differ between endometrium versus fat (34/54 vs. 20/27; $p=0.23$, Chi-square test).

All endometrial components, i.e., surface epithelium (Fig 4.2E), glands (Fig 4.2F) and stromal cells (Fig 4.2G) were capable of attaching to serosal surfaces of visceral peritoneum. Due to shorter culture times, attachments were simple adhesions.

4.4.1.2 Health score of tissues during culture period

Prior to culture, the endometrium of all dogs and pigs were healthy (score 0; Table 4.5) whereas endometrium from two sheep (2/3) received a score of 1. Likewise, the smooth muscle fibers (of broad ligament in pig and omentum in sheep) prior to culture were healthy (score of 0). Smooth muscle fibers were not observed in broad ligament samples of dogs (except in two samples of fat attachment), hence were not scored. During the culture period, majority of endometrial pieces and smooth muscle fibres of visceral peritoneum in all species remained healthy (score 0 and 1) at 24h but began to undergo degenerative changes (score 2 and 3) by 48h and 72h (Table 4.5).

Table 4.4 Proportion of samples with successful attachments at 24, 48 and 72 h of in vitro whole-tissue explant culture between endometrium/fat and visceral peritonuem in dogs, pig and sheep {n=3 animals per species; two samples (endometrium) and one sample (fat) from each animal for each time point were incubated}.

Species/ Type of tissue	Endometrium			Fat		
	Time point			Time point		
	24h	48h	72h	24h	48h	72h
Dogs	5/6	4/6	2/6	2/3	2/3	0/3
Pig	6/6	3/6	1/6	3/3	3/3	1/3
Sheep	4/6	5/6	4/6	3/3	3/3	3/3

Table 4.5 Scores for degree of attachment and health of tissue (based on Table 4.1 and 4.2, respectively) at 24, 48 and 72 h of in vitro whole-tissue explant culture between endometrium/fat and visceral peritoneum (broad ligament in dogs and pig, omentum in sheep); Red: first animal, Blue: second animal, Green: third animal in each species). All scores were 0 to 3, 'X' indicates that the given tissue component was not present in section for scoring and '–' indicates the given sample remained unattached. The value within the parentheses (black number) is the median score for a given time point.

Time point/ Tissue	Degree of attachment	Mesothelial cells of visceral peritoneum	Endometrium	Smooth muscle fibers of visceral peritoneum
Attachment of endometrium and visceral peritoneum				
Dogs				
0h	X	220 (2)	000 (0)	X
24h	11312- (1)	32332- (3)	00003- (0)	X
48h	-1321- (1.5)	-3333- (3)	-1122- (1.5)	X
72h	-11--- (1)	-33--- (3)	-13--- (2)	X
Pig				
0h	X	312 (2)	000 (0)	000 (0)
24h	321112 (1.5)	313321 (2.5)	112211 (1)	001022 (0.5)
48h	-02-1- (1)	-03-2- (2)	-32-0- (2)	-22-1- (2)
72h	----2- (2)	----1- (1)	----1- (1)	----0- (0)
Sheep				
0h	X	321 (2)	011 (1)	000 (0)
24h	122-3- (2)	113-2- (1.5)	011-3- (1)	00-1- (0)
48h	-11232 (2)	-03323 (3)	-12333 (3)	-01033 (1)
72h	-23-22 (2)	-03-02 (1)	-13-33 (3)	-12-11 (1)
Attachment of fat and visceral peritoneum				
Dogs				
24h	-33 (3)	-03 (1.5)	X	- X 0 (0)
48h	33- (3)	20- (1)	X	0 X – (0)
72h	---	---	X	---
Pig				
24h	233 (3)	022 (2)	X	221 (2)
48h	332 (3)	223 (2)	X	122 (2)
72h	--2 (2)	--2 (2)	X	--2 (2)

Sheep				
24h	223 (2)	323 (3)	X	001 (0)
48h	133 (3)	103 (1)	X	301 (1)
72h	222 (2)	233 (3)	X	312 (2)

4.4.1.3 Presence or absence of mesothelial cells on visceral peritoneum

Confocal microscopy was used to identify mesothelial cells on peritoneum by immunofloursecence with pancytokeratin antibody. Prior to culture, samples of visceral peritoneum {broad ligament in dog (3/3), pig (2/3) and omentum in sheep (2/3)} had identifiable mesothelial cells lining it. Mesothelial cells were not detectable lining the broad ligament of dogs (score 3) (Fig 4.2H) in 9/11 of samples at different time points of culture. In pig and sheep, mesothelial cells were detectable upto 72h (Fig 4.2E) of culture (score of 0 to 2, 6/10 and 8/13, respectively). None of the samples of broad ligament in dogs had mesothelial cells at the site of attachment with endometrium (score 0 and 1) whereas approximately 40% of samples of visceral peritoneum in pig (4/10) and sheep (5/13), had mesothelial cells at the site of attachment between endometrium and omentum/broad ligament. Majority of samples (13/20; data combined among species and time points) had mesothelial cells between fat and visceral peritoneal attachment.

4.4.2 Surgical induction of endometriosis by autologous tissue grafting

4.4.2.1 Proportions of successful transplants and adhesions

Single or multiple fluid filled structures were observed at euthanasia. Structures ≥ 1cm were defined as cysts and those less than 1 cm were defined as vesicles. Majority (19/20) of endometrial tissue grafts in dogs developed into endometriotic lesions with single or multiple cysts (Figs 4.4 B,D); remaining one graft on the bladder developed into a solid lesion. Endometrial grafts in pigs developed into solid (8/16) or cystic lesions (7/16; Figs 4.4F,H) with no lesion from one graft. In sheep, the lesions included solid lesions (5/20), small vesicles (5/20), cysts (5/20) (Figs 4.4J,L) and absence of lesions (5/20). The proportion of cystic lesions was greater ($p<0.01$) in dogs (19/20) than in pig (8/16) and sheep (5/20). The proportion of successful transplantations and those with cystic lesions did not differ ($p > 0.05$) between

the left (non-epithelial side touching peritoneum) and the right (epithelial side touching peritoneum) sides of surgeries in dogs (10/10 vs 10/10 and 9/19 vs. 10/19 respectively), pig (7/8 vs 8/8 and 3/7 vs. 4/7) or sheep (7/10 vs 8/10 and 2/5 vs. 3/5). There was no difference ($p>0.05$) in proportions of successful tissue grafts on serosal surface of visceral vs. parietal peritoneum in dogs (10/10 vs. 10/10), pig (7/8 vs. 8/8) or sheep (7/10 vs. 8/10). Fat tissue grafts in treatment and control group dogs (8/20 and 6/20, respectively) and sheep (9/20 and 9/20) were seen as remnants or were completely undetectable (Figs 4.4 B,D,J,L) whereas some fat grafts in pig were well preserved (11/16 in treatment group and 7/12 in control group) while remaining were undetectable (Figs 4.4 F,H).

Adhesions were considered as present if grossly visible at the time of euthanasia or if grafted tissue/lesion localization at euthanasia required the use of scissors or scalpel blade. Adhesions between abdominal wall grafts and mesentery were observed in all treatment group dogs (5/5) but only in one control group (1/5) dog ($p=0.04$). One of the treatment dogs had adhesions between right endometrial graft on urinary bladder and cervix (1/5). Equal number of treatment (2/4) and control group (2/3) pigs developed adhesions between intestinal (mostly jejunum) mesentery and incision site and one (1/4) had adhesions between broad ligament of uterus and urinary bladder. All sheep in treatment group (5/5) had varying degrees of adhesion between uterus, uterine or abdominal grafts and mesentery of intestine whereas two of five sheep in control group developed adhesion between abdominal grafts and mesentery ($p=0.16$). Combined among grafting sites (visceral and parietal peritoneum) and species, a greater proportion ($p=0.015$) of surgical sites had adhesions in treatment group (12/14) versus control group (5/13). Combined among species and treatment groups, proportion of surgical sites with adhesions was greater ($p<0.01$) for parietal (12/19) compared to visceral (7/19) peritoneum.

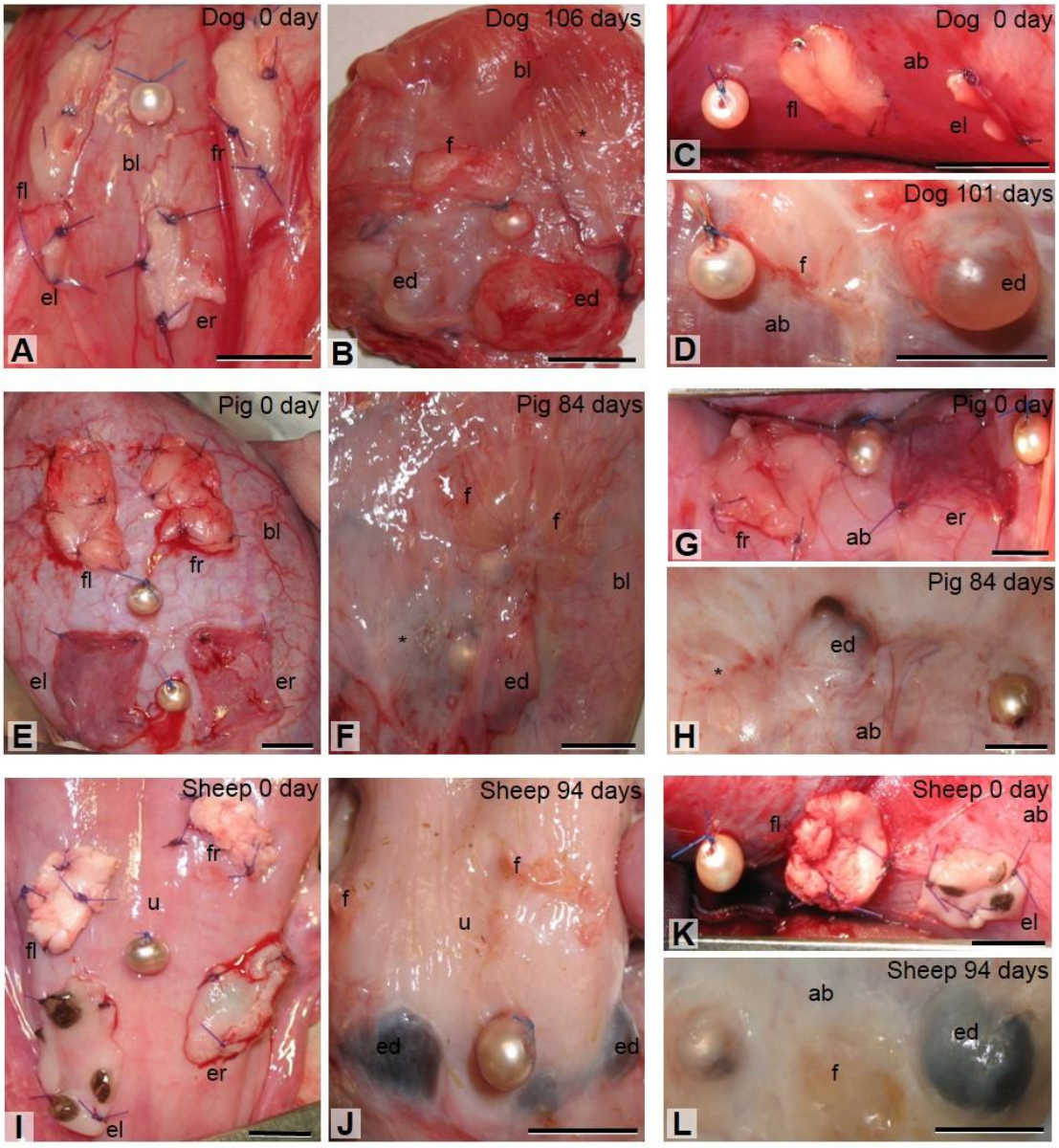

Figure 4.4. Endometrial and fat grafts at the time of surgical transplantation (Fig. A, C, E, G, I, K) and lesions post surgery (Fig. B, D, F, H, J, L; at the time of euthanasia) in dogs (Fig. A-D), pig (Fig. E-H) and sheep (Fig. I-L) on the serosal surface of visceral peritoneum (dorsal wall of urinary bladder in Fig. A, B, E, F and dorsal wall of uterus in Fig. I, J) and parietal peritoneum (dorsal surface of abdominal wall in Fig. C, D, G, H, K, L). Species and days post-surgery are indicated at the upper right corner of each figure. Plastic jewelry beads were sutured as markers. A variety of lesions including endometriotic cysts {Fig B, D, F (right), H, J, L}, vesicles, solid lesions and absence of lesions {Fig. F (left)} was noticed. Fat was either seen as remnants {Fig. B (left), D, F, J, L} or absence of lesion {Fig. B (right), H} Scale bar = 1 cm; ab, abdomen; bl, urinary bladder; ed, endometriotic cyst; el, left endometrial graft; er, right endometrial graft; f, remnants of fat; fl, left fat graft; fr, right fat graft; u, uterus; * absence of lesion

4.4.2.2 Comparison of size of transplanted grafts at surgery versus endometriotic lesions at euthanasia

The area of grafted tissues (length x width) at the time of surgery and endometriotic lesions at the time of euthanasia are listed in Table 4.6. There was no difference ($p > 0.05$; t-test) between size of left and right grafts/lesions on bladder/uterus and abdomen in dogs, pig and sheep either at the time of surgery or at 3 months after surgery; therefore, data from the left and right grafts/lesions were combined to obtain mean sizes.

In dogs, endometriotic lesions on serosal surface of the urinary bladder were more than double the size compared to endometrial grafts transplanted at surgery ($p=0.005$; paired t-test). Cystic lesions on abdominal wall followed a similar pattern (i.e. became larger) although not statistically significant different than at the time of surgery ($p=0.21$). Overall (combined between urinary bladder and abdominal grafts), the size of endometriotic lesions at 3 months post-surgery was larger (0.89 ± 0.11 cm^2) compared to endometrial grafts at the time of surgery (0.50 ± 0.09 cm^2) in dogs. Fat grafts were either seen as remnants or were not detectable and shrank in size ($p<0.05$) in both treatment and control group dogs. In pig and sheep, the size of endometrial lesions decreased by half or more ($p<0.05$) by 3-months post-surgery. Fat grafts in treatment and control group also decreased in size ($p<0.05$) in both pig and sheep.

Table 4.6. Comparison between size (cm^2; mean ± S.E.M.) of endometrial and fat grafts transplanted on visceral and parietal peritoneum at the time of surgery (S) and 3 months post-surgery (PS; at euthanasia) in the treatment group. Data were analyzed by paired T-tests between "S" and "PS" columns (*$p < 0.05$, **$p < 0.01$). Control group animals had only fat grafts (last 4 columns).

	Treatment group								**Control group**			
Species	**Endometrial grafts (cm^2) on**				**Fat grafts (cm^2)**				**Mean size of fat grafts (cm^2)**			
	visceral peritoneum		**parietal peritoneum**		**visceral peritoneum**		**parietal peritoneum**		**visceral peritoneum**		**parietal peritoneum**	
	S	**PS**	**S**	**PS**	**S**	**PS**	**S**	**PS**	**S**	**PS**	**S**	**PS**
Dogs	0.46 ± 0.08	1.09 ± 0.18**	0.54 ± 0.17	0.70 ± 0.12	0.64 ± 0.19	0.09 ± 0.06**	0.60 ± 0.12	0.31 ± 0.09*	1.25 ± 0.19	0.35 ± 0.15**	1.02 ± 0.18	0.04 ± 0.04*
Pig	1.45 ± 0.08	0.42 ± 0.11**	1.52 ± 0.19	0.64 ± 0.14**	1.50 ± 0.12	0.76 ± 0.17**	1.63 ± 0.12	0.28 ± 0.12**	2.17 ± 0.48	1.42 ± 0.11*	2.00 ± 0.25	0.25 ± 0.35**
Sheep	1.53 ± 0.15	0.29 ± 0.08**	1.11 ± 0.08	0.45 ± 0.11**	1.37 ± 0.09	0.41 ± 0.17**	1.13 ± 0.12	0.15 ± 0.08**	1.93 ± 0.23	0.33 ± 0.09**	0.93 ± 0.04	0.06 ± 0.04**

4.4.2.3 Histological characterization of endometriotic lesions

Histological characteristics of lesions in different species are illustrated in Figs 4.5, 4.6 and 4.7.

In dogs, irrespective of stage of estrous cycle at the time of surgery and site of transplantation (bladder versus abdomen), endometriotic lesions contained single or multiple cysts of varying sizes (Figs 4.5 A,B) with clear-serous, serosanguinous or sanguineous fluid. The wall of the cyst was composed of lining epithelium, endometrial glands, smooth muscles and stromal tissue (Figs 4.5 C,D) surrounded by the mesothelial cells (facing the peritoneal cavity).The lining epithelium of cysts varied from simple squamous-cuboidal to low/high cuboidal (Fig 4.5 E), cuboidal-columnar or columnar epithelium (Fig 4.5G). Apical surface of cuboidal/columnar cells was lined by varying number of short microvilli (Fig 4.5C inset). There were papillary projections into the lumen and infoldings of the lining epithelium (Fig 4.5F) in some cysts. Intraepithelial glands (Figs 4.5G) were seen in the lining epithelium as well. Cytoplasmic changes like stratified squamous metaplasia with keratinization (Fig 4.6A) and ciliated epithelium were observed in the lining epithelium of few cysts. Cyst luminal contents consisted of white blood cells (WBC; neutrophils, lymphocytes and macrophages), red blood cells (RBC), sloughed epithelial cells and secretions. There was considerable vascularization to the cyst in the form of numerous capillaries intimately surrounding the lining epithelium (Fig 4.5E). Normal, dilated (Fig 4.6B) and cystic (Fig 4.6C) endometrial glands were seen in the wall of the cysts. Some dilated and cystic glands had similar contents as that of luminal contents whereas others had secretory products. Varying amount of smooth muscle fibers surrounded the cysts through which endometrial glands were seen invading (Fig 4.5E), both in parietal and visceral peritoneal grafts. Smooth muscles fibers were either organized in a layer or were scattered in the wall. Stromal bleeding was evident with numerous hemosiderin-laden macrophages (Fig 4.6D). Numerous pseudoxanthoma cells (Fig 4.6E) having autofluorescence (Fig 4.6F) were seen surrounding the cyst wall of abdominal endometrial graft in one dog.

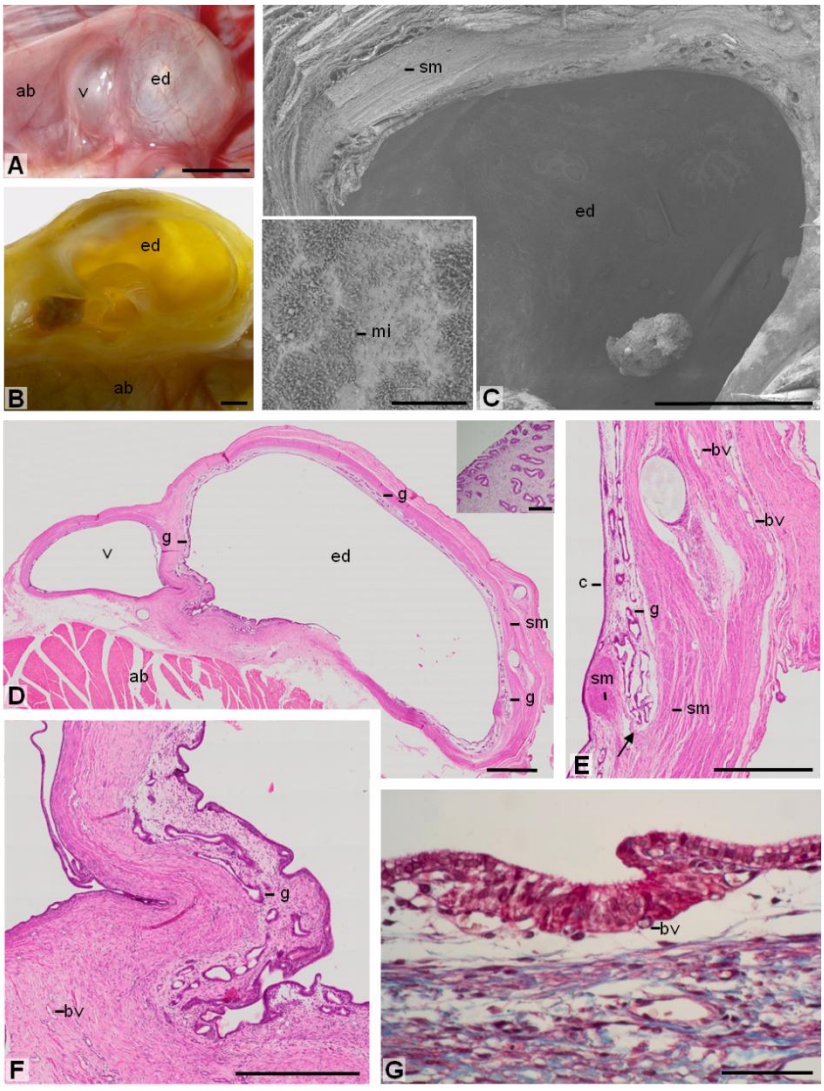

Figure 4.5 Histopathological features of endometriotic cyst in a dog. Right endometrial graft developed into multiple endometriotic cysts 105 days post –surgery at the time of euthanasia (Fig.A, external appearance in fresh lesion; Fig.B, cross section through the cysts after tissue fixation, transmitted light). Scanning electron microscopy of the cyst cavity (Fig.C) show smooth surface of the cyst lined with cells having short microvilli and hexagonal borders (inset). There is also a projection into the cavity (Fig.C). Histological section of the lesion (Fig.D) shows an endometriotic cyst and vesicle on the abdomen surrounded by endometrial glands. Inset shows number of glands present at surgery in endometrium. Note that a considerable number of glands surround the cyst at euthanasia. Low cuboidal epithelium (Fig. E, F, G) with occasional intraepithelial glands (Fig.G) was seen lining the cysts with endometrial stromal and glandular cells surrounding the cyst (Fig.E, F). A well-defined layer of smooth muscle was seen surrounding the cyst (Fig.E). Note invasion of endometrial glands (arrow) through smooth muscle (Fig.E). Cyst had infoldings and projections within the cyst wall (Figs. D, F) and was vascularized with capillaries closely associated with epithelium (Fig. G). Fig. D-F, H&E staining and bright-filed microscopy), Fig. G Masson's trichrome staining (epithelium and cells, red; collagen fibres, blue). ab, abdomen; bv, blood vessel; ed, endometriotic cyst; c, cuboidal epithelium; g, endometrial glands; mi, microvilli; sm, smooth muscle fibres; v, vesicle. Scale bars: Fig. A= 1 cm, Fig. B,C,D=1 mm, Inset in Fig. C=5 µm, Inset in Fig.D=200 µm, Fig. E,F= 500 µm, Fig. G= 50 µm.

Stage of estrous cycle brought about normal physiological changes in endometrium of uterus that were seen on histology. Similar physiological changes were also seen in endometriotic cysts including secretory changes in endometrial glands and lining epithelium of cysts with respect to high progesterone during diestrous, increased vascularity during proestrous-estrous etc.

In 1 of the 5 treatment group dogs, endometriotic cyst had epithelial, papillary (vascular) projections (Fig 4.6G) from the cyst wall. These papillae had a hyalinized papillary core (Figs 4.6H,I) surrounded by a single layer of high cuboidal epithelial cells (Figs 4.6H,I) with foamy/bubbly cytoplasm (Fig 4.6J), irregularly shaped nucleus with nuclear atypia (prominent nucleoli, irregularly shaped nucleus) (Fig 4.6K). Some of these epithelial cells were also seen as groups scattered within the lumen of the cyst (Fig 4.6J). PAS with digestion cleared out glycogen from the cytoplasm of epithelial cells lining papillae and some areas of lining epithelium of cyst (Fig 4.6L). However, some areas of epithelium lining the cyst wall (Fig 4.6M) and some of the secretory products within endometrial glands contained mucin (Figs 4.6N,O) (i.e., not cleared with PAS digestion). Atypical hyperplasia (enlarged, rounded, irregularly shaped nuclei, prominent nucleoli) was also seen in endometrial glands (Fig 4.6O).

In pigs, cysts were lined by cuboidal-columnar epithelium with a few papillary projections (Fig 4.7A). Cyst luminal contents consisted of numerous RBC and few WBC. Stromal bleeding with hemosiderin-laden macrophages and hemorrhage was observed. Normal (Fig 4.7C), dilated and cystic endometrial glands (Fig 4.7D) were seen but they were few in number (Fig 4.7B) compared to dogs. Hyperplasia without atypia was observed in few glands. Degeneration of endometrial glands and lining epithelium was also seen. Fibrosis of the incision site with osseous metaplasia (Fig 4.7B inset) was common in areas where abdominal grafts were transplanted.

In sheep, cysts (Figs 4.7E,F) were lined by simple cuboidal-columnar epithelium. Cyst luminal contents consisted of pink eosinophillic secretion (Fig 4.7G), numerous RBC and few WBC.

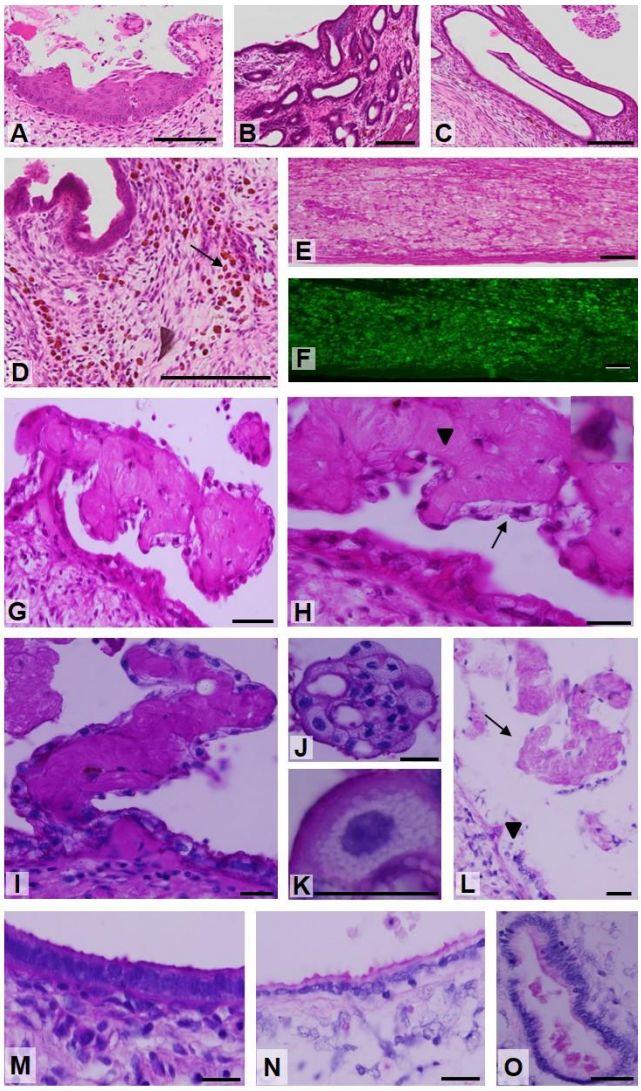

Figure 4.6 Histomorphological characterization and identification of cytoplasmic and neoplastic changes in endometriotic cyst of a dog. Squamous metaplasia with keratinization of epithelial lining of cyst in one dog (Fig. A); normal, dilated (Fig.B) and cystic glands (Fig.C) in the wall of cysts; evidence of stromal bleeding (Fig.D) with numerous hemosiderin-laden macrophages (arrow); pseudoxanthoma cells (Fig.E) that were autofluorescing (Fig.F); and papillary projections (Fig,G) from the wall of a cyst lined by simple cuboidal epithelial cells (Fig.H) with abundant bubbly/foamy cytoplasm (arrow), irregularly shaped nucleus with nuclear atypia (two prominent nucleoli; inset) and hyalinized papillary core (arrowhead). PAS staining showing papillary projection (Fig.I) and clusters of sloughed off epithelial cells in the lumen of a cyst (Fig.J) with bubbly/foamy cytoplasm and nuclear atypia with prominent nuclei (Fig.K). PAS with diastase digestion cleared out glycogen from the cytoplasm of epithelial cells lining papillae (arrow) and the some parts of lining epithelium (arrow head) of cyst (Fig.L); other parts of lining epithelium of cyst wall did not get cleared following digestion (Fig.M without digestion, N with digestion) indicating presence of mucin. Epithelial cells of some endometrial glands also stained for mucin and contained mucinous secretory products within the lumen (Fig.O). Fig A-H H&E staining, Fig. I-K, M PAS staining; Fig L, N,O PAS staining after diastase digestion; scale bars: Fig A-F=100 µm, G= 50 µm, H-O= 20 µm.

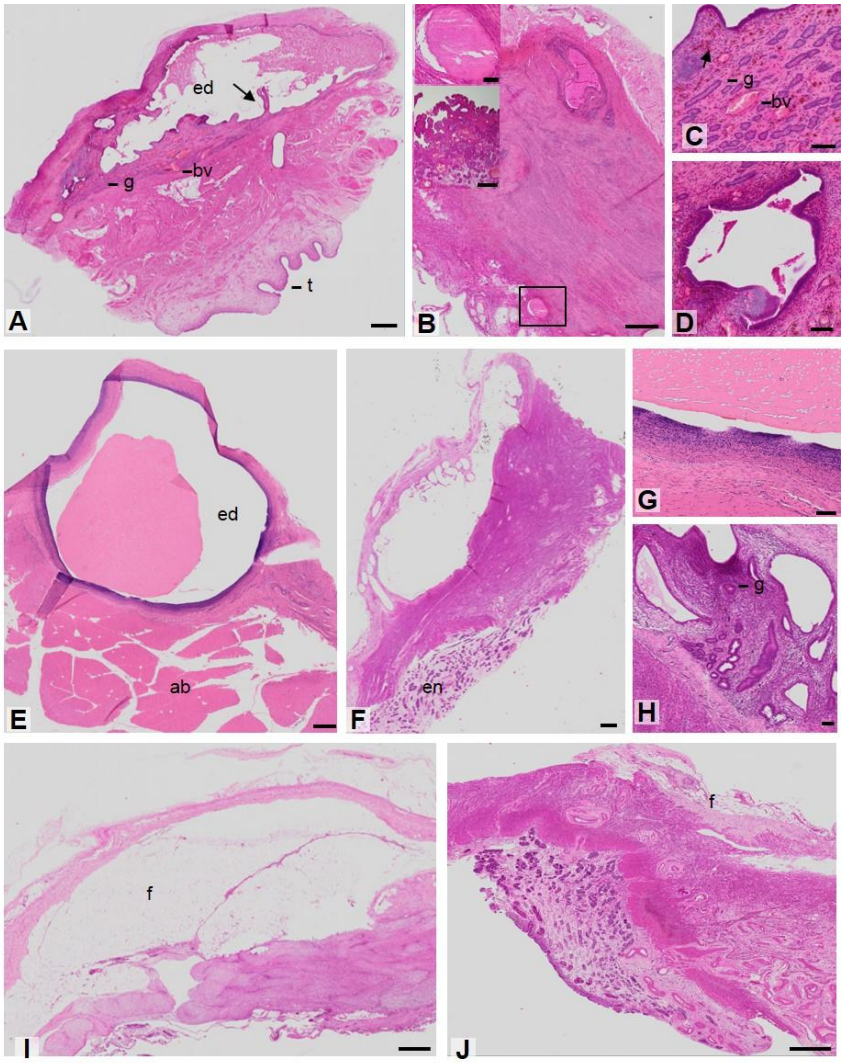

Figure 4.7 Histopathology of endometriotic lesions/cysts in pig and sheep. Cyst on the urinary bladder in pig lined by cuboidal epithelium, surrounded by glands and blood vessels, filled with blood and papillary projections (arrow) protruding into the lumen of the cyst (Fig.A), Blood filled dilated gland surrounded by normal glands. First inset (area indicated by square) shows osseous metaplasia. Second inset shows number of glands present in endometrium at surgery. Note that there is considerable reduction in number of glands in lesions at euthanasia (Fig.B), Normal glands interspersed with numerous blood vessels (Fig.C; arrow indicates hemosiderin-laden macrophages) and cystic glands (Fig.D) were seen in the cyst wall of pigs, Endometriotic cyst on parietal peritoneum in sheep with no glands in cyst wall (Fig.E), Cyst on the serosal surface of uterus in sheep with absence of glands. Note the number of glands in endometrium (en) of uterus seen below compared to no glands in lesion (Fig.F), Pink eosinophillic secretion within lumen of cyst (Fig.G), Normal, dilated and cystic glands seen in very few endometriotic lesions in sheep. Notice pink secretory products within lumen of cystic gland on the extreme left (Fig.H), well preserved (Fig.I) and remnants of fat (Fig.J) in pig and sheep respectively of the control group. ab, abdomen; bv, blood vessel; ed, endometriotic cyst; en, endoemtrium; f, remnants of fat; g, endometrial glands; t, transitional epithelium of urinary bladder Scale bars: Fig. A,B,E,F,I,J= 0.5 mm, Fig. C,D,G,H and 1st inset in B= 0.05 mm, 2nd inset in B= 0.2 mm.

No papillary projections were observed. Very few endometrial glands (Fig 4.7H) were observed with some lesions having no glands. Dilated glands if present were lined by cuboidal epithelium with few RBC and WBC. Hemosiderin-laden macrophages, hemorrhage and melanin (melanocytes are normally present in sheep caruncular areas) was observed. Degeneration of cyst lining epithelium was also seen.

In the control group of dog, pig (Fig 4.7I) and sheep (Fig 4.7J), areas of fat grafts consisted of normal adipocytes with no tissue changes.

4.4.2.4 Concentration of plasma estrogen and progesterone

Stage of estrus cycle was not known for sheep and pig at the time of surgery, therefore, weekly concentrations of estrogen and progesterone were not used to calculate mean concentrations; values for individual animals are illustrated in Fig 4.8. Based on stage of estrus cycle (proestrus, diestrus, anestrus) plasma levels of estrogen and progesterone for dogs were compared between treatment and control groups. There was an interaction between week and group for plasma estrogen concentration (Fig 4.9) in proestrus dogs. Treatment group dogs in proestrus at the time of surgery had higher plasma estrogen concentrations at week 0 followed by lower concentrations at week 6 and 9 compared to dogs in control group (group*week interaction, $p=0.02$); there was no difference in plasma progesterone concentration among groups ($p=0.24$). For dogs in anestrus at the time of surgery, there was no difference between plasma concentrations of estrogen ($p=0.81$) and progesterone ($p=0.66$) between treatment and control group.

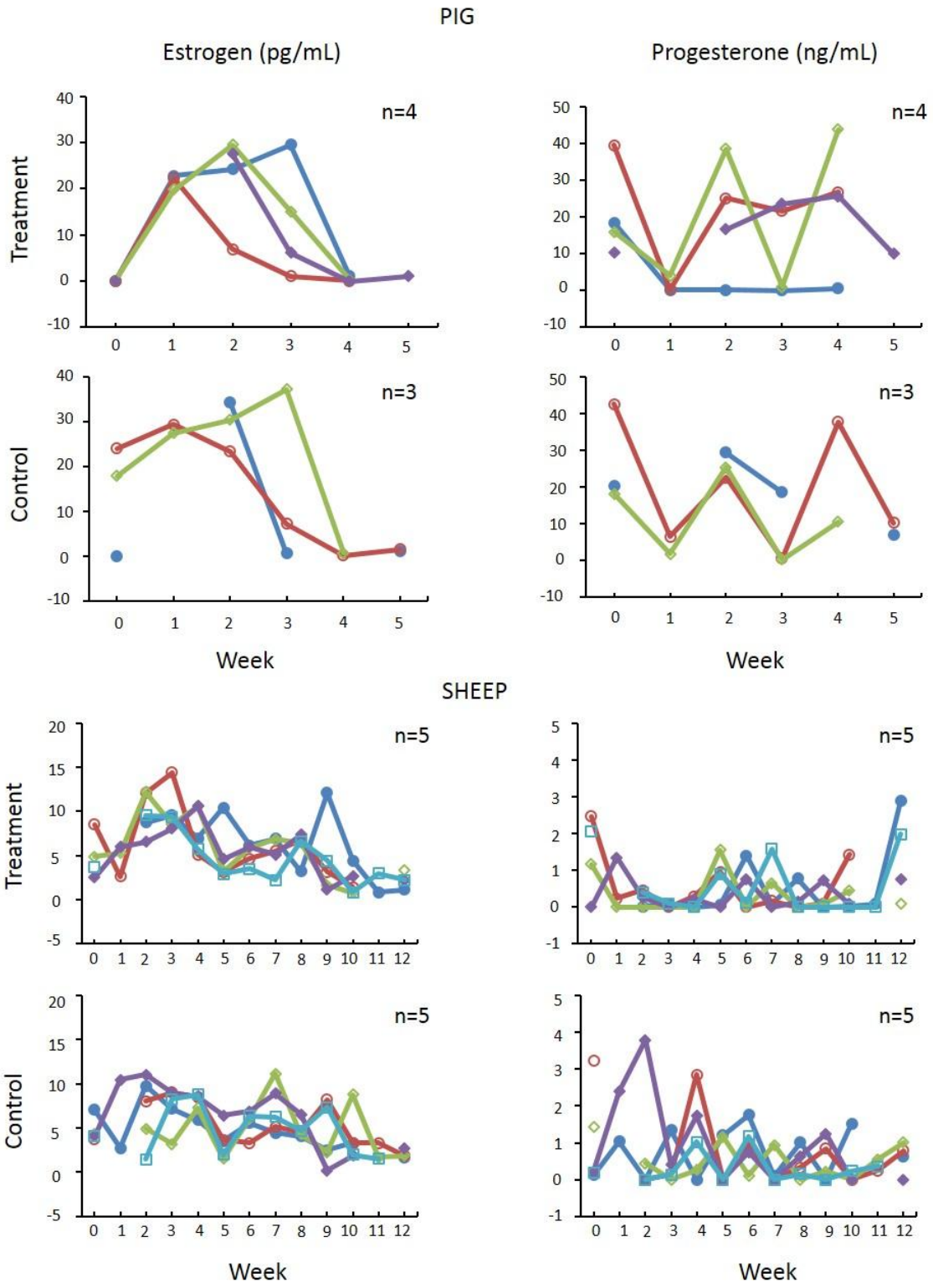

Figure 4.8 shows plasma concentrations of estrogen and progesterone in pig and sheep in treatment (n=4, n=5 respectively) and control (n=3, n=5 respectively) groups.

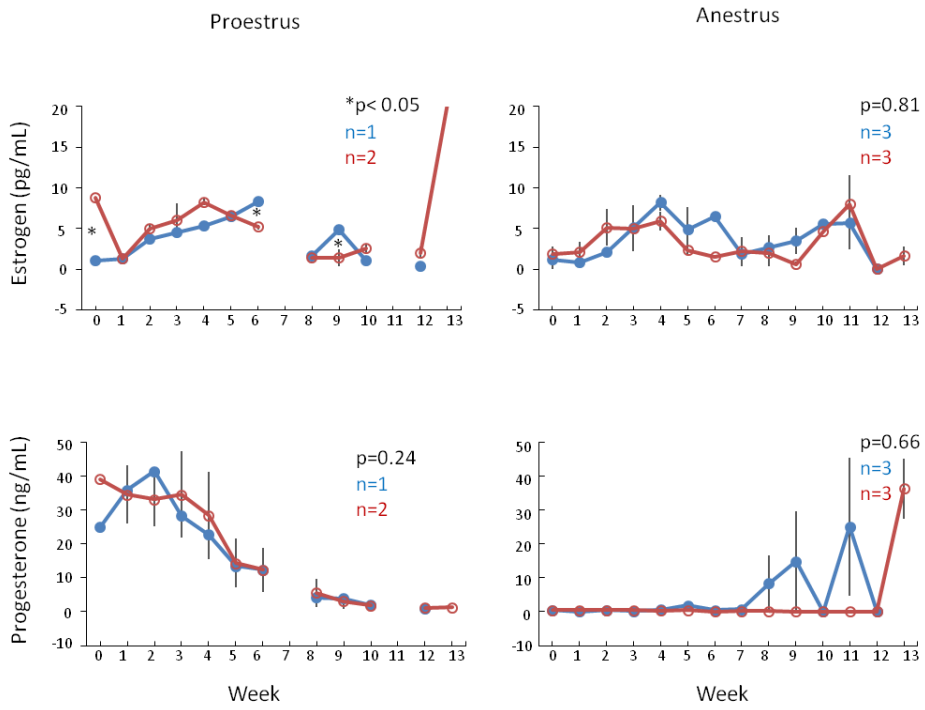

Figure 4.9 shows plasma concentrations of estrogen and progesterone in dogs based on stage of estrus cycle (proestrus and anestrus) in treatment (red) and control group (blue).

4.5 Discussion

Our objective was to develop a domestic animal model for endometriosis that is suitable for performing sequential and repeated examinations to assess the efficacy of diagnostic imaging procedures and treatments. In vitro whole-tissue explant culture and surgical induction of endometriosis were carried out in dogs, pig and sheep. Whole-tissue explant study documented that all endometrial components, i.e., surface epithelium, glands and stroma, are capable of attaching to peritoneum within 24 h of in vitro culture. A variety of outcomes (endometriotic cysts containing serosanguinous fluid, solid lesions, vesicles, absence of lesions) were noticed after surgical transplantation of endometrium to visceral and parietal peritoneum in dogs, sheep and pig. The proportion of cystic lesions was greater in dogs (19/20) than in pig (8/16) and sheep (5/20). Endometriotic lesions in dogs at euthanasia were larger than endometrial grafts at surgery while the size of lesions decreased by half in pig and sheep. Similar to those

found in women, the wall of endometriotic cysts in dogs was characterized by simple cuboidal/columnar epithelium, vascular papillary projections, and normal, dilated and/or cystic endometrial glands. Some cysts also showed evidence of stromal bleeding and contained hemosiderin-laden macrophages and/or pseudoxanthoma cells. Evidence of growing endometriotic cysts in dogs with histological characteristics similar to those described in ovarian endometriotic cysts in women (Czernobilsky and Fox 2003) led us to conclude that dogs is the most promising domestic animal model for testing imaging probes and therapy agents for the diagnosis and treatment of endometriosis in women.

During the whole-tissue explant in vitro culture of dog, pig and sheep endometrium with peritoneum, endometrial components were able to attach to peritoneum within 24 h of incubation. Comparable results were recorded in women after similar experimentation (Witz et al 1999; Witz et al 2001). In our study, endometrial components such as uterine surface epithelium, stromal and endometrial gland cells were capable of attaching to serosal surfaces with or without an intact layer of mesothelial cells in three animal species tested. It is interesting to note that when endometrium from normal women (i.e., without endometrioisis) were co-cultured in vitro, endometrial implants attached to an intact layer of mesothelium within 1 h (Witz et al 2001). In our study, although most attachments were via stromal cells, there were number of samples where glands were directly attached to peritoneum and this attachment could occur irrespective of the presence or absence of an intact mesothelial lining. It is noteworthy that there was lesser contact area between endometrium and peritoneum in odgs (<30%) compared to pig and sheep. Also, 40% of samples of cultured samples in pig and sheep had mesothelial cells at the site of attachment between endometrium and peritoneum compared to complete absence in dogs. This could indicate that mesothelial cells lining the serosal surfaces could play an important role in the initial attachment of endometrium. Human study (Witz et al 1999) suggested that early invasion of stromal cells into serosa was possible in less than 24h of culture. However, as expected, majority of the explanted samples in our study showed only simple attachment or adhesion of the tissue due to short duration of the culture system.

There was a similar degree of attachment between fat samples and visceral peritoneum (control cultures) in all three species when compared to endometrial-peritoneal interaction. Therefore, the innate ability of epithelial and stromal components of peritoneum to adhere to other tissues is equally important in both in vitro and in vivo conditions. Endometrium and smooth muscle fibres of peritoneum (omentum in sheep and broad ligament in pig) remained healthy prior to culture and until 24h into culture, but began to show degenerative changes by 48h. It is interesting to note that a greater proportion of endometrial samples attached at 24h compared to 72h. It is likely that changes after initial 24h of culture may result in loss of tissue health over the remaining culture period. Hence, it can be concluded that in-vitro culture of endometrium and peritonteum should preferably not exceed 48h.

The findings from the whole tissue explant in vitro culture provided promising and comparable results to human in vitro studies and paved the way for the in vivo trial wherein three domestic animal species (dogs, pig and sheep) were used to evaluate their suitability as a model for endometriosis. Lesions in dogs developed into endometriotic cysts whereas cysts and solid lesions were seen in pig and sheep. Development of similar endometriotic cysts and solid masses have been observed in laboratory animals like rat, rabbit after surgical grafting (Jacobson 1922; Schenken and Asch 1980; Vernon and Wilson 1985). In women, a lesion at ectopic sites is considered diagnostic of endometriosis when it has endometrial stromal and glandular components with (or evidence of) hemorrhage or hemosiderin-laden macrophages (Czernobilsky and Fox 2003). Dogs provided promising results with development of vascularized cysts surrounded by endometrial glands and stroma with hemorrhage and/or hemosiderin-laden macrohpages. Although cysts in pig and sheep contained the classical features of lesions seen in endometriosis, there were fewer or no glands (normal/dilated) in most lesions with evidence of epithelial and glandular degeneration compared to dogs.

In laboratory animals studies, either complete uterine wall (Vernon and Wilson 1985)} or endometrial layer (Schenken and Asch 1980) was used for transplantation. Our study design allowed direct comparison of ability of uterine surface epithelium versus endometrial gland/stromal components in

establishing the initial adhesion and further developing into lesions on serosal surface of visceral and parietal peritoneum. Majority of grafts in dogs developed into cysts regardless whether the epithelial or non-epithelial surface faced the serosal surface of peritoneum. Similar results were obtained in pig and sheep. From biological perspective, our results from both in vitro and animal experiments provide direct evidence of ability of both epithelial components (surface epithelium and glands) and stromal tissues to attach, adhere and re-vascularize at ectopic location within the body cavity.

Luminal content of cysts was filled with RBC and WBC which indicated an inflammatory response by the body. However, surrounding cells (stroma and glands) did not undergo cell death; appeared healthy and there was no major evidence of avtive ing=flammatory cell infirltration in the cyst walls. Similar hypothesis is proposed as one of the main reasons for development of endometriosis in women (Nap 2012). Cysts in dogs were encapsulated by thick wall (fibrous capsule with or without smooth muscle layer) which could have limited the escape of luminal contents leading to formation of huge cysts. In contrast, peritoneal lesions in women appear as red, black or white lesions based on the extent of vascularization and age of lesion, red being an initial vascularized lesion and white corresponding to an aged, devascularized lesion (Donnez et al 2012; (Nisolle and Donnez 1997). Conversely, ovarian endometriosis in women is usually characterized by endometriotic cysts lined by endometrial-type epithelium, with endometrial glands (inactive or proliferative type with or without hyperplasia). Cysts in dogs were similar to ovarian endometriotic cysts in women. Further development of the dogs model need to focus on devising an experimental procedure for inducing surface (flat) form of peritoneal endometriosis and to test responsiveness of endometriotic cysts to phases of reproductive cycle and to hormones such as estradiol and progesterone.

Furthermore, epithelial atypia such as squamous metaplasia, stratification and pleomorphic or hyperchromatic nuclei observed in the lining of ovarian endometriotic cysts in women are most often due to local inflammation but can also be neoplastic (Czernobilsky and Morris 1979). Similar epithelial atypia such as squamous differentiation and mucinous changes were observed in the epithelial lining of cysts in

dogs. Mucinous changes are usually associated with atypia, with columnar cells having basal nuclei and abundant pale supranuclear cytoplasm that conatins mucin (Mazur and Kurman 2005). Secondary changes occurring in lesions due to bleeding or fibrosis can transform areas of endometriosis into granulation tissue with numerous histiocytes also called pseudoxanthoma cells which contain ceroid (degradation products of blood) capable of autoflurescing (Clement et al 1988); Czernobilsky and Fox 2003). Similar pseudoxanthoma cells were found in the cyst wall of one dog. Movement of endometrial gland and/or stroma leaving the well-defined endometrium was observed in a few lesions which could indicate invasive capability of endometrial components. Further evaluations by euthanasia after a longer period of time (8-9 months) could help in assessing if cysts retain these characteristics or undergo secondary changes due to bleeding and fibrosis. Another intriguing finding was preliminary evidence of pathologic features resembling clear cell carcinoma (papillary pattern and clear cell type). Such carcinomas are frequently (58%) associated with endometriosis and endometriotic cysts in women (Montag et al 1989; Lee 2006). The cytoplasm of clear cells is usually described as clear or bubbly (Lee 2006) due to presence of glycogen (Sugiyama and Tsuda 2011). The clear cells in our study also had similar morphology and contained glycogen, not mucin. These findings also strengthen our model, however further work would be needed to assess pre-neoplastic potential of endometriotic cysts in dogs by possibly prolonging the duration of the study.

In conclusion, in vitro whole tissue explants culture documented that endometrial components (epithelium, stromal and glandular cells) of dog, pig and sheep are capable of attaching to serosal surfaces. Surgical transplantation of endometrium was successful in dogs, pig and sheep, however consistent development of endometriotic lesions was only observed in dogs. Development of a greater proportion of growing endometriotic cysts in dogs with classic combination of endometrial stroma, glands and evidence of hemorrhage and/or hemosiderin-laden macrophages within cysts compared to sheep and pig led us to conclude dogs as the most suitable domestic animal model for endometriosis among the three species tested. Dog model can be used for repeated and sequential medical imaging such as

ultrasonography, PET-CT, MRI for diagnostic and treatment trials and therefore have significant advantage over laboratory animal models.

CHAPTER 5: POTENTIAL OF A DOMESTIC ANIMAL MODEL OF ENDOMETRIOSIS FOR IMAGING

Emy.E.Varughese, Paul Babyn, Gregg.P.Adams, Pritpal Malhi, James Montgomery, Elisabeth Snead, Jaswant Singh

5.1 Abstract

Endometriosis is a reproductive disease affecting women in their prime reproductive years and is characterized by presence of endometrial glands and stroma in ectopic locations. There is no specific and sensitive non-invasive test and definitive diagnosis usually requires laparoscopic examinatiuon and histopathology. In a recent study to develop an animal model for endometriosis, we reported that all dogs developed cystic lesions after surgical transplantation of endometrium while results were variable in sheep. The objective of this study is to assess the usefulness and limitations of ultrasonography, magnetic resonance imaging (MRI) and positron emission tomography-computed tomography (PET-CT) in detecting cystic endometriotic lesions in dog and sheep. Surgical induction of endometriois was performed in dogs (n=5) and sheep (n=5) using autologous endometrial grafts (n=4 grafts per animal) and fat grafts sutured to visceral peritoneum (urinary bladder in dogs, uterus in sheep) and parietal peritoneum (ventral abdominal wall). Weekly ultrasonography was performed from Week 1-9 post-surgery and day of euthanasia (Week 14-15). T1 and T2 weighted weighted MRI images (n=2 each for dog and sheep) were obtained and PET-CT (n=3 dog, n=1 sheep) using ^{18}F-fluorodeoxyglucose (^{18}F-FDG) as radiolabel was performed between Week 13-15 post-surgery in dog and sheep. Gray-scale B-mode ultrasonography was able to detect endometriotic cysts (0.25-1.75mm) on urinary bladder and abdominal wall in dogs; endometrial grafts Week 1 post-surgery appeared as a homogenous, hypoechoic masses, following which they grew larger with evidence of cyst formation by Week 5. Cysts were undetectable from Week 10-13, whereas they appeared as homogenous masses with a hypoechoic fluid-filled cavity with diffuse hyperechoic echoes and low vascularisation (Color-Doppler imaging) by Week 14-15. In sheep, endometrial grafts were detected as hypoechoic masses Week 1 post-surgery that became smaller until no detectable lesions were visible beyond Week 6-7. Cysts in dogs and sheep appeared hyperintense on T2 and hypointense on T1 weighted images. ^{18}F -FDG PET-CT did not show hypermetabolic activity in endometriotic cysts in dogs and sheep. In conclusion, MRI appeared to provide the most definitive diagnostic images of endometriotic cysts in dogs and sheep, particularly for lesions in sheep which were

not evident by ultrasonography. However, ultrasonography was sufficient to characterize most endometriotic cysts in dogs. Further research needs to be carried out to develop specific PET tracers for endometriosis.

Keywords: Domestic animal model, dogs, endometriosis, endometriotic cysts, imaging, medical imaging, MRI, PET-CT, sheep model, ultrasonography

5.2 Introduction

Endometriosis is defined as the presence of ectopic endometrial glands and stroma primarily affecting the pelvic peritoneum, ovaries, and rectovaginal septum (Burney and Giudice 2012). An estimated 176 million women worldwide have endometriosis primarily during their prime reproductive years (Adamson et al 2010) with an estimated prevalence rate of 10% with highest incidence in women aged 25-30 years (Meuleman et al 2009, Eskenazi and Warner 1997). Further, the incidence of endometriosis in women undergoing laparoscopic evaluation for infertility is even higher, as much as 50% (Senapati and Barnhart 2011) with serious implications for future reproductive success. Endometriosis also has high economic importance as the total annual societal burden of endometriosis amounts to many millions of Euros (Simoens et al 2012).

Laparoscopy and histopathology are considered the gold standard for diagnosis and detection of endometriotic lesions in women (Dunselman and Beets-Tan 2012). As laparoscopy is invasive and expensive, endometriosis is often diagnosed many years (8-11 years) after the occurrence of the first complaint (Dunselman and Beets- Tan 2012). Various non-invasive imaging modalities including transvaginal ultrasonography (Mais et al 1993), magnetic resonance imaging (MRI) (Dallaudière et al 2013) and positron emission tomography- computed tomography (PET-CT) (Fastrez et al 2011) have been tried in women with endometriosis with varying degree of success. There remains significant need for better non-invasive diagnostic imaging tests that are more specific and sensitive especially in the detection of early and/or flat peritoneal endometriotic lesions which may be small and less invasive.

The ideal animal model for testing diagnostic modalities and assessing response to treatment would be a spontaneous primate model; however, ethical and practical constraints limit the study of pathogenesis and progression of endometriosis in women and non-human primates. Laboratory animal models such as mice (Chen et al 2010, Defrère et al 2006), rats (Umezawa et al 2008) and rabbits (Rosa-e-Silva et al 2010) have been tested. Rodent models are cost-effective but the lesions that develop are small and difficult to identify (Tirado-Gonzalez et al 2010) making them poorly suited as animal models for imaging studies. Xenografting of human endometrial tissue in immunodeficient mice have also been tried but this model does not permit assessment of immunoregulatory factors that may be involved in the pathogenesis of the disease (Fazleabas 2012). Rabbits are induced ovulators and lack a spontaneously occurring luteal phase (D'Hooghe, 1997), unlike the menstrual cycle in women. Considering above facts, animals comparable in size to humans may be a better model for mimicking the conditions required for assessing the sensitivity and specificity of various non-invasive imaging modalities.

In a previous study, our research group evaluated dogs, pig and sheep as potential models for surgical induction of endometriosis on serosal surfaces of the visceral (urinary bladder/uterus) and parietal (abdominal wall) peritoneum. Cystic endometriotic lesions developed from all endometrial grafts in dogs, while results were variable in sheep. The objective of this study is to assess the usefulness and limitations of ultrasonography, magnetic resonance imaging (MRI) and positron emission tomography-computed tomography (PET-CT) in detecting ednometriotic lesions in dogs and sheep.

5.3 Materials and Methods

The study was approved by the University Committee on Animal Care and Supply, Animal Research Ethics Board, University of Saskatchewan. Surgery, ultrasonography, and MRI were conducted at the Western College of Veterinary Medicine, University of Saskatchewan while PET-CT was performed at Royal University Hospital, Saskatoon, Saskatchewan, Canada.

5.3.1 Surgical induction of endometriosis

Surgical induction of endometriosis using autologous endometrial grafts was performed in dogs (mixed-breed Husky; n=5; body weight= 15-20kg; aged between 2-4 years of age) and sheep (Suffolk; n=5; body weight=80-90kg; aged between 1-2 years). At the time of surgery, dogs were in proestrus (n=2), and anestrus (n=3) stage of estrous cycle.

In brief, animals were premedicated for surgery, anesthesia induced by intravenous injection and maintained on general anesthesia with isoflurane as described (Chapter 3). Following laparotomy, unilateral hysterectomy of the left uterine horn was performed. The endometrium was separated aseptically from other layers of uterus and dissected into several small pieces (approximately 1 X 1 cm in dogs and 2 X 1 cm in sheep). A total of 4 endometrial pieces were sutured on the serosal surface of caudodorsal aspect of visceral peritoneum (urinary bladder in dogs and uterus in sheep; left and right endometrial grafts) and the parietal peritoneum of the ventral abdominal wall (left and right graft). Plastic jewellery beads (4mm diameter; one on bladder and two on each side of abdomen) were sutured adjacent to each graft and served as markers to identify them during imaging (Fig 5.1). Pieces of fat (n=4, approximately 2 X 1 cm; obtained from the falciform ligament in dogs and ligaments of bladder in sheep) were also sutured on visceral peritoneum and abdomen cranial to the endometrial grafts (Fig 5.1). The fat grafts served as internal controls. Grafting on the left side was performed with non-epitheial side of endometrium/non-serosal side of fat touching the serosal (mesothelial) surface of peritoneum whereas right side grafts were placed with epithelial side of endometrium/sersosal side of fat touching the serosal surface of peritoneum (Fig 5.1).

The size (length and width) of all grafts (endometrium and fat) were measured before closing the abdomen. Abdominal incisions were closed in a routine manner. Post-operative analgesics were administered to any animal that showed signs of pain. All the animals recovered uneventfully with no complications demonstrable with daily activities such as feeding, voiding etc.

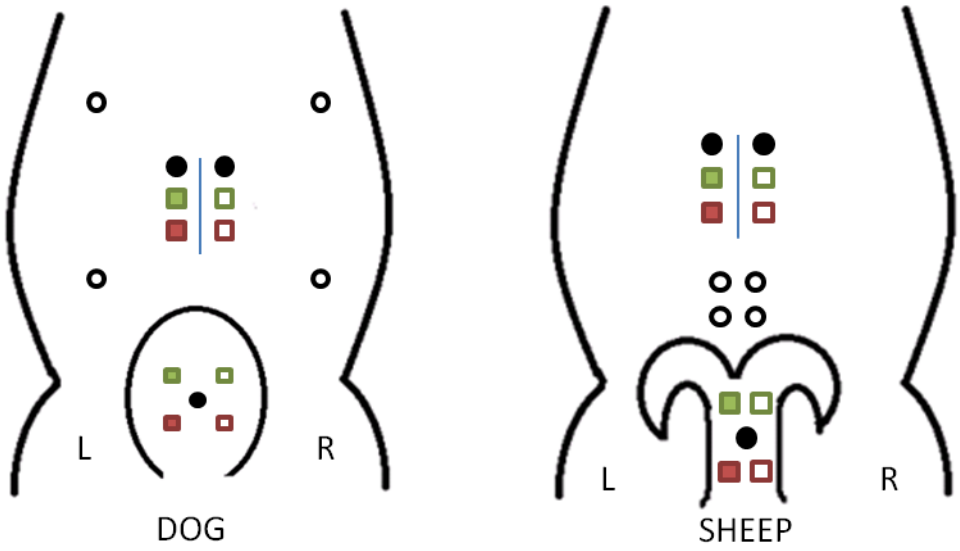

Figure 5.1 Dorso-ventral view of abdomen showing the site of incision (line; mid-ventral incision along linea alba) in relation to mammary glands (teats shown as open circles) in the dogs and sheep. Endometrial (red) and fat (green) pieces were sutured on the caudodorsal and craniodorsal aspect respectively of visceral peritonuem (urinary bladder in dogs and uterus in sheep) and dorsal aspect of ventral abdominal wall in animals. Grafts were placed with either epithelial/serosal (clear boxes) or non-epithelial/non-serosal side (i.e., stromal tissue, solid boxes) of the graft touching the visceral/parietal peritoneum. Plastic beads (solid black circles) served as markers for imaging.

5.3.2 Imaging of animals

5.3.2.1 Ultrasonography

Ultrasonography was performed once per week in dogs and sheep from Week 1-9 and in the day of euthanasia (Week 14-15). Ultrasonography was not performed from Week 10-13 as lesions were not detectable after Week 7 in dogs and Week 6 in sheep. Sedation (Acepromazine, Atravet, Boehringer Ingelheim, Burlington, Ontario, Canada) was used in dogs, if required. Grafts on the urinary bladder were imaged using a transrectal approach with a 12 MHz linear-array transducer (SN0152; MyLab5, Esaote North America, Inc., Indianapolis, IN, USA) in dogs, and a 5-7.5 MHz linear-array transducer (LV513; MyLab5) in sheep. Following initial localization of the urinary bladder/uterus, the plastic beads were

located and grafts were identified based on their location either cranial (fat graft) or caudal (endometrial graft), and left or right of midline. Abdominal grafts in both species were imaged by transcutaneous approach using a 5 MHz convex-array transducer (EC1123; MyLab5). To locate peritoneal abdominal wall grafts, the incision line scar was used for initial identification, with subsequent localization of the adjacent marker beads. Gray-scale B-mode was used to locate the grafts and colour flow Doppler mode (1400Hz pulse repetition frequency and 65-70% color gain) was used to ascertain blood flow to grafts. Cineloops of ultrasonographic examinations were stored (about 300 frames per video) and visibility, sonographic appearance and size of grafts (length and width) were recorded.

5.3.2.2 Positron Emission Tomography / Computed Tomography (PET/CT) and Magnetic resonance imaging (MRI)

MRI and PET-CT imaging were performed in anesthetized animals. Drugs and doses used for premedication and induction are as described previously (Chapter 3). Animals were maintained under general anesthesia using sevoflurane (SEVOrane, AbbVie Corporation, Saint-Laurent, Quebec, Canada).

Whole body ^{18}F –FDG PET-CT was performed in three dogs at Week 12-13 and one sheep at Week 13 post-surgery using ^{18}F-fluorodeoxyglucose (^{18}F-FDG) as radiolabel. A Discovery 710 (General Electric, Milwaukee, USA) PET-CT scanner located in the Royal University Hospital, Saskatoon, Canada was used. Blood glucose levels were measured prior to procedure and were within normal levels. Animals were positioned in dorsal recumbency and given an intravenous dose of ^{18}F –FDG (dose: 4.5 MBq/kg) with an uptake phase set at 60 minutes. An initial ultra-low dose CT was performed for attenuation correction, followed by a PET scan at 60 minutes and a full dose CT with intravenous contrast agent (Iopamidol, Isovue Multipack, Bracco Imaging Canada, Montreal, Quebec, Canada). Animals were then transported back to theholding facility and maintained in wards until all surface dose rates of radiation were less than 5µSv/h. MRI of mid-abdomen through pelvis region was performed in two dogs at Week 15 and two sheep at Week 13 post-surgery with a 1.5T scanner (Symphony, Syngo MRA35 software,

Siemens). Different slice orientations including axial and sagittal planes with spin-echo (SE) and fast spin-echo (FSE) T1 (repetition time 477-609 ms, echo time 12-13 ms and slice thickness 3-5.5 mm) and turbo spin-echo (TSE) T2 (repetition time 3940-6490 ms, echo time 91-108 ms and slice thickness 4-5 mm) weighted (W) images with and without fat suppression were obtained. Pre and post contrast axial FSE T1 W images with fat suppression was performed in only one dog and not performed in any sheep to evaluate for the usefulness of using a contrast agent. Gadolinium-based contrast agent (Optimark; dose-5mL/animal) was used to obtain post-contrast images.

5.3.3 Euthanasia and recovery of lesions

All dogs and sheep were euthanized using pentobarbital Sodium (Euthanyl Forte, Bimeda-MTC Animal Health Inc, Cambridge, Ontario, Canada) at a dose of 1mL/5kg BW intravenously between 84-110 days post-surgery and endometriotic lesions were recovered fro confirmation of medical imaging findings. All cysts were macroscopically visible and digital camera images were obtained using macro setting (Canon Power Shot A620, Canon Inc., China). The sizes (length and width) of cysts were measured for comparison.

5.3.4 Image analysis

Ultrasound images were evaluated over time for visibility, size, echogenicity and blood flow of grafts/cysts in dogs and sheep. Ultrasound and gross images were compared for anatomical aspects such as septation and presence of solitary or multiple cysts. All MRI sequences were evaluated at the same location to evaluate T1/T2 W images with and without fat suppression/contrast. PET and CT images were evaluated alone and in conjunction with MRI for comparison.

5.4 Results

5.4.1Experimental animals

5.4.1.1 Ultrasonography

The number of endometrial and fat grafts observed over weeks in dogs and sheep is shown in Fig. 5.2. Following surgical transplantation in dogs, proportion of endometrial grafts detected by ultrasonography over weeks gradually decreased from Week 3 to 6 (Fisher's Exact Test; $P<0.01$). Transplanted tissue grafts were not detected for following 3 weeks (Week 7 to 9), therefore ultrasonographic examinations were discontinued. Endometrial grafts initially appeared as a homogenous, hypoechoic mass on Gray-scale B-mode ultrasonography (Fig 5.3A). By Week 3, the endometrial grafts grew larger in size with evidence of prominent circumferential and internal vascularization (Fig 5.3B) on color-flow Doppler ultrasonography. By Week 5 and 6, cyst formation was evident (n=11 and 7 cysts respectively, out of 20) with hypoechoic fluid filling the cavity surrounded by moderate vascularization (Fig 5.3C,D). On the day of euthanasia (Week 14-15), ultrasonography performed on live dogs detected endometriotic cysts (n=19 grafts out of 20, n=5 animals) which appeared as a homogenous, hypoechoic mass with some focal hyperchoic echoes. Septations within some cysts was evident and low vascularisation was detected by clor-flow Doppler imaging (Fig 5.3E). Some dogs (n=3) had multiple cysts (Fig 5.3F) within one endometrial graft location. Following surgical transplantation, all fat grafts appeared as hyperechoic masses on B-mode ultrasonography (Fig 5.3A) between Week 1-6. Proportion of detectable fat grafts ($p<0.01$) and size of fat grafts decreased from Week 1-6 and were not recognizable on the day of euthanasia (Week 14-15).

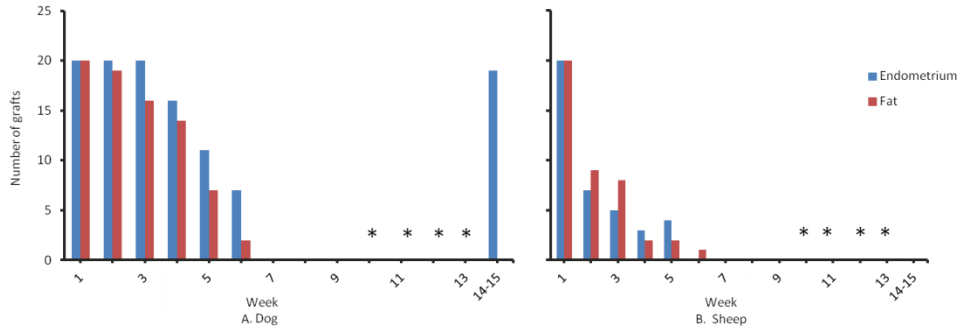

Figure 5.2 shows number of endometrial (blue) and fat (red) grafts visible on ultrasonography in dogs (A) and sheep (B) over 14-15 Weeks post-surgery. Blank spaces indicate weeks where lesions were not detectable. (*) indicates weeks where ultrasonography was not performed.

In sheep following surgical transplantation, sutured endometrial grafts appeared as a homogenous, hypoechoic mass whereas fat grafts appeared hyperechoic on B-mode ultrasonography (Fig 5.3G). By Week 3 and 4 most of endometrial grafts reduced in size and appeared as a hypoechoic mass (Fig 5.3H). It was difficult to discern the boundaries of the graft. Fat grafts appeared hyperechoic with reduction in size (Fig 5.3I) by Week 2. By Week 6, no lesions were seen in sheep. At the time of euthanasia, plastic marker beads were detectable with no evidence of abdominal or uterine endometriotic lesions in sheep (Fig 5.3J,K).

5.4.1.2 MRI

Endometriotic cysts on ventral abdominal wall and urinary bladder in dogs appeared hyperintense on TSE T2 W images (Fig 5.4B) and TSE T2 W fat-suppressed images. Cysts appeared hypointense on SE T1 W images (Fig 5.4C) and SE T1 W fat-suppressed images (Fig 5.4D). Cysts on the urinary bladder had signal intensity similar to fluid in bladder on TSE T2 W images and SE T1 W image. Contrast enhancement along cyst wall was observed in both bladder and abdominal cysts on FSE T1 W fat-suppressed images (Fig 5.4E) following administration of contrast agent. FSE T1 W fat-suppressed images revealed hyperintense spots (Fig 5.4G) within endometriotic cysts. Following euthanasia, cut section of the same cyst revealed presence of blood (Fig 5.4F). Multilocularity of cysts with a clear dividing septae was predominatly seen on sagittal TSE T2 W (Fig 5.4I) image which was not evident on axial orientation.

MRI of endometriotic cysts in one sheep revealed similar characteristics as those in dogs. No lesions/cysts were detected in the other sheep. Endometriotic cysts (both abdominal and uterus) appeared hyperintense on TSE T2 W images (Fig 5.5 B) and TSE T2 W fat-suppressed images (Figs 5.5 C,G,H) and hypointense

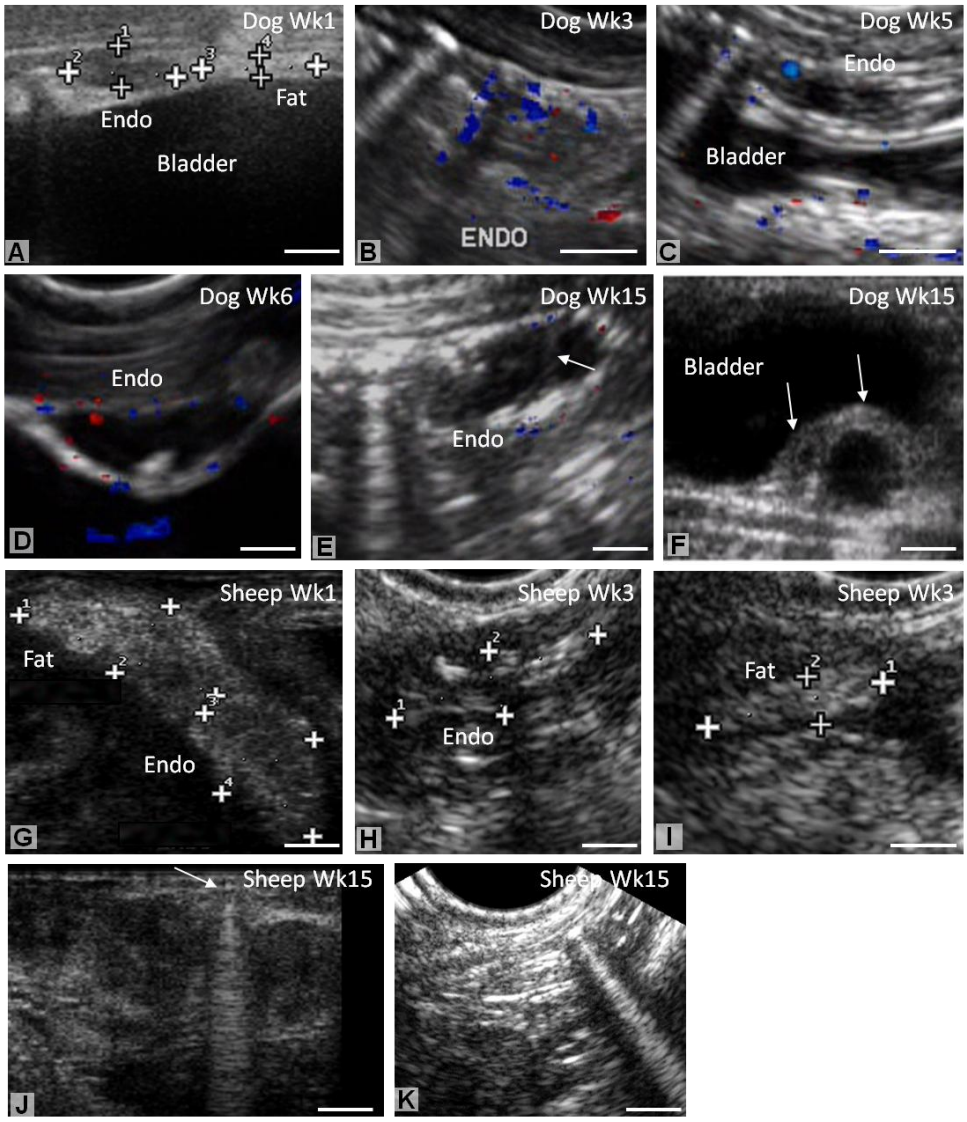

Figure 5.3 Gray-scale B-mode and color Doppler ultrasonography imaging of endometriotic lesions and fat in dogs (Fig. A-F) and sheep (Fig. G-K). Following surgery (Week 1), endometrial (Endo) grafts appeared as a homogenous, hypoechoic mass whereas fat grafts appeared hyperechoic in dogs (Fig.A). By Week 3, endometrial grafts grew larger in size with evidence of prominent circumferential and internal vascularization on Doppler ultrasonography (Fig.B), By Week 5 and 6, cyst formation was evident with hypoechoic fluid filling the cavity surrounded by moderate vascularization (Fig C,D). Notice the hyperechoic spot within the lumen of the cyst which could be blood (Fig.D), On the day of euthanasia (Week 14-15), endometriotic cysts appeared as a hypoechoic mass with diffuse hyperchoic echoes within lumen with low vascularization. Septations (arrow) were seen within the cyst (Fig.E), Multiple cysts of varying sizes (arrows) were also seen in some (n=3) dogs at euthanasia (Fig.F), In sheep, endometrial grafts appeared as a homogenous, hypoechoic mass whereas fat grafts appeared hyperechoic (similar to dogs) at Week 1 (Fig.G), By Week 3 and 4, endometrial grafts reduced in size in sheep and appeared as a hypoechoic mass (Fig.H), However, fat grafts appeared hyperechoic with reduction in size (Fig.I), On the day of euthanasia (Week 14-15), marker beads were seen (arrow) with no endometriotic lesions or remnants of fat on uterus (Fig.J) or abdomen (Fig.K). Bladder=Urinary bladder, Endo=Endometrial graft, Fat= Fat graft, Wk=Week. Scale bar: Fig A-K= 0.5cm.

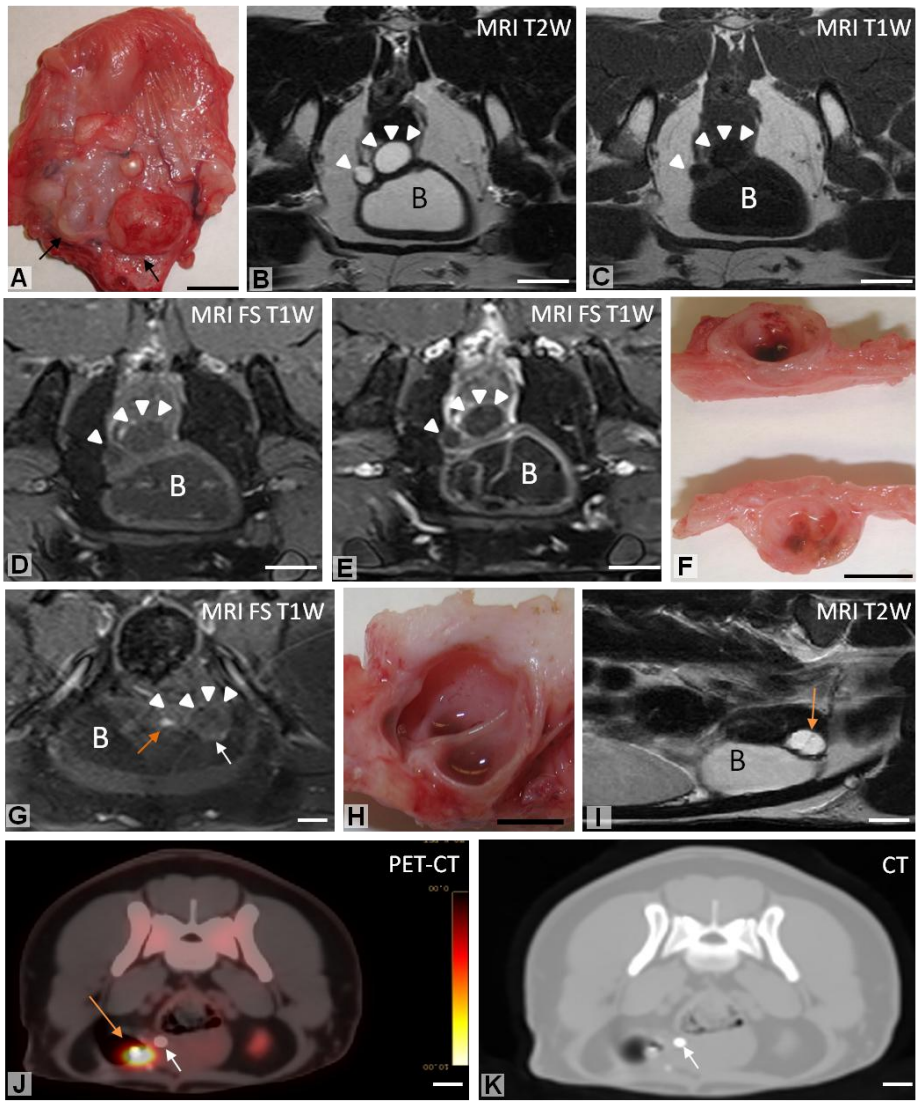

Figure 5.4 Endometriotic lesions in dogs viewed grossly, by MRI, PET-CT and CT. Dorsal surface of urinary bladder following euthanasia shows left (small) and right (big) endometriotic cysts (arrows) with a marker bead located cranial to the cysts (Fig.A), Axial TSE T2 W image shows the presence of hyperintense cysts (both left and right, arrowheads) with signal intensity similar to fluid in urinary bladder (Fig.B), Axial SE T1 W image shows the presence of hypointense cysts with signal intensity similar to fluid in urinary bladder (Fig.C), Axial FSE T1 W fat- suppressed image before (Fig.D) and after (Fig.E) administration of contrast indicates contrast enhancement along cyst wall (Fig.E), Cut section of an endometriotic cyst on bladder reveals a unilocular cavity with blood (top section) (Fig.F), Axial FSE T1 W fat- suppressed image of the same cyst shows hyperintensity spots along the dependent portion of cysts, brighter on the left (orange arrow) than the right cyst (white arrow) indicating possible presence of blood (Fig.G), Cut section of right endometriotic lesion on urinary bladder reveals a multilocular septated cavity with serosanguineous fluid (Fig.H), Sagittal TSE T2 W image shows a clear septae (orange arrow) dividing the big endometriotic cyst which is not evident on axial orientation (Fig.E) (Fig.I), PET-CT (Fig.J) and CT (Fig.K) images did not clearly identify the presence of cysts but demonstrated evidence of bead (white arrow) which had similar intensity as that of bone. FDG excretion via urine depicted by bright positive activity (orange arrow). B=Urinary Bladder, Spin-echo=SE, Fast spin-echo=FSE, Turbo spin-echo=TSE, Weighted=W, Fat suppression=FS. Scale bar Fig A-E,G,I-K= 1cm, Fig. F,H= 0.5 cm.

on SE T1 W images (Figs 5.5 D,F). Abdominal cysts were detected as small vesicles (Fig 5.5G). It was difficult to identify cysts on T1 W images since they were small and not as evident as that in dogs.

5.4.1.3 PET-CT/CT

None of the ^{18}F -FDG PET-CT/CT images demonstrated hypermetabolic activity around urinary bladder or ventral abdominal wall endometriotic cysts in dogs (Fig 5.4J) or around uterine or ventral abdominal wall endometriotic lesions in sheep (Figs 5.5 I,J). Marker beads with similar attenuation to bone were identified in dog (Fig 5.4K) and sheep (Figs 5.5K,L). Urinary excretion of ^{18}F –FDG leads to accumulation in bladder denoted by positive activity.

5.4.2 Gross evaluation of endometriotic cysts

As reported previously (Chapter 3), majority of endometrial grafts (19/20) in dogs (n=5) developed into endometriotic cysts that were larger than initial grafts. Remaining graft on the urinary bladder developed into a solid lesion. Cysts presented as single (Fig 5.4A) or multiple cysts. Cysts were unilocular (Fig 5.4F) or multilocular (Fig 4H)}. For the purpose of this study, vesicles were identified as structures less than 1cm, whereas a cyst was ≥ 1cm. In sheep, the lesions included solid lesions (5/20), single or multiple small vesicles (5/20), cysts (5/20) (Fig 5.5 A,E) and absence of lesions (5/20).

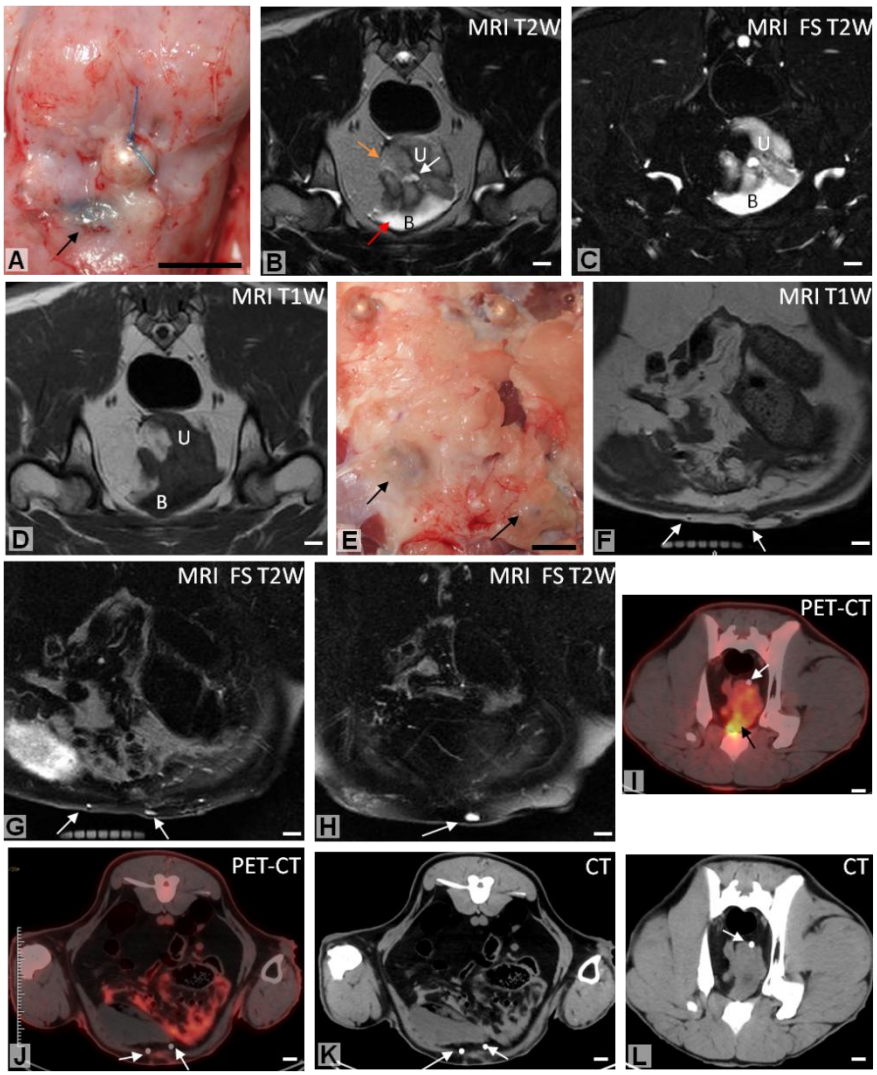

Figure 5.5 Endometriotic lesions in a sheep viewed grossly after euthanasia, by MRI, PET-CT and CT. Gross image of uterus following euthanasia shows left endometriotic cyst (arrow) with a bead in the cranial aspect (Fig.A), Axial TSE T2 W image shows presence of uterus (orange arrow), urinary bladder (red arrow) and hyperintense left endometriotic cyst (white arrow) on the uterus with signal intensity similar to bladder (Fig.B), Axial TSE T2 W fat-suppressed image shows brighter intensity of cyst with signal intensity similar to urinary bladder (Fig.C), Axial SE T1 W image does not reveal a clear identifiable cyst (Fig.D) compared to TSE T2 W image with (Fig.C) or without (Fig.B) fat-suppression, Macroscopic image of the abdomen following euthanasia shows endometriotic cysts left and right (arrows) of midline with two beads in the far cranial aspect. Notice that the right cyst is caudal compared to left cyst (Fig.E), Axial SE T1 W image shows small hypointense left and right abdominal cysts (arrows) (Fig.F) , Axial TSE T2 W fat suppressed image shows hyperintense left and right abdominal cysts (Fig.G), Since the right cyst was caudal to left cyst, a different section revealed a slightly bigger cyst on axial TSE T2 W fat suppressed image (Fig.H), PET-CT (Fig.I,J) and CT (Fig.K,L) images of pelvis (Fig.I,L) and abdomen (Fig.J,K) did not reveal the presence of cysts but demonstrated evidence of a bead (white arrow). FDG excretion via urine depicted by bright positive activity (black arrow). B- Urinary Bladder, Spin-echo=SE, Fast spin-echo=FSE, Turbo spin-echo=TSE, Weighted=W, Fat suppression=FS, U= Uterus. Scale bar Fig. A-L= 1cm.

5.5 Discussion

One of the major limitations with diagnosing endometriosis is the lack of a highly specific and sensitive non-invasive diagnostic test. Animal models can provide insight into developing better non-invasive tests for early and accurate diagnosis. The objective of our study was to use imaging modalities to detect endometriotic cysts in previously described dog and sheep models of endometriosis. To assist with detection of lesions, plastic marker beads were sutured at the site of graft transplantation. Gray-scale and color Doppler ultrasonography was able to detect progression of endometriotic lesions for 5 to 6 weeks post-surgery in both dog and sheep. In contrast to fat grafts, endometrial grafts appeared "hypoechoic" with evidence of fluid filled cavities and moderate vascularization of peripheral areas. As the lesions became smaller in sheep, they could not be detected for several weeks, however cystic endometriotic lesions in dogs were detected at all locations by 14 to 15 weeks post-surgery and confirmed by necropsy. MRI was also able to detect endometriotic lesions, particularly in T2 W images. This modality detected lesions in sheep that were not visible on ultrasonography. A somewhat surprising finding was the inability of CT and PET-CT with ^{18}F-FDG to detect lesions indicating that developing endometriotic cysts does not have hypermetabolic activity (i.e., enhanced glucose uptake) or acute inflammatory reaction. Since ^{18}F-FDG is not specific for endometriosis, development of an endometriosis-specific PET tracer may help to detect small and early microinvasive lesions.

Our previous study (chapter 3) tested the suitability of dog, pig and sheep to develop endometriotic lesions after surgical grafting of endometrium on visceral and parietal peritoneum. Majority of developing lesions in dogs at Week 14-15 post-surgery were in the form of cysts with characteristics similar to endometriomas in women as described in literature. Although not all endometrial grafts grew in sheep, a variety of outcomes (small vesicles, solid lesions, complete absorption, cystic lesions) were discovered at necropsy. Ultrasound data from this study documents that progression of the endometrial lesions during first month after surgical intervention parallels the fat tissue in both dog and sheep; however, at necropsy, important differences were documented between the two species. Microscopically, cysts were surrounded

by endometrial glandular and stromal cells with hemorrhage and/or hemosiderin-laden macrohpages in dogs with normal, dilated and cystic endometrial glands were observed in the cyst wall. In the small number of grafts that developed into endometiotic cysts in sheep, very few endometrial glands were observed with some lesions having no glands. Therefore, based on necropsy and histopathological finding, dog model was considered the most optimal model.

On ultrasonography, 95% of endometriomas in women present as homogenous, hypoechoic masses with low level echoes (Volpi et al 1995; Patel et al 1999). Multilocularity seen as septations together with presence of hyperechoic foci within the wall of a mass and the absence of neoplastic features increases the suspicion of an endometrioma (Spencer and Weston 2003). In our study, endometriotic cysts in dogs presented as hypoechoic masses with focal hyperchoic echoes, septations within cyst, variable sizes (Fig. 5.4B), features typical of those described in women. The initial development of endometriotic cysts in dogs was characterized by moderate levels of vascularisation (Week 2-6) followed by low levels of vascularisation on the day of euthanasia (Week 14-15). Similar blood flow characteristics were seen in women with endometriomas featuring low vascularisation (Aleem et al 1995). Ultrasonography was particularly useful for the detection of growing endometriotic cysts in dogs. Plastic beads sutured near grafts (easily detected with ultrasonography as intensely reflective objects with vertical shadows due to reverberation) served as excellent landmarks to differentiate between absence or presence of endometriotic and fat lesions.

MRI readily identified endometriotic cysts in both dog and sheep. In our study, these appeared hyperintense on TSE T2 W images (with and without fat suppression) and hypointense on SE T1 W images. Endometriomas in women commonly appear hyperintense on T1 W and hypointense on T2 W images on MRI (Glastonbury 2002; Saba et al 2015). It is speculated that the loss of signal intensity on T2 W images results from the presence of more concentrated blood products in older endometriomas (Glastonbury 2002). It has also been proposed that predominance of glandular component/dilated endometrial glands within endometriotic lesions can lead to high signal intensity on T2 W images (Del

Frate et al 2006; Saba et al 2015). In such cases use of contrast agent may demonstrate contrast enhancement (Del Frate et al 2006). A few hyperintense foci were noted within cysts in dogs on FSE T1 W fat-suppressed images possibly related to blood. The reason for hyperintensity within endometriotic cysts on T2 W images in dogs could be attributed to the numerous dilated and cystic endometrial glands that were evident on histopathology and little hemorrhage. In our study, cysts appeared late (Week 14-15 post surgery) with little blood/blood products to contribute to classic high and low signal intensity on T1 and T2 W images respectively as seen in women. Therefore, prolonging the duration of the study (9-12 months) to compare the effect of time on signal changes (i.e., 3 versus 9-12 months post-surgery) in cysts could provide details regarding microstructure of cysts.

In our study, T2 W (with and without fat suppression) MRI images showed clear evidence of cysts. However, FSE T1 W fat-suppressed images were particularly useful in identifying possible accumulation of blood. Contrast enhancement surrounding cyst walls corresponded with the amount of fibrous tissue which encapsulated all cysts. Axial and sagittal orientations helped to demonstrate multilocularity and cyst septations. Therefore, it was essential to perform all sequences {T1W and T2W (especially with and without fat suppression)} and orientations (axial and sagittal) so that lesions can be characterized in all aspects without missing essential information. On comparing ultrasonograpy and MRI in sheep, ultrasonography could not detect endometriotic lesions in sheep nearing euthanasia. However, although lesions were small, MRI was capable of detecting lesions that were not readily seen on ultrasonography.

PET-CT imaging using ^{18}F –FDG for diagnosis of endometriosis in women has yielded mixed results (Jeffry et al 2004, Fastrez et al 2011, Ge et al 2015) with most studies showing no detection of hypermetabolic anomaly (Fastrez et al 2011) except when associated with inflammation (Jeffry et al 2004). Our studies showed similar results with no hypermetabolic activity in endometriotic cysts following ^{18}F –FDG PET-CT in dogs and sheep. The major limitation attributed to PET-CT studies with ^{18}F –FDG is the lack of specificity to endometrial tissue (Fastrez et al 2011). For example, Gamma scintigraphy and PET studies using rabbit as an endometriosis model to assess the uptake of radiolabelled

(^{99m}Tc or ^{68}Ga) GAP-EDL via estrogen-receptor mediated process (Takahashi et al 2007) provided promising results. There was increased uptake of ^{99m}Tc-GAP-EDL via gamma scintigraphy and ^{68}Ga-GAP-EDL via PET in uterine graft implants proving to be useful functional estrogen receptor imaging agents (Takahashi et al 2007). Therefore, further research in the development of endometriosis/estrogen receptor specific PET tracers will markedly increase the potential of PET-CT in the diagnosis of endometriosis. In addition, although MRI is the most optimal imaging modality to diagnose and define the exact extent of endometriosis in women (Kinkel et al 2006), significant limitations include sub-optimal detection of small implants and adhesions (Zanardi et al 2003).

In conclusion, MRI was the best imaging modality in diagnosis of enodmetriotic cysts in dogs and sheep. Ultrasonography was sufficient to characterize most endometriotic cysts in dogs but not sheep. In addition, MRI is capable of providing information related to content of cysts, in addition to presence of locularity and septation. Endometriotic cysts in dogs and sheep were undetectable and did not show hypermetabolic activity on ^{18}F –FDG PET-CT. Further research needs to be carried out in the development of more specific PET tracers for endometriosis that could significantly improve the diagnosis of solid/or small lesions that may be difficult to detect using MRI/ultrasonography in women. Our success suggests that the dog model for endometriosis was useful for imaging and can be used for improving existing non-invasive tests.

CHAPTER 6: DISCUSSION

Endometriosis is defined as the presence of endometrial glands and stroma in ectopic locations, primarily the pelvic peritoneum, ovaries, and rectovaginal septum (Burney and Giudice 2012). An estimated 176 million women worldwide have endometriosis primarily during their prime reproductive years (Adamson et al 2010). On a personal level, women with endometriosis suffer severe pelvic pain, dysmenorrhea, dyspareunia, gastrointestinal symptoms such as painful defecation, diarrhea, constipation or both, nausea and vomiting, and bladder symptoms such as painful dysuria, urgency-frequency and painful bladder sensation (Arnaud et al 2013). On a global level, the total annual societal burden of endometriosis-associated symptoms accounts to billions of euros (Simeons et al 2012). The most striking finding was that the cost of productivity loss was double the health care costs per woman indicating drastic reduction in the quality of life once affected with the disease (Simeons et al 2012). Famous celebrities have known to be affected, the most notable one being Marilyn Monroe who was thought to have become addicted to painkillers that she took for endometriosis that resulted in her death (Boseley et al 2015). Considering the above facts, endometriosis is a disease that is gaining significant importance due its serious implications.

To understand the pathogenesis of this complex disease is challenging especially when combined with the fact that it is unethical, impractical and difficult to study the progression of the disease in women. Therefore, animal models proved to be indispensable to increase our understanding of the disease that is affecting a multitude of women of today's age. Several small animal models have been tried but they pose several disadvantages with respect to size of lesions that are difficult to identify and dissimilar estrus cycles. Despite the numerous advantages associated with using non-human primates as models, they are expensive to maintain and is ethically sensitive to carry out such experiments in these animals (Tirado-Gonzalez et al 2010). Laparoscopy and/or histopathology remains to be the gold standard diagnostic test for detection of endometriotic lesions (Dunselman and Beets-Tan 2012). Since laparoscopy is invasive, expensive and not the primary diagnostic choice, endometriosis is often diagnosed several years (8-11

years) after the occurrence of the first complaint (Dunselman and Beets- Tan 2012). Therefore, there seems to be an ever-increasing need for the development of an animal model with size comparable to humans to allow for serial non-invasive tests that is both specific and sensitive for the detection of early endometriosis where the lesions are particularly small and sometimes micro-invasive.

To address the prevailing issues, three studies were conducted as part of the thesis. First study involved in vitro assessment of attachment characteristics of endometrium to serosal surfaces in dogs, pig and sheep (Chapter 3). After successfully determining that endometrium is capable of attaching to serosal surfaces, surgical induction of endometriosis was carried out in dogs, pig and sheep to determine the most suitable domestic animal model for endometriosis (Chapter 3). Since dogs proved to be the most optimal animal model, currently available imaging modalities were performed to determine their capability in identifying endometriotic lesions (Chapter 4).

The in vitro study provided significant evidence that endometrial epithelial, stromal and glandular cells are capable of attaching to visceral peritoneum (omentum/broad ligament) within 24 hours with and without an intact layer of mesothelial cells in dogs, pig and sheep. Endometrium and smooth muscle fibers of visceral peritoneum remained healthy prior to culture and until 24 hours, but began to show degenerative changes by 48 and 72 hours. This demonstrates that endometrial components of endometrium are capable of strong attachment within 24h and our results were similar to those found in women (Witz et al 1999, Witz et al 2001). In our study we observed that although most attachments were via stromal cells and some amount of stromal cells always surrounds glands, there was considerable number of samples where glands were directly attached to serosal surface in all species. The endometrial epithelium was also capable of attaching to serosal surfaces. Although previous studies (Witz et al 1999) concluded that endometrial stromal cell and not epithelium attached to peritoneum, our study observed differently where endometrial stromal, glandular and epithelial cells were capable of attaching. It can be concluded that in-vitro culture of endometrium and visceral peritonuem should preferably not exceed 48h

and is a good method to assess early attachment characteristics in dogs, pig and sheep. This provided evidence that endometrial cells are capable of attaching to serosal surfaces which paved the way for our in vivo study.

Large animals as models provide several advantages. They would have longer estrus cycles length which are comparable to women when compared to short cycles in laboratory animals. They would develop lesions that are detectable compared to small lesions that are difficult to identify in smaller animals. In addition, domestic animals would have body size comparable to women. Large animal models can provide additional advantage as they can be used for serial imaging with currently available imaging modalities for endometriosis and also for testing treatment options. Our study was conducted by surgical induction of endometriosis using autologous endometrial grafts sutured onto serosal surfaces of organs (urinary bladder in dogs and pig, uterus in sheep) and parietal peritoneum (ventral abdominal wall) in dogs, pig and sheep. Dogs provided the most promising results with grafts (19/20) developing into endometriotic cysts characterized by endometrial stromal and glandular cells with hemorrhage and/or hemosiderin-laden macrophages. These features were characteristic of endometriosis in women, especially those related to ovarian endometriotic cysts (Czernobilsky and Fox 2003). Cysts were also observed in pig and sheep with hemorrhage and/or hemosiderin-laden macrohpages in stroma. The most striking feature in dog and sheep was the reduction in number of glands (normal/dilated) or no glands in most lesions with evidence of epithelial and glandular degeneration. Thus we concluded that among the three species tested, dogs are the most suitable domestic animal model for endometriosis.

Cystic endometrial hyperplasia in the bitch is primarily seen during diestrus (luteal phase) stage of the estrus cycle frequently associated with inflammation leading to pyometra (Dow 1958, Schlafer and Gifford 2008). This illustrates that the dog endometrium has an innate ability to develop cysts. However in our study, endometrial grafts from dogs at different stages of estrus cycle developed into endometriotic cysts suggesting a different pathogenesis. Also, eutopic ednometrium in these dogs were normal and did not show any signs of cystic endometrial hyperplasia.

Dogs were then utilized to assess their utility as an endometriosis model for imaging using currently used imaging modalities such as ultrasonography, MRI, CT and PET-CT. On ultrasonography, endometriotic cysts appeared as a homogenous, hypoechoic mass with diffuse hyperchoic echoes within cyst. MRI was particularly useful in detecting cysts as they appeared hyperintense on T2 weighted (W) image and hypointense on T1 W images. Cysts on the bladder had signal intensity similar to fluid in bladder. T1 W fat-suppressed images revealed small foci of hyperintensity within cysts indicating possible presence of blood/hemorrhage. It was noteworthy that, endometriotic cysts could not be detected on ultrasonography in sheep, whereas MRI was capable of detecting cysts with signal intensity similar to cysts in dogs nearing euthanasia. None of the ^{18}Flourine-fluorodeoxyglucose (^{18}F –FDG) PET-CT/CT images were capable of detecting hypermetabolic activity in endometriotic cysts in dogs and sheep, however beads were seen with signal intensity similar to bone.

In our study, MRI was the best imaging tool in diagnosis of enodmetriotic cysts in dogs. However, ultrasonography was sufficient to characterize most endometriotic cysts in dogs. Although MRI is the most optimal imaging modality to diagnose and define the exact extent of endometriosis (Kinkel et al 2006), significant limitations include sub-optimal detection of small implants and adhesions (Zanardi et al 2003). Further research needs to be carried out in the development of specific PET tracers for endometriosis which will prove to be a boon in the diagnosis of solid and or microscopic/small lesions that may be difficult to detect using MRI/ultrasonography. An accurate non-invasive test that is both specific and sensitive will eliminate the need for invasive laparoscopy and early diagnosis of endometriosis, where lesions may be small, as more women are likely to get imaged than undergo laparoscopy. Early diagnosis will lead to better prognosis and significantly improved quality of life.

CHAPTER 7: FUTURE DIRECTIONS

Since our study was a preliminary study to establish a suitable domestic animal model, further characterization of endometriotic lesions in dogs would prove highly beneficial. Characterisation of proliferative potential of glandular vs stromal cells and evaluation of apoptotic index using immunohistochemical techniques would better our understanding since proliferation and escape from apoptosis is an important component of endometriotic lesions in women. Assessment of estrogen receptors and local production of estrogen would give a complete idea of how the lesion is behaving in response to changes in the estrus cycle, since endometriosis is an estrogen dependant disease in women. Considering the inflammatory nature of the disease, evaluation of local, peripheral and peritoneal fluid levels of inflammatory cytokines such as interleukins could provide more details about the nature of the lesions in dogs. Since cadherins specifically E-cadherin is involved in cell-cell adhesion and N-cadherin is involved in invasiveness, changes in types of cadherins could provide information regarding why neoplastic changes were seen in only two dogs. Since endometriosis in women occurs when endometrial cells undergo retrograde menstruation, mimicking this process in dogs by intraperitoneal injection of endometrial cells separated from endometrium would prove to be more identical to the situation in women. Lastly, increasing the duration of the study would help us understand if the lesions would persist, grow or change features that are presently seen.

CHAPTER 8: GENERAL CONCLUSIONS

In conclusion, the results of studies presented in this thesis suggest that in vitro culture can be used as a quick tool to assess attachment characteristics of endometrium to serosal surfaces of visceral peritoneum. Dogs proved to be a suitable domestic animal model for endometriosis since they developed endometriotic lesions with features characteristic to those described in women. Dogs can also be used for various imaging modalities thus extending their potential use for being used as models to develop improved non-invasive tests and testing treatment options.

REFERENCES

Abrao MS, Gonçalves MO, Dias JA Jr, Podgaec S, Chamie LP, Blasbalg R. 2007. Comparison between clinical examination, transvaginal sonography and magnetic resonance imaging for the diagnosis of deep endometriosis. Human Reproduction 22: 3092-3097.

Acosta AA, Buttram VC Jr, Besch PK, Malinak LR, Franklin RR and Vanderheyden JD. 1973. A proposed classification of pelvic endometriosis. Obstetrics and Gynecology 42: 19–25.

Adamson GD and Pasta DJ. 2010. Endometriosis fertility index: the new, validated endometriosis staging system. Fertility and Sterility 94: 1609-1615.

Adamson GD, Kennedy S and Hummelshoj L. 2010. Creating solutions in endometriosis: global collaboration through the World Endometriosis Research Foundation. Journal of Endometriosis 2: 3-6.

Adamson GD. 2013. Endometriosis Fertility Index: is it better than the present staging systems? Current Opinion in Obstetrics and Gynaecology 25: 186–192.

Aghajanova L, Horcajadas JA, Weeks JL, Esteban FJ, Nezhat CN, Conti M and Giudice LC. 2010. The protein kinase A pathway- regulated transcriptome of endometrial stromal fibroblasts compromised differentiation and persistent proliferative potential in endometriosis. Endocrinology 151: 1341-1355.

Agic A, Xu H, Rehbein M, Wolfler MM, Ebert AD and Hornung D. 2007. CCR1 and mRNA expression in peripheral blood as a diagnostic test for endometriosis. Fertility and Sterility 87: 982-984.

Akira S, Taga T and Kishimoto T. 1993. Interleukin-6 in biology and medicine. Advances in Immunology 54: 1-78.

Aleem F, Pennisi J, Zeitoun K and Predanic M, 1995. The role of color Doppler in diagnosis in endometriomas. Ultrasound in Obstetrics and Gynecology 5: 51-54.

Arici A, Oral E, Attar E, Tazuke SI and Olive DL. 1997. Monocyte chemotactic protein-1 concentration in peritoneal fluid of women with endometriosis and its modulation of expression in mesothelial cells. Fertility and Sterility 67:1065–1072

Arnaud F, Stéphanie S, Cyrille H, Horace R, Pierre P and Philippe D. 2013. Comparison of patient- and physician-based descriptions of symptoms of endometriosis a qualitative study. Human Reproduction 28: 2686-2694.

Badawy SZ, Cuenca V, Marshall L, Munchback R, Rinas AC and Coble DA. 1984. Cellular components in peritoneal fluid in infertile patients with and without endometriosis. Fertility and Sterility 42: 704-708.

Baghaei H, Wong WH and Li H. 2013. Principles of positron emission tomography imaging. (2nd ed). 2013. Kim EE, Lee MC, Inoue T and Wong WH. Clinical PET and PET/CT: Principles and applications pp 3-28. Springer Science + Business Media, New York, USA.

Banu SK, Starzinski-Powitz A, Speights VO, Burghardt RC, Arosh JA. 2009. Induction of peritoneal endometriosis in nude mice with use of human immportalized endometriosis epithelial and stromal cells: a potential experiment tool to study molecular pathogenesis of endometriosis in humans. Fertility and Sterility 91: 2199-2209 (Supple).

Barcz E, Skopinska Rózewska E, Kaminski P, Demkow U, Bobrowska K and Marianowski L. 2002. Angiogenic activity and IL-8 concentrations in peritoneal fluid and sera in endometriosis. International Journal of Gynecology and Obstetrics 79: 229-235.

Barczyk M, Carracedo S and Gullberg D. 2010. Integrins. Cell and Tissue Research 339: 269-280.

Béliard A, Donnez J, Nisolle M and Foidart JM. 1997. Localization of laminin, fibronectin, E-cadherin, and integrins in endometrium and endometriosis. Fertility and Sterility 67: 266-272.

Béliard A, Noël A and Foidart JM. 2004. Reduction of apoptosis and proliferation in endometriosis. Fertility and Sterility 82: 80-85.

Bobbio A, Damotte D, Gompel A and Alifano M. 2012. Extra-abdominal endometriosis (ed). 2012. Endometriosis –Science and practice pp 108-114. Wiley Blackwell publication, United Kingdom.

Boseley S, Glenza J and Davidson H. 2015. Women don't have to suffer in silence. The Guardian Weekly pp 34-35.

Bruner-tran K L, Eisenberg E, Yeaman GR, Anderson TA, Mcbean J and Osteen KG. 2002. Steroid and cytokine regulation of matrix metalloproteinase expression in endometriosis and the

establishment of pexperimental endometriosis in nude mice. Journal of Clinical Endocrinology and Metabolism 87: 4782-4791.

Bulun SE, Yang S, Fang Z, Gurates B, Tamura M and Sebastian S. 2002. Estrogen production and metabolism in endometriosis. Annals of the New York Academy of Sciences 955: 75-85

Burney RO and Giudice LC. 2012. Pathogenesis and pathophysiology of endometriosis. Fertility and Sterility 98: 511-519.

Burney RO, Talbi S, Hamilton AE Vo KC, Nyegaard M, Nezhat CR, Lessey BA and Giudice LC. 2007. Gene expression analysis of endometrium reveals progesterone resistance and candidate susceptibility genes in women with endometriosis. Endocrinology 148: 3814-3826.

Buttram VC Jr. 1978. An expanded classification of endometriosis. Fertility and Sterility 30: 240–242.

Carlberg M, Nejaty J, Fröysa B, Guan Y, Söder O and Bergqvist A. 2000. Elevated expression of tumour necrosis factor α in cultured granulose cells from women with endometriosis. Human Reproduction 15: 1250-1255.

Chapron C, Chopin N, Borghese B, Foulot H, Dousset B, Vacher-Lavenu MC, Vieria M, Hasan W and Bricou A. 2006. Deeply infiltrating endometriosis: pathogenic implications of the anatomical distribution. Human Reproduction 21: 1839-1845.

Chen DB, Yang ZM, Hilsenrath R, Le SP, Harper MJ. 1995. Stimulation of prostaglandin (PG) F2 alpha and PGE2 release by tumour necrosis factor-alpha and interleukin-1 alpha in cultured human luteal phase endometrial cells. Human Reproduction 10: 2773-2780.

Chen QH, Zhou WD, Su ZY, Huang QS, Jiang JN, Chen QX. 2010. Change of proinflammatory cytokines follows certain patterns after induction of endometriosis in a mouse model. Fertility and Sterility 93: 1448-1454.

Clement PB, Young RH and Scully RE. 1988. Necrotic Pseudoxanthomatous nodules of ovary and peritoneum in endometriosis. The American journal of surgical pathology 12: 390-397.

Concannon PW. 2011. Reproductive cycles of the domestic bitch. Animal Reproduction Science 124: 200-210.

Crain DA, Janssen SJ, Edwards TM, Heindel J, Ho SM, Hunt P, Iguchi T, Juul A, McLachlan JA, Schwartz J, Skakkebaek N, Soto AM, Swan S, Walker C,Woodruff TK, Woodruff TJ, Giudice LC and Guillette LJ Jr. 2008. Female reproductive disorders: the roles of endocrine-disrupting compounds and developmental timing. Fertility and Sterility 90: 911-940.

Culling CFA. 1974. Basic staining and mounting procedures. In Culling CFA (3rd ed) 1974. Handbook of Histopathological and Histochemical Techniques pp 192-200. Butterworths and Co, London UK.

Czernobilsky B and Fox H. 2003. Endometriosis. (5th ed). 2003. Obstetrical and Gynecological Pathology vol 2 pp 963-987. Elsevier Science Limited, United Kingdom.

Czernobilsky B and Morris WJ. 1979. A histologic study of ovarian endometriosis with emphasis on hyperplastic and atypical changes. Obstetrics and gynecology 53: 318-323.

Dallaudière B, Salut C, Hummel V, Pouquet M, Piver P, Rouanet JP and Maubon A. 2013. MRI atlas of ectopic endometriosis. Diagnostic and Internventional Imgaing 94: 263-280.

DeBerardinis RJ, Lum JJ, Hatzivassiliou G and Thompson CB. 2008. The biology of cancer: metabolic reprogramming fuels cell growth and proliferation. Cell metabolism 7: 11-20.

Defrère S, Van Langendonckt A, González Ramos R, Jouret M, Mettlen M, Donnez J. 2006. Quantification of endometriotic lesions in amurine model by fluometric and morphometric analyses. Human Reproduction 21: 810-817.

Del Frate C, Girometti R, Pittino M, Del Frate G, Bazzocchi M and Zuiani C. 2006. Deep retroperitoneal pelvic endometriosis: MR imaging appearance with laproscopic correlation. Radiographics 26: 1705-1718.

D'Hooghe T. 1997. Clinical relevance of the baboon as a model for the study of endometriosis. Fertility and sterility 68: 613-625.

D'Hooghe TM, Bambra CS, De Jonge I, Lauweryns JM, Koninckx PR. 1996. The prevalence of spontaneous endometriosis in the baboon (Papio anubis, Papio cynocephalus) increases with the duration of captivity. Acta Obstetrica et Gynecologica Scandinavica 75: 98-101.

D'Hooghe TM, Bambra CS, Raeymaekers BM, De Jonge I, Lauweryns JM and Koninckx PR. 1995. Intrapelvic injection of menstrual endometrium causes endometriosis in baboons (Papio cynocephalus and Papio Anubis). American Journal of Obstetrics and Gynecology 173: 125-134.

D'Hooghe TM, Bambra CS, Suleman MA, Dunselman GA, Evers HL, Koninckx PR. 1994. Development of a model of retrograde menstruation in baboons (Papio anubis). Fertility and Sterility 62: 635-638.

Donnez J and Squifflet J. 2004. Laparoscopic excision of deep endometriosis. Obstetrics an Gynecology Clinics of North America 31: 567-580.

Donnez J, Donnez O, Lousse Jean-Christophe and Squifflet J. 2012. Peritoneal, Ovarian, and Rectovaginal Endometriosis are Three Different Entities. (ed). 2012. Endometriosis –Science and practice pp 92-107. Wiley Blackwell publication, United Kingdom.

Donnez J, Nisolle M, Gillet N, Smets M, Bassil S and Casanas- Roux F. 1996. Large ovarian endometriomas. Human Reproduction 11: 641-646.

Donnez J, Smoes P, Gillerot S, Casanas-Roux F and Nisolle M. 1998. Vascular endothelial growth factor (VEGF) in endometriosis. Human Reproduction 13: 1686-1690.

Doonez J and van Langendonckt A. 2004. Typical and subtle atypical presentation of enodmetriosis. Current opinion in Obstetrics and Gynecology 16: 431-437.

Dow C. 1958. The cystic hyperplasia-pyometra complex in the bitch. Veterinary Record 70: 1102-1110.

Dunselman GAJ and Beets-Tan RGF. 2012. Diagnosis of Endometriosis: Imaging. (ed). 2012. Endometriosis –Science and Practice pp 299-308. Wiley Blackwell publication, United Kingdom.

Eskenazi B and Warner ML. 1997. Epidemiology of endometriosis. Obstetrics and Gynecology Clinics 24: 235-258.

Fassbender A, Overbergh L, Verdrengh E, Kyama CM, Vodolazakaia A, Bokor A, Meuleman C, Peeraer K, Tomassetti C, Waelkens E, Mathieu C and D'Hooghe T. 2011. How can macroscopically normal peritoneum contribute to the pathogenesis of enodmetriosis? Fertility and Sterility 96: 697-699.

Fastrez M, Nogarède C, Tondeur M, Sirtaine N, Rozenberg S. 2011. Evaluation of 18FDG PET-CT in the diagnosis of endometriosis: a prospective study. Reproductive Sciences 18: 540-544.

Fazleabas TA. 2012. Models of Endometriosis: Animal Models II – Non-human Primates. (ed). 201 2. Endometriosis –Science and Practice pp 285-291. Wiley Blackwell publication, United Kingdom.

Gaetje R, Kotzian S, Herrmann G, Baumann R and Starzinski-Powitz A. 1997. Nonmalignant epithelial cells, potentially invasive in human endometriosis, lack the tumor suppressor molecule E-cadherin. The American Journal of Pathology 150: 461-467.

Gagné D, Rivard M, Page M, Shazand K, Hugo P and Gosselin D. 2003. Blood leukocyte subsets are modulated in patients with endometriosis. Fertility and Sterility 80: 43-53.

Ge J, Zuo C, Guan Y and Zhang X. 2015. Increased ^{18}F-FDG uptake of widespread endometriosis mimicking ovarian malignancy. Clinical Nuclear Medicine 40: 186-188.

Gellersen B and Brosens J. 2003. Cyclic AMP and progesterone receptor cross-talk in human endometrium: a decidualizing affair. Journal of Endocrinology 178: 357-372.

Gellersen B, Brosens IA and Brosens JJ. 2007. Decidualization of the human endometrium: mechanisms, functions, and clinical perspectives. Seminars in Reproductive Medicine 25: 445-453.

Glastonbury CM. 2002. The Shading Sign. Radiology 224: 199-201.

Groothuis PG. 2012. Angiogenesis and Endometriosis. (ed). 2012. Endometriosis –Science and Practice pp 190-199. Wiley Blackwell publication, United Kingdom.

Grümmer R, Schwarzer F, Bainczyk K, Hess-Stumpp H, Regidor PA, Schindler AE, Winterhager E. 2001. Peritoneal endometriosis: validation of an iv-vivo model. Human Reproduction 16: 1736-1743.

Halme J, Hammond MG, Hulka J, Raj SG and Talbert LM. 1984. Retrograde menstruation in healthy women and in patients with endometriosis. Journal of the American College of Obstetricians and Gynecologists 64: 151-154.

Hammond MG, Oh ST, Anners J, Surrey ES and Halme J. 1993. The effect of growth factors on the proliferation of human endometrial stromal cells in culture. American Journal of Obstetrics and Gynecology 168: 1131-1138.

Hansen AE, McEvoy F, Engelholm SA, Law I and Kristensen AT. 2011. FDG PET/CT imaging in canine cancer patients. Veterinary Radiology and Ultrasound 52: 201-206.

Harirchian P, Gashaw I, Lipskind ST, Braundmeier AG, Hastings JM, Olson MR, Fazleabas AT. 2012. Lesion kinetics in a non-human primate model of endometriosis. Human Reproduction 27: 2341-2351.

Healy DL, Rogers PAW, Hii L and Wingfield M. 1998. Angiogenesis: a new theory for endometriosis. Human Reproduction Update 4: 736-740.

Hirata T, Osuga Y, Yoshino O, Hirota Y, Harada M, Takemura Y, Morimoto C, Koga K, Yano T, Tsutsumi O, Taketani Y. 2005. Development of an experimental model of endometriosis using mice that uqiquitously express green fluorescent protein. Human Reproduction 20: 2092-2096.

Honoré GM. 1999. Extrapelvic endometriosis. Clinical Obstetrics and Gynecology 42:699-711.

Hori Y and SAGES Guidelines Committee. 2008. Diagnostic laparoscopy guidelines : This guideline was prepared by the SAGES Guidelines Committee andreviewed and approved by the Board of Governors ofthe Society of American Gastrointestinal and EndoscopicSurgeons (SA GES), November 2007. Surgical Endoscopy 22: 1353-1383.

Hughesdon PE. 1957. The structure of endometrial cysts of the ovary. Journal of Obstetrics and Gynecology British Empire 44: 69-84.

Huhtinen K, Desai R, Stahle M, Salminen A, Handelsman DJ, Perheentupa A and Poutanen M. 2012. Endometrial and endometriotic concentrations of estrone and estradiol are determined by local metabolism rather than circulating levels. Journal of Clinical Endocrinology and Metabolism 97: 4228-4235.

Humphries M J. 2000. Integrin cell adhesion receptors and the concept of agonism. Trends in Pharmacological Sciences 21: 29-32.

Iwabe T1, Harada T, Tsudo T, Nagano Y, Yoshida S, Tanikawa M, Terakawa N. 2000. Tumor necrosis factor-alpha promotes proliferation of endometriotic stromal cells by inducing interleukin-8 gene and protein expression. Journal of Clinical Endocrinology and Metabolism 85:824-829.

Jacobson VC. 1922. The autotransplantation of endometrial tissue in the rabbit. Archives of Surgery 5: 281-300.

Javert CT. 1949. Pathogenesis of endometriosis based on endometrial homeoplasia, direct extension, exfoliation and implantation, lymphatic and hematogenic metastasis. Cancer 2: 399-410.

Jeffry L, Kerrou K, Camatte S, Metzger U, Lelièvre L, Talbot JN, Lecuru F. 2004. Endometriosis with FDG uptake on PET. European Journal of Obstetrics, Gynecology and Reproductive Biology 117: 236-239.

Jones LM, Gardner MJ, Catterall JB and Turner GA. 1995. Hyaluronic acid secreted by mesothelial cells: a natural barrier to ovarian cancer cell adhesion. Clinical and Experimental Metastasis 13: 373-380.

Joseph IBJK, Currie WD and Rawlings NC. 1992. Effects of time after ovariectomy, season and oestradiol on luteinizing hormone and follicle-stimulating hormone secretion in ovariectomized ewes. Journal of Reproduction and Fertility 94: 511-523.

Keenan JA, Chen TT, Chadwell NL, Torry DS and Caudle MR. 1994. Interferon-gamma (IFN-gamma) and interleukin-6 (IL-6) in peritoneal fluid and macrophage-conditioned media of women with endometriosis. American Journal of Reproductive Immunology 32: 180-183.

Khan KN, Masuzaki H, Fujishita A, Kitajima M, Hiraki K, Sekine I, Matsuyama T and Ishimaru T. 2005. Interleukin-6- and tumour necrosis factor alpha-mediated expression of hepatocyte growth factor by stromal cells and its involvement in the growth of endometriosis. Human Reproduction 20: 2715-2723.

Khanjani S, Al-Sabbagh MK, Fusi L and Brosens JJ. 2012. Role of steroid hormones: Progesterone signaling. (ed). 2012. Endometriosis –Science and Practice pp 145-152. Wiley Blackwell publication, United Kingdom.

Kinkel K, Frei KA, Balleyguier C and Chapron C. 2006. Diagnosis of endometriosis with imaging: a review. European Radiology 16: 285-298.

Kinkel K, Frei KA, Balleyguier C and Chapron C. 2006. Diagnosis of endometriosis with imaging: a review. European Radiology 16: 285-298.

Kistner RW, Siegler AM, Behrman SJ. 1977. Suggested classification for endometriosis: relationship to infertility. Fertility and Sterility 28: 1008–1010.

Klemmt PAB and Starzinski-Powitz A. 2012. Biology of Eutopic and Ectopic Endometrium in Women with Endometriosis. (ed). 2012. Endometriosis –Science and Practice pp 117-129. Wiley Blackwell publication, United Kingdom.

Kushner PJ, Agard DA, Greene GL, Scanlan TS, Shiau AK, Uht RM and Webb P. 2000. Estrogen receptor pathways to AP-1. Journal of Steroid Biochemistry and Molecular Biology 74: 311-317.

Laird SM, Li TC and Bolton AE. 1993. The production of placental protein 14 and interleukin 6 by human endometrial cells in culture. Human Reproduction 8: 793-798.

Laird SM, Tuckerman EM, Saravelos H and Li TC. 1996. The production of tumour necrosis factor α (TNF-α) by human endometrial cells in culture. Human Reproduction 11: 1318-1323.

Laschke MW, Korbel C, Rudzitis-Auth J, Gashaw I, Reinhardt M, Hauff P, Zollner TM and Menger MD. 2010. High-resolution ultrasound imaging. The American Journal of Pathology 176: 585-593.

Lebovic DI, Bentzien F, Chao VA, Garrett EN, Meng YG and Taylor RN. 2000. Induction of an angiogenic phenotype in endometriotic stromal cell cultures in interleukin-1β. Molecular Human Reproduction 6: 269-275.

Lebovic DI, Mueller MD and Taylor RN. 2001. Immunobiology of enodmetriosis. Fertility and Sterility 75: 1-10.

Lee HY, Lee MC and Kim EE. 2013. Normal and variable patterns in PET. (2nd ed). 2013. Kim EE, Lee MC, Inoue T and Wong WH. Clinical PET and PET/CT: Principles and applications pp 99-106. Springer Science + Business Media, New York, USA.

Lee KR. 2006. The pathology of surface epithelial-stromal tumors of the ovary (ed). 2006. Crum CP and Lee KR. Diagnostic Gynecologic and Obstetric Pathology pp 839-903. Elsevier Saunders, USA.

Mais V, Guerriero S, Ajossa S, Angiolucci M, Paoletti AM and Melis GB. 1993. The efficiency of transvaginal ultrasonography in the diagnosis of endometrioma. Fertility and Sterility 60: 776-780.

Martínez S, Garrido N, Coperias JL, Pardo F, Desco J, García-Velasco JA, Simón C and Pellicer A. 2007. Serum interleukin-6 levels are elevated in women with minimal-mild endometriosis. Human Reproduction 22: 836-842.

Matrisian LM. 2000. Matrix metalloproteinases. Current Biology 10: 692.

Matsui T, Nakata N, Nagai S, Nakatani A, Takahashi M, Momose T, Ohtomo K, Koyasu S. 2009. Inflammatory cytokines and hypoxia contribute to 18F-FDG uptake by cells involved in pannus formation in rheumatoid arthritis. Journal of Nuclear Medicine 50: 920-926.

Mazur TM and Kurman RJ. 2005. Endometrial Hyperplasia, Endometrial intraepithelial carcinoma and epithelial cytoplasmic change (2nd ed). 2005. Diagnosis of endometrial biopsies and curettings pp 178-207. Springer Science, NY, USA

McLaren J, Prentice A, Charnock-Jones DS and Smith SK.1996. Vascular endothelial growth factor (VEGF) concentrations are elevated in peritoneal fluid of women with endometriosis. Human Reproduction 11: 220-223.

Merrill JA. 1966. Endometrial induction of endometriosis across Millipore filters. American Journal of Obstetrics and Gynecology 94: 780-790.

Meuleman C, Vandenabeele B, Fieuws S, Spiessens C, Timmerman D, D'Hooghe T. 2009. High prevalence of endometriosis in infertile women with normal ovulation and normospermic partners. Fertility and Sterility 92:68–74.

Montag AG, Jenison EL, Griffiths CT, Welch WR, Lavin PT and Knapp RC. 1989. Ovarian clear cell carcinoma: A clinicopathologic analysis of 44 cases. Intenational Journal of Gynecological Pathology 8: 85-96.

Mori H, Sawairi M, Nakagawa M, Itoh N, Wada K and Tamaya T. 1992. Expression of interleukin-1 (IL-1) beta messenger ribonucleic acid (mRNA) and IL-1 receptor antagonist mRNA in peritoneal macrophages from patients with endometriosis. Fertility and Sterility 57: 535-542.

Motta PM, van Blerkom J and Mekabe S. 1992. Changes in the surface morphology of ovarian germinal epithelium during the reproductive life and in some pathological conditions. Submicroscopy cytology 99: 664-667.

Nezhat F, Nezhat C, Allan CJ, Metzger DA and Sears DL. 1992. A clinical and histological classification of endometriomas: implications for a mechanism of pathogenesis. Journal of Reproductive Medicine 37: 771-776.

Nap AW. 2012. Theories on the pathogenesis of endometriosis. Giudice L C, Evers JLH, Healy DL. (ed). 2012. Endometriosis –Science and practice pp 42-53. Wiley Blackwell publication, United Kingdom.

Nisolle M and Donnez J. 1997. Peritoneal endometriosis, ovarian endometriosis and adenomyotic nodules of the rectovaginal septum are three different entities. Fertility and Sterility 68: 585-596.

Noble LS, Simpson ER, Johns A and Bulun SE. 1996. Aromatase expression in endometriosis. Journal of Clinical Endocrinology and Metabolism 81: 174-179.

Oosterlynck DJ, Cornillie FJ, Waer M, Vandeputte M and Koninckx PR. 1991. Women with endometriosis show a defect in natural killer activity resulting in a decreased cytotoxicity to autologous endometrium. Fertility and Sterility 56: 45-51.

Osteen KG, Yeaman GR and Bruner-Tran KL. 2003. Matrix metalloproteinases and endometriosis. Seminars in Reproductive Medicine 21: 155-164.

Patel MD, Feldstein VA, Chen DC, Lipson SD and Filly RA. 1999. Endometriomas: diagnostic performance of ultrasound. Radiology 210: 739-745.

Pelch KE, Schroder AL, Kimball PA, Sharpe-Timms KL, Davis JW, Nagel SC. 2010. Aberrant gene expression profile in a mouse model of endometriosis mirrors that observed in women. Fertility and Sterility 93: 1615-1627.

Rana N, Braun DP, House R, Gebel H, Rotman C, Dmowski WP. 1996. Basal and stimulated secretion of cytokines by peritoneal macrophages in women with endometriosis. Fertility and Sterility 65: 925-930.

Ridley JH and Edwards IK. 1958. Experimental endometriosis in the human. American Journal of Obstetrics and Gynecology 76: 783-790.

Rodgers WH, Matrisian LM, Giudice LC, Dsupin B, Cannon P, Svitek C, Gorstein F and Osteen KG. 1994. Patterns of matrix metalloproteinase expression in cycling endometrium imply differential functions and regulation by steroid hormones. Journal of Clinical Investigation 94: 946-953.

Rogers PA, D'Hooghe TM, Fazleabas A, Giudice LC, Montgomery GW, Petraglia F, Taylor RN. 2013. Defining future directions for endometriosis research: workshop report from the 2011 World Congress of Endometriosis in Montpellier, France. Reproductive Sciences 20: 483-499.

Rosa-e-Silva JC, Garcia SB, de Sá Rosa-e-Silva AC, Candido-dos-Reis FJ, Poli-Neto OB, Ferriani RA, Nogueira AA. 2010. Increased cell proliferation in experimentally induced endometriosis in rabbits. Fertility and Sterility 93: 1637-1642.

Rossi D and Zoltnik A. 2000. The biology of chemokines and their receptors. Annual review of Immunology 18: 217-242.

Saba L, Sulcis R, Melis GB, de Cecco CN, Laghi A, Piga M and Guerriero S. 2015. Endometriosis: the role of magnetic resonance imaging. Acta Radiologica 56: 355-367.

Sampson JA. 1921. Perforating hemorrhagic (chocolate) cysts of the ovary: their importance and especially their relation to pelvic adenomas of endometrial type (adenomyoma of the uterus, rectovaginal septum, sigmoid, etc). Archives of Surgery 3: 245–323.

Sampson JA. 1925. Hetertropic or misplaced endometrial tissue. American Journal of Obstetrics and Gynecology 10: 649-664.

Sampson JA. 1927. Peritoneal endometriosis due to menstrual dissemination of endometrial tissue into the peritoneal cavity. American journal of Obstetrics and Gynaecology 14: 422–469.

Sampson JA. Perforating hemorrhagic (chocolate) cysts of ovary. 1921. Their importance and especially their relation to pelvic adenomas of endometriotic type (‘‘adenomyoma’’ of the uterus, rectovaginal septum etc.). Archives of Surgery 3: 245–261.

Sasson IE and Taylor HS. 2008. Stem cells and the pathogenesis of endometriosis. Annals of the New York Academy of Sciences 1127: 106–115.

Schall TJ, Bacon K, Toy KJ and Goeddel DV. 1990. Selective attraction of monocytes and T lymphocytes of the memory phenotype by cytokine RANTES. Nature 347: 669-671.

Schenken RS and Asch RH. 1980. Surgical induction of endometriosis in the rabbit: effects on fertility and concentrations of peritoneal fluid prostaglandins. Fertility and sterility 34: 581-587.

Schlafer DH and Gifford AT. 2008. Cystic endometrial hyperplasia, pseudo-placentational endometrial hyperplasia, and other cystic conditions of the canine and feline uterus. Theriogenology 70: 349-358.

Senapati Sand Barnhart K. Managing endometriosis-associated infertility. 2011. Clinical Obstetrics and Gynecology 54:720–726.

Sillem M, Prifti S, Neher M and Runnebaum B. 1998. Extracellular matrix remodeling in the endometrium and its possible relevance to the pathogenesis of endometriosis. Human Reproduction Update 4: 730-735.

Simoens S, Dunselman G, Dirksen C, Hummelshoj L, Bokor A, Brandes I, Brodszky V, Canis M, Colombo GL, Falcone T, Graham B, DeLeire T, Halis G, Horne A, Kanj O, Kjer JJ, Kristensen J, Lebovic D, Mueller M, Vigano P, Wullschleger M and D’Hooghe TM. 2012. The burden of endometriosis:costs and quality of life of women with enodmetriosis and treated in referral centres. Human Reproduction 27: 1292-1299.

Simpson JL, Elias S, Malinak LR and Buttram VC Jr. 1980. Heritable aspects of endometriosis. I. Genetic studies. American Journal of Obstetrics and Gynecology 137: 327-331.

Sironi M, Breviario F, Proserpio P, Biondi A, Vecchi A, Van Damme J, Dejana E and Mantovani A. 1989. IL-1 stimulates IL-6 production in endothelial cells. Journal of Immunology 142: 549-553.

Somigliana E, Infantino M, Benedetti F, Arnoldi M, Calanna G and Ragni G. 2006. The presence of ovarian endometriomas is associated with a reduced responsiveness to gonadotropins. Fertility and Sterility 86: 192-196.

Somigliana E, Vigano P, Gaffuri B, Candiani M, Busacca M, Di Blasio AM and Vignali M. 1996. Modulation of NK cell lytic function by endometrial secretory factors: potential role in endometriosis. American Journal of Reproductive Immunology 36: 295-300.

Spencer JA and Weston MJ. 2003. Imaging in endometriosis. The British Institue of Rdaiology 15: 63-71.

Stewart BW. 1994. Mechanisms of apoptosis: integration of genetic, biochemical, and cellular indicators. Journal of National Cancer Institute 86: 1286-1296.

Stovall DW, Anners JA and Halme J. 1992. Immunohistochemical detection of type I, III and IV collagen in endometriosis implants. Fertility and Sterility 57: 984-989.

Sugiyama T and Tsuda H. 2011 Clear cell carcinoma of the ovary (ed). 2011. Reed N, Green JA, Gerhenson DM, Siddiqui N and Connor R. Rare and Uncommon Gynecological Cancers: A Clinical Guide pp 91-104. Springer Heidelberg Dordrecht, New York.

Takahashi N, Yang DJ, Kurihara H, Borne A, Kohanim S, Oh CS, Mawlawi O, Kim EE. 2007. Functional imaging of estrogen receptors with radiolabelled-GAP-EDL in rabbit endometriosis model. Academic Radiology 14: 1050-1057.

Taylor E and Williams C. 2010. Surgical treatment of endometriosis: location and patterns of disease at reoperation. Fertility and Sterility 93: 57-61.

Tirado-González I, Barrientos G, Tariverdian N, Arck PC, García MG, Klapp BF, Blois SM. 2010. Endometriosis research: animal models for the study of a complex disease. Journal of Reproductive Immunology 86: 141-147.

Uchiide I, Ihara T and Sungamata M. 2002. Pathological evaluatin of the rat endometriosis model. Fertility and Sterility 78: 782-786.

Umaria N and Olliff JF. 2000. MRI appearances of bladder endometriosis. The British Journal of Radiology 73: 733-736.

Umezawa M, Sakata C, Tanaka N, Kudo S, Tabata M, Takeda K, Ihara T and Sugamata M. 2008. Cytokine and chemokine expression in a rat endometriosis is similar to that in human endometriosis. Cytokine 43: 105-109.

Vernon MW and Wilson EA. 1985. Studies on the surgical induction of endometriosis in the rat. Fertility and sterility 44: 684-694.

Vigano P, Gaffuri B, Somigliana E, Busacca M Di Blasio AM and Vignali M. 1998. Expression of intercellular adhesion molecule (ICAM)-1 mRNA and protein is enhanced in endometriosis versus endometrial stromal cells in culture. Molecular Human Reproduction 4: 1150-1156.

Volpi E, de Grandis T, Zuccaro G, la Vista A and Sismondi P. 1995. Role of transvaginal ultrasonography in the detection of endometriomata. Journal of Clinical Ultrasound 23: 163-167.

Von Recklinghausen F. 1896. Adenomyomas and cystadenomas of the wall of the uterus and tube: their origin as remnants of the wolffian body. Wien Klin Wochenschr 8: 530.

Walker GV, Niikura N, Yang W, Rohren E, Valero V, Woodward WA, Alvarez RH, Lucci A Jr, Ueno NT and Buchholz TA. 2012. Pretreatment staging positron emission tomography/computed tomography in patients with inflammatory breast cancer influences radiation treatment field designs. International Journal of Radiation Oncology, Biology, Physics 83: 1381-1386.

Wang DB, Zhang SL, Niu HY, Lu JM. 2005. A nude mouse model of endometriosis and its biological behaviours. Chinese Medical Journal 118: 1564-1567.

Wang N, Hong S, Tan J, Ke P, Liang L, Fei H, Liu B, Liu L, Liu Y and Yu B. 2014. A red fluorescent nude mouse model of human endometriosis: advantages of a non-invasive imaging method. European Journal of Obstetrics and Gynecology and Reproductive Biology 176: 25-30.

Wang N, Hong S, Tan J, Ke P, Liang L, Fei H, Liu B, Liu L, Liu Y and Yu B. 2014. A red fluorescent nude mouse model of human endometriosis: advantages of a non-invasive imaging method. European Journal of Obstetrics and Gynecology and Reproductive Biology 176: 25-30.

Witz CA, Cho S, Montoya-Rodriguez IA, Schenken RS. 2002a. The α2β1 and α3β1 integrins do not mediate attachment of endometrial cells to peritoneal mesothelium. Fertility and Sterility 78: 796–803.

Witz CA, Montoya-Rodriguez IA, Cho S, Centonze VE, Bonewald LF and Schenken RS. 2001. Composition of the extracellular matrix of the peritoneum. Journal of the Society for Gynecologic Investigation 8: 299-304.

Witz CA, Allsup KT, Montoya-Rodriguez IA, Vaughn SL, Centonze VE and Schenken RS. 2002b. Culture of menstrual endometrium with peritoneal explants and mesothelial monolayers confirms attachment to intact mesothelial cells. Human Reproduction 17: 2832-2838.

Witz CA, Monotoya-Rodriguez IA and Schenken RS. 1999. Whole explants of peritoneum and endometrium: a novel model of the early endometriosis lesion. Fertility and Sterility 71: 56-60.

Witz CA, Thomas MR, Montoya-Rodriguez IA, Nair AS, Centonze VE and Schenken RS. 2001. Short-term culture of peritoneum explants confirms attachment of endomterium to intact peritoneal mesothelium. Fertility and Sterility 75: 385-390.

Witz CA. 2003. Cell adhesion molecules and endometriosis. Seminars in Reproductive Medicine 21: 173-181.

Yaegashi N, Fujita N, Yajima A and Nakamura M. 1995. Menstrual cycle dependent expression of CD44 in normal human endometrium. Human Pathology 26: 862-865.

Yung S, Li FK and Chan TM. 2006. Technological advances in peritoneal dialysis. Peritoneal Dialysis International 26: 162-173.

Zanardi R, Del Frate C, Zuiani C and Bazzocchi M. 2003. Staging of pelvic endometriosis based on MRI findings versus laparoscopic classification according to the American Fertility Society. Abdominal Imaging 28: 733-742.

Zanetta GM, Webb MJ, Li H and Keeney GL. 2000. Hyperestrogenism: A relevant risk factor for the development of cancer from endometriosis. Gynecologic Oncology 79:18-22.

Zhang H, Li J, Sun W, Hu Y, Zhang G, Shen M and Shi X. 2014. Hyaluronic Acid-Modified Magnetic Iron Oxide Nanoparticles for MR Imaging of Surgically Induced Endometriosis Model in Rats. PLoS ONE 9: e94718.

Zhang RJ, Wild RA and Ojago JM. 1993. Effect of tumour necrosis factor-alpha on adhesion of human endometrial stromal cells to peritoneal mesothelial cells: an invitro system. Fertility and Sterility 59: 1196-1201.

Zheng W, Li N, Wang J, Ulukus EC, Ulukus M, Arici A and Liang SX. 2005. Initial endometriosis showing direct morphologic evidence of metaplasia in the pathogenesis of ovarian endometriosis. International Journal of Gynecological Pathology 24: 164-172.